Coordination of Insulin-mediated Neural Stem Cell Proliferation and Stem Cell Niche Development

Xin Yuan

Tianjin, China

B.S., University of Iowa, 2013

A Dissertation presented to the Graduate Faculty of the University of Virginia in Candidacy for the Degree of Doctor of Philosophy

Department of Biology

University of Virginia

December 2019

Abstract

During development, early undifferentiated progenitors called stem cells generate functional tissue through cell growth and proliferation. Stem cells are either pluripotent or multipotent, capable of differentiating into a variety of cell types depending on their intrinsic properties and environmental cues. Precise regulation of stem cell proliferation, differentiation, and quiescence ensures the development of specialized daughter cells with spatial and temporal accuracy. This is essential for establishing functional organs and maintaining tissue homeostasis. One such population of undifferentiated progenitors are neural stem cells, which generate the neurons and glia in the brain responsible for life and survival. In *Drosophila*, neural stem cells, named neuroblasts (NBs), are maintained in a microenvironment termed the NB stem cell niche. NBs enter a dormancy state termed quiescence at the end of embryogenesis, and reactivate after larval feeding. Dietary nutrients promote stem cell proliferation within the niche through activation of the canonical Insulin/PI3K/AKT/TOR growth signaling pathway.

In this dissertation, I sought to uncover the cellular interactions between neural stem cells and their niche cells in response to dietary nutrients. I demonstrated that the cellular architecture of the *Drosophila* NB stem cell niche establishment requires dietary nutrients during early stages of development. We show that NBs in the central brain reside in a complex niche microenvironment consisting of cortex glia and cerebral trachea, the gas exchange organ that delivers oxygen to the brain. The establishment of this complex niche cytoarchitecture (cellular architecture) is nutrient and PI3-Kinase dependent. Additionally, we

uncovered nutrient instructed coordination of growth between NBs, cortex glia, and trachea. NB reactivation from quiescence requires activated PI3-Kinase in both cortex glia and trachea. Conversely, glial membrane growth requires reactivated NBs. The nutrient-responsive growth of NBs and glia are mediated through *Drosophila* insulin-like peptide 2 (Dilp-2). In addition, through single Dilp mutant analysis of the 7 Dilps, we found that Dilp-1 and Dilp-7 are also required for NB reactivation in the central brain. The pancreatic β cell analogous organ, insulin producing neurons, are the cellular source of Dilp-2. Circulating Dilp-2 in the insect blood hemolymph, and Dilp-2 locally released onto the Dilp-recruiting neurons are both potential sources of insulin to reactivate quiescent NBs. These findings demonstrate that both NB exit from quiescence, and niche cytoarchitecture development are established through intercellular communication and nutrient signaling coordination. This work highlights the interplay of insulin-mediated neural stem cell proliferation, stem cell niche development and insulin-responsive neural circuitry essential for proper brain growth and development.

Dedication

To Mackenzie, Chyna, Antarctica, Bon Bon, Soufflé and Ryan, for being with me through every laugh and every tear.

Acknowledgement

I thank past and present members of the Siegrist lab, my advisor Dr. Sarah Siegrist; my lab mates Dr. Matthew Pahl, Dr. Susan Doyle, Dr. Conor Sipe, Chhavi Sood, Emily Ross, Nahid Ausrafuggaman, Dr. Karsten Siller; undergraduate research assistants Lindsay Ardiff, Sandy Hoang, Jamie Null, Siddharth Patel, Morgan Brazel, Tori Rodgers, Ricky Anjorin, Jackie Lee, Jungmin Choi, Zach Whiting, Courtney Doran, Will Moles, Jeremy Rigaldies, Ky Nguyen, Lucie Rigaldies, Julien Rigaldies, Rashika Budhathoki, Virginia Justis, Katie Woods, Jonathan Day and Catherine Shen for intellectual inspiration, technical assistance, and support in all aspects for the completion of this dissertation.

I thank my dissertation committee, chaired by Dr. Sarah Kucenas, and members of the committee, Dr. Barry Condron, Dr. Paul Adler, Dr. Eyleen O'Rouke, and Dr. Michelle Bland for intellectual discussions and mentorship.

I thank members of the Kucenas lab, Dr. Sarah Kucenas, Dr. Cody Smith, Dr. Yunlu Zhu, Dr. Angela Morris, Dr. Laura Fontanes for technical assistance and expertise in live imaging, fluorescent dye injection, and their generosity in sharing equipment and reagents.

I thank all of my fellow graduate students in my cohort, in particular Jennifer McDaniels, Dr. Ryan Grippo, Dr. Yunlu Zhu, Kerry Micheals, and Dr. Cory Weller for spiritual and technical support during graduate school.

I thank my family for emotional and financial support for the completion of my PhD.

I thank Dr. Ryan Grippo, Dr. Susan Doyle, Dr. Sarah Kucenas and Dr. Barry Condron for insightful comments of this dissertation.

Last but not least, I thank the taxpayers for putting their hard-earned money in support of this research.

Throughout Chapter II, the names of specific co-authors that have made a significant contribution to the research are highlighted in bold.

List of Abbreviations

HSC: hematopoietic stem cell

SVZ: subventricular zone

VZ: ventricular zone

V: ventricle

SGZ: subgranular zone

NSC: neural stem cell

ISC: intestinal stem cell

MSC: mesenchymal stem cell

GSC: germline stem cell

IML: inner molecular layer

GCL: granular cell layer

GC: mature granular cell

IGC: immature granular cell

RA: radial astrocyte

IPC1: intermediate progenitor 1

IPC2: intermediate progenitor 2

NB: neuroblast

OL: optic lobe

GMC: ganglion mother cell

SPG: subperineurial glia

PEDF: pigment epithelium-derived factor

Dlp: Dally-like

Gbb: Glass bottom boat

AD: Alzheimer's disease

T2DM: type II diabetes mellitus

VEGF: vascular endothelial growth factor

HIF-1α: hypoxia-inducible transcriptions factors α

ESC: embryonic stem cell

CSF: cerebral spinal fluid

BBB: blood-brain barrier

UAS: Upstream activating sequence

PI3K: PI3-Kinase

InR: Insulin receptor

GFP: Green fluorescent protein

RFP: Red fluorescent protein

Dpn: Deadpan

Scrib: Scribble

Dilp-1: *Drosophila* insulin-like peptide 1

Dilp-2: *Drosophila* insulin-like peptide 2

Dilp-3: *Drosophila* insulin-like peptide 3

Dilp-4: *Drosophila* insulin-like peptide 4

Dilp-5: *Drosophila* insulin-like peptide 5

Dilp-6: *Drosophila* insulin-like peptide 6

Dilp-7: *Drosophila* insulin-like peptide 7

Dilp-8: *Drosophila* insulin-like peptide 8

IPC: insulin producing cells

Imp-L2: Ecdysone-inducible gene L2

IGF: insulin-like growth factor

IGFBP: insulin-like growth factor binding proteins

CB: central brain

VNC: ventral nerve cord

CNS: central nervous system

PNS: peripheral nervous system

FB: fat body

FH: freshly hatched

SOG: subesophageal ganglion

DIC: Differential interference contrast

APF: after pupal formation

Table of Contents

Chapter I

General Introduction

Stem Cell Quiescence

Stem cells divide to self-renew and generate specialized daughter cells that make up a complex variety of tissues and organs in metazoans (1,2). Beyond their role in early development, stem cells also respond to injury, and repair damage to maintain tissue homeostasis (3). In order to maintain stemness, the ability to self-renew and differentiate into different cell types (4), stem cells utilize a dormancy strategy termed quiescence, where they cease proliferation but actively maintain their potential to remain undifferentiated (5). Precocious exit from quiescence can lead to premature differentiation and subsequent stem cell pool depletion (6). Proliferating eukaryotic cells go through four phases of the cell cycle, G1 (gap1), S (synthesis), G2 (gap2) and M (mitosis) (7). When intrinsic or extrinsic mechanisms instruct stem cells to enter quiescence, they exit the cell cycle at G1 phase and enter a G0 quiescent phase (Figure 1) (5,8). Recent studies have demonstrated heterogeneity of the quiescence state where some quiescent stem cells undergo cell cycle arrest at G2 (9–11). This heterogeneity is further demonstrated by certain quiescent stem cells exhibiting a “deeper” quiescent state with a higher reactivation threshold of growth factors (8,10,12). Quiescence is distinct from terminal differentiation of cells and senescence because it is reversible (13).

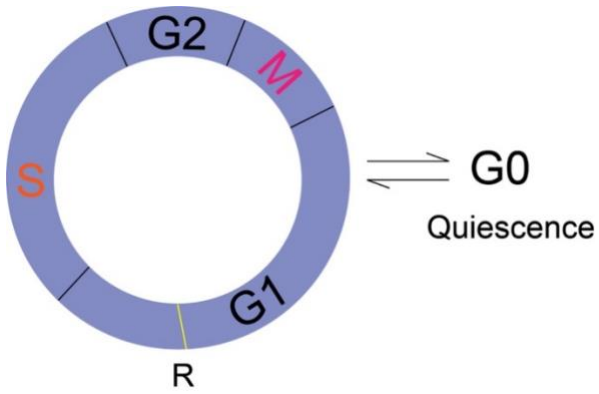

Figure 1. Quiescence is a reversible state. The cell cycle is comprised of S, G2, Mitosis and G1 phase. Stem cells can exit cell cycle during G1 phase before reaching the restriction point (R), and enter the G0 quiescence phase. Adapted from Rumman et al. (5)

Quiescence is also an evolutionarily conserved phenomenon that occurs in a wide range of organisms (13–16). Lower phylogenetic organisms often utilize quiescence for self-preservation against harsh environments. *C. elegans* and bacteria enter a resting phase with suppressed metabolism and cell cycling rate in response to harsh environmental challenges such as high temperature and scarce food supply (16). The conservation also occurs at the molecular level, since nuclear FOXO is required for both *C. elegans* dauer, a hibernation state for *C. elegans*, and mammalian hematopoietic stem cell (HSC) quiescence (15). Stem cell quiescence has been described and studied in many stem cell models (13). In rodents, quiescence protects HSCs in the adult bone marrow from accumulation of genetic mutations, and maintains HSCs' capacity to replenish blood cells

throughout adulthood (8). In adult murine brains, a pool of adult neural stem cells (NSCs) is maintained in the subventricular zone (SVZ) and subgranular zone (SGZ) of the hippocampus, and generates neurons, astrocytes and oligodendrocytes (Figure 2) (17–20). NSCs in these two regions maintain their stemness through entry and exit from quiescence (21). Mis-regulation of quiescence will lead to early differentiation of NSCs, and depletion of the stem cell pool (22,23). The existence of quiescent NSCs is promising for therapeutic repair of the aging brain, but because of the lack of clear molecular markers for quiescent NSCs and other technical challenges of human studies, it remains a debate whether adult NSCs exist in humans, leaving the exact regenerative capacity of the human brain a mystery (24–26)

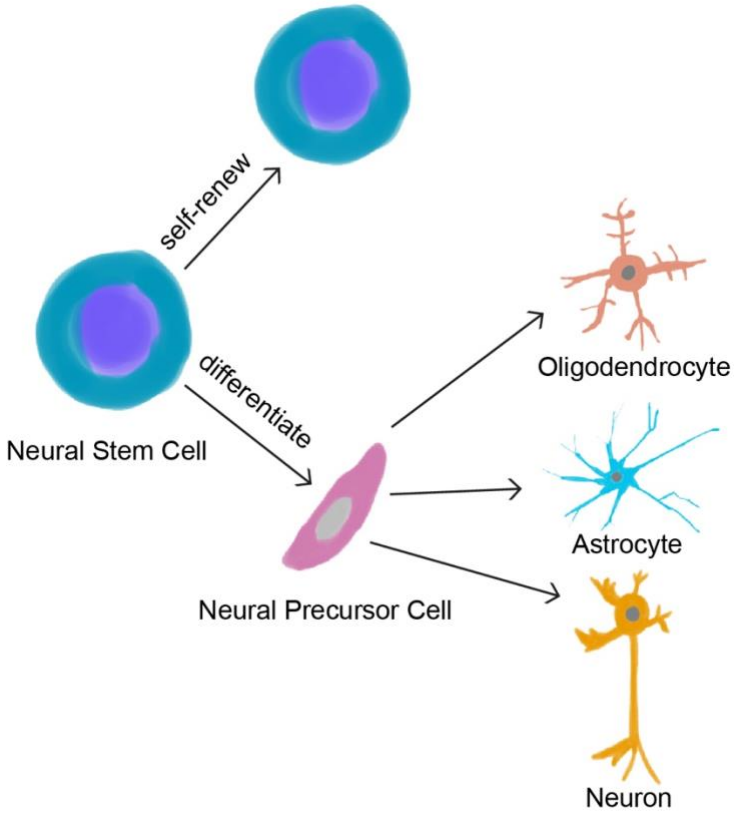

Figure 2. Neural stem cell self-renewal and differentiation. NSCs undergo asymmetric cell divisions to self-renew, and produce a more differentiated neural precursor cell that will then in turn generate more specialized cells such as oligodendrocytes, astrocytes and neurons. Adapted from (27).

Dietary Nutrients and Stem Cells

Regulation of stem cell proliferation, differentiation and maintenance is tightly linked to dietary nutrients (28). During development, poor maternal nutrition results in stunted growth of offspring (29). Dietary nutrients regulate stem cell homeostasis in both children and adults. Bone formation requires a constant supply of nutrients as inadequate nutrition will lead to bone loss and subsequent bone damage associated with osteoporosis (30). Mesenchymal stem cells (MSCs) require proper

nutrients for osteogenic differentiation (31). Researchers have shown that MSCs in obese mice display impaired osteogenic and chondrogenic potential (32). In muscle tissues, dietary restriction improves the regeneration capacity of the muscle stem cells. In addition, transplant experiments reveal that donor muscle stem cells from normal fed mice engraft more productively during calorie restriction in the recipient mice (33). Nutrient regulation of these two stem cell models is critical for maintenance of proper stem cell functions.

In the intestinal epithelium, both rapid cycling and quiescent intestinal stem cells (ISCs) are present to maintain intestinal tissue homeostasis (34). When ISCs enter a state of quiescence, they are protected from environmental insults through maintenance of quiescence by PTEN (a tumor suppressor, and phosphatase of PIP_3) expression (35). Rapid cycling ISCs are sensitive to environmental insults such as nutrient deprivation and fail to cycle in these conditions (36,37). When nutrient availability is restored, quiescent ISCs reactivate through release of PTEN inhibition, and activation of the nutrient sensing PI3K/AKT/mTOR signaling pathway to regenerate the intestine (35).

Calorie restriction creates a more favorable stem cell niche that keeps ISCs in a poised state to maintain the stem cell pool. Calorie restriction also reduces mTORC1 signaling in ISC niche cell called Paneth cells, and induces expression of bone stromal antigen 1 which strengthens the proliferation of the ISCs (38). Having both rapid cycling ISCs and quiescent ISCs with divergent cellular responses to changes in nutrient status ensures fast tissue regeneration, and prevents premature exhaustion of the stem cell population (34).

The highly conserved InR/PI3K/AKT nutrient-sensing pathways are readily accessible to study in *Drosophila* stem cell models by using timed feeding assays. Nutrient sensing occurs through either direct binding of particular nutrients such as amino acids, lipids and carbohydrates to the sensor, or through indirect molecular expression such as insulin, that gauges nutrient levels (39). There are 8 *Drosophila* insulin-like peptides (Dilps) that have been identified (40). Dilp 1-6 are homologs of insulin/IGF. Dilp 1-5 resembles insulin, and *Dilp6* resembles IGF base on sequence homology (41). Dilp7-8 resemble relaxin, a hormone that effects the female reproductive system and pregnancy (42)(43,44). Dilp 1-7 are typically thought to be able to signal through the insulin receptor (InR) (43). With powerful genetic tools, how the nutrient sensing insulin signaling pathway regulates stem cell proliferation in flies remains an important and accessible area of study.

The *Drosophila* germline stem cell (GSC) niche is a well characterized niche model system with respect to its response to dietary nutrients. When starved of protein, GSCs reduce proliferation and ultimately are lost (36). However, activated insulin signaling in the niche cells is able to maintain a small pool of GSCs in response to starvation (36). Proliferation and quiescence of *Drosophila* NSCs, neuroblasts (NBs), are also nutrient regulated (45–48). Understanding how dietary nutrients regulate stem cell proliferation, quiescence and stem cell niche function is crucial for therapeutic considerations of stem cells' regenerative capacity, and ultimately improving animal well-being and life span.

Drosophila Neuroblast Entry and Exit from Quiescence

Drosophila NBs share functional homology to mammalian NSCs and generate various neuron subtypes that are essential for circuit formation (49). NBs are specified during early embryogenesis, and undergo reductive cell size divisions to generate neurons and glia that make up a functional early larval brain (50). At the end of embryogenesis, NBs enter a period of quiescence through expression of a series of spatial Hox proteins and temporal identity factors (51). A subset of NBs, called mushroom body NBs, and a lateral NBs, never enter quiescence and maintain proliferation (45,46). Activated Hippo signaling maintains NBs in quiescence through inhibition of the transcriptional factor Yorki. Intercellular transmembrane proteins Crumbs and Echinoid in both NBs and neighboring glial cells modulate Hippo signaling to inhibit reactivation (52). In the optic lobe (OL), glia neighboring the OL NBs also secrete a glycoprotein, anachronism, to inhibit OL NBs from reactivation from quiescence (53,54). *Drosophila* perlecan, Trol, activates OL NBs from quiescence (53). When larvae hatch and begin feeding, dietary amino acids signal through the fat body, a white adipose tissue and liver equivalent organ in *Drosophila*, which sends an unknown fat body-derived signal (FDS) to the central nervous system (CNS) (45,48,55). The subperineurial glia (SPG) of the blood-brain barrier (BBB) then secrete *Drosophila* insulin-like peptide 6 (Dilp6) via calcium pulses of the gap junctions between the SPGs (56), and activate InR/PI3K/AKT signaling pathways in the NBs to reactivate quiescent NBs (Figure 3) (48,55,56). Dilp-6 has also been shown to drive cortex glial growth in the ventral nerve cord via activation of PI3-K signaling in response to dietary

nutrients (57). STRIPAK members act as an intrinsic molecular switch to coordinate Hippo and InR pathways (58).

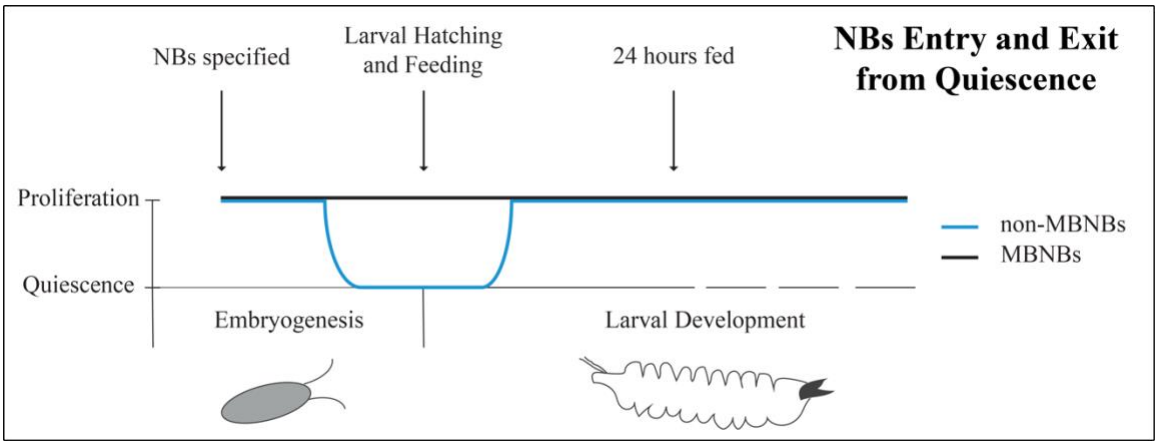

Figure 3. Schematic of NB entry and exit from quiescence.

Much of the known model describing NB entry and exit from quiescence focuses on the NBs in the thoracic region of the ventral nerve cord (VNC) where NBs are in close contact with the BBB, and the SPGs make up the neurovascular niche of the NBs in the VNC (59). Whether 1) the central brain (CB) shares the same NB niche cytoarchitecture as the VNC, 2) whether the niche cytoarchitecture establishment is nutrient-responsive, and 3) whether NB reactivation requires niche establishment remain unclear.

Neural Stem Cell Niche in Mammals and Flies

Adult neural stem cell niche in the mammalian subventricular zone

Stem cells self-renew and produce differentiated progenies in a highly specialized, three-dimensional architecture, termed the stem cell niche (1,60). Proper interaction between niche cells and stem cells is important for maintaining stem cell multipotency. The mammalian subventricular zone (SVZ), and subgranular zone (SGZ) are among the most well-studied adult neurogenic niches. In the SVZ of rodents, quiescent and activated neural stem cell (NSC) Type-B1 cells interact with a diverse group of cells that comprise the neurogenic niche including; astrocytes, pericytes, neuroblasts, post-mitotic neurons, intermediate progenitors (INPs), ependymal cells, and endothelial cells of the vasculature (Figure 4A) (61). Researchers have characterized the SVZ neural stem cell-niche interaction using both in *vitro* and in *vivo* methods. Astrocytes derived from neurogenic regions promote neuronal fate commitment of the neural stem cells in culture (62). Ependymal cells induce astrocyte fate via secretion of Noggin, and promote self-renewal of the neural stem cells through secreting pigment epithelium-derived factor PEDF (63). The apical side of the Type-B1 stem cell reaches through the pinwheel shaped ependymal cells and contacts the cerebral spinal fluid (CSF); basally, Type-B1 stem cells' end feet are in contact with endothelial cells of the blood vessels (64). Through contact of the ependymal cells, NSCs also have access to the cytokines and growth factors in the CSF (65). Through contact with the endothelial cells of the vasculature, quiescence of Type-B1 cells is regulated through Notch and Ephrin signaling (66). The presence of cytokines and growth factors in the CSF, and the frequency of contact with endothelial cells both

influence neural stem cell proliferation (64,67). Interactions with a multitude of niche cells enable Type-B1 stem cells to integrate various inputs from their surrounding environment.

Adult neural stem cell niche in the mammalian subgranular zone

In the dentate gyrus of the hippocampus, radial astrocytes (RAs), the neural stem cells, contact cells present in the granular cell layer (GCL) and inner molecular layer (IML) via the long shafts of their polarized cell bodies (Figure 4B) (68). RAs interact with; blood vessels, neighboring RAs, intermediate progenitor cells, granular cells, and other glial cells, axons and synaptic terminals in the inner molecular layer (69). RAs are intimately associated with endothelial cells and blood vessels on the Hillus side (69). In the SGZ, neurogenesis and angiogenesis co-occur, possibly through vascular endothelial growth factor (VEGF), promoting neural progenitor proliferation (70). Overexpression of Noggin, which is normally expressed in granular cells, the hillus and the RAs, increases RA proliferation (71). Similar to SVZ Type B1 cells, RAs in the SGZ present an exceptional stem cell model that interacts with various niche cells across several domains. Altogether these studies demonstrate the importance of identifying the necessary components that constitute the cytoarchitecture of a stem cell niche. Understanding the stem cell niche cytoarchitecture is essential to decipher the regulation of stem cell proliferation and advance stem cell therapy.

Drosophila neuroblast stem cell niche

With available genetic tools and makers, and ease of feeding assays, *Drosophila* neuroblasts (NBs), are a great model system to study the neurogenic niche and

nutrient regulation of stem cell proliferation and niche development. *Drosophila* NBs reside in a much simpler stem cell niche compared to their mammalian counterpart. In the central brain (CB), *Drosophila* NBs are in direct contact with both cortex glia and NBs' new-born daughters, ganglion mother cells (GMCs) (Figure 4C and Figure 5) (72–74). NBs utilize activated PI3K to build an adhesive niche between themselves, cortex glia and their GMCs (72). Cortex glia are thought to functionally mimic mammalian astrocytes (75), and are considered the niche glia that provide support for NBs (57). In the thoracic region of the ventral nerve cord (VNC), NBs also make contact with the subperineural glia (SPG) (55,59). Blood-brain barrier (BBB) glia, specifically the SPGs, provide a barrier between the CNS and the hemolymph through formation of tight junctions with one another (76), similar to mammalian endothelial cells (59,77). The SPGs are implicated in NB exit from quiescence (55,56). Aside from cortex glia and the SPGs, the most outer layer of the BBB, comprised of perineural glia, instructs NB proliferation at third instar larval stage through expression of Dally-like (Dlp), a heparan sulfate proteoglycan, and Glass bottom boat (Gbb), a BMP homolog (78). The functionally analogous cell types in the brain of *Drosophila* and mammals present an advantage to study neural stem cell niche regulation of neural stem cell quiescence in a much simplified system.

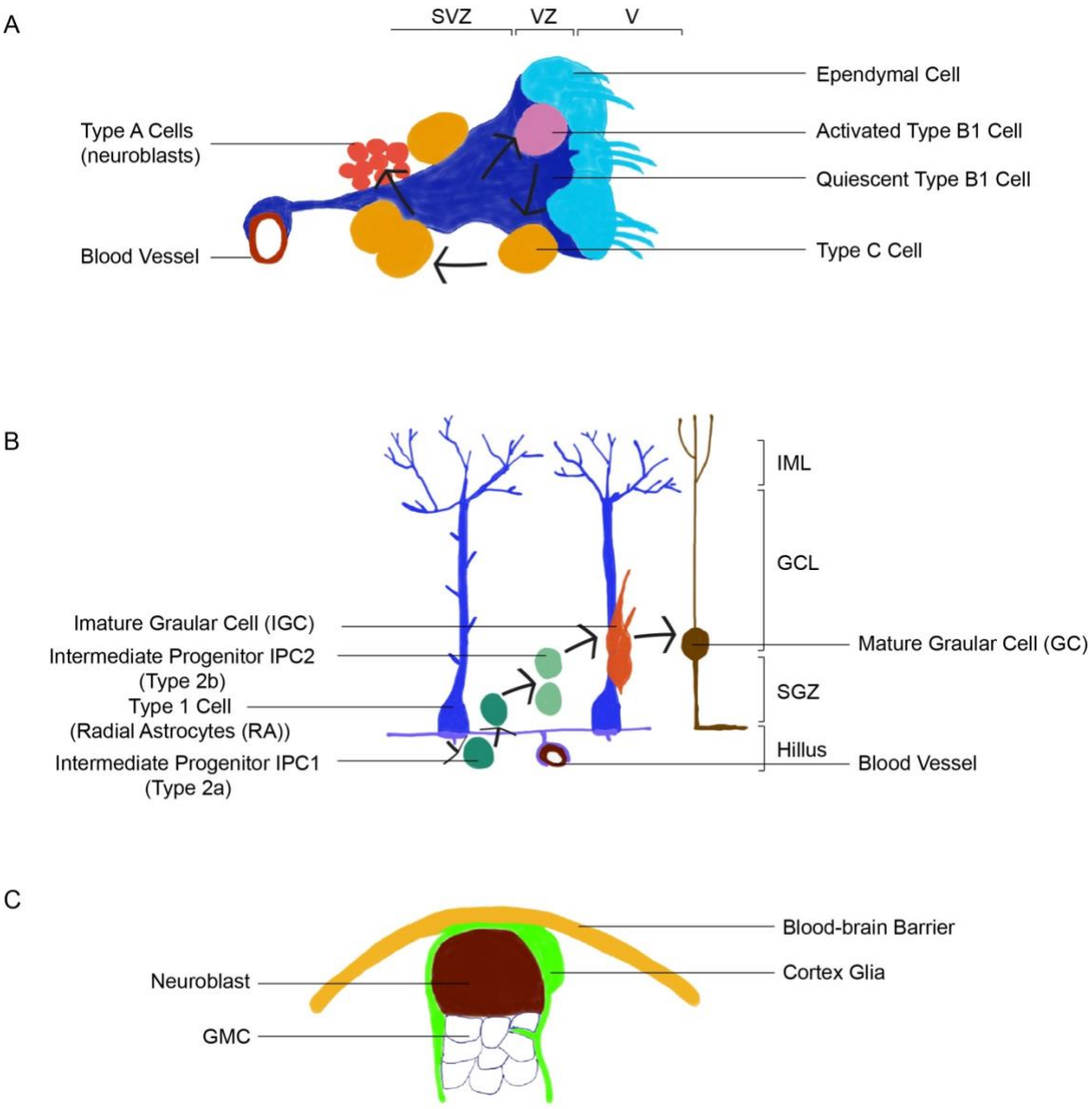

Figure 4. Neural stem cell niche in rodent SVZ, SGZ and *Drosophila* CB.

(A). Simplified version of adult neurogenic niche in the SVZ. Arrows denote the NSC differentiation path. Type B1 cell: NSCs. Type C cell: transient amplifying progenitor. (B). Simplified version of adult neurogenic niche in the SGZ. Arrows denote the NSC differentiation path. IML: inner molecular layer. GCL: granular cell

layer. (C). *Drosophila* NB stem cell niche. A and B adapted from Fuentealba et al., 2012 (69).

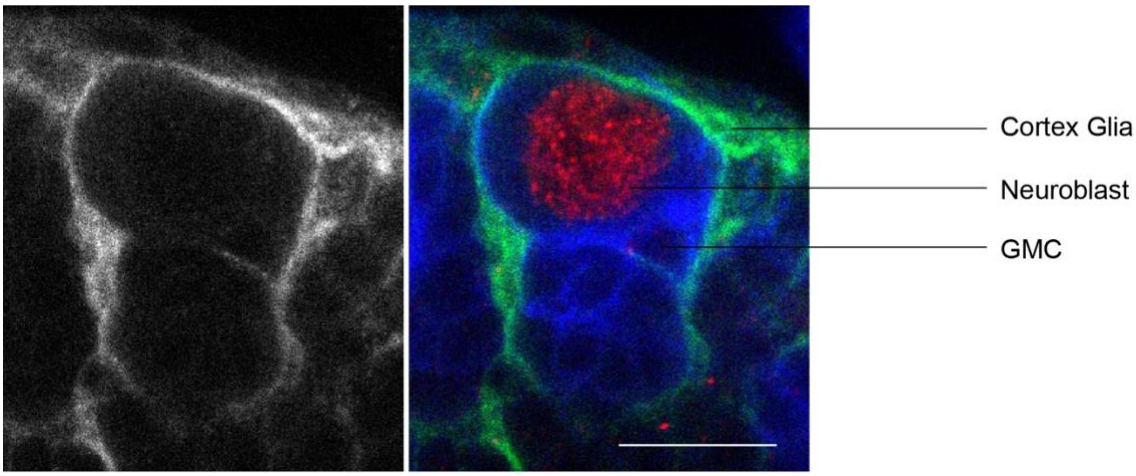

Figure 5. Neuroblasts reside in glial cells. Image shows a single Z plane. Greyscale channel on the left. demonstrates glial niche morphology. Merged channel image on the right. Developmental stage: 72 hours after larval hatching.

Roles of Oxygen in the Stem Cell Niche

Oxygen availability is an important component of the stem cell niche that influences stem cell proliferation and differentiation fate (79). Human embryonic stem cells (ESCs) differentiate under an ambient oxygen concentration of around 21% 0_2 (80). Oxygen concentration *in vivo* is often much lower than ambient air. It is well accepted that the physiological normoxia is 2% - 9% 0_2 (81). A higher physiological concentration of oxygen helps ESCs maintain proliferation as well as differentiate (80). Oxygen tension in the brain can be as low as 1% (81). In the rodent SVZ, lower oxygen tension maintains neural stem cells in quiescence and helps them maintain their multipotency through induction of VEGF by hypoxia-inducible transcriptions factors α (HIF-1α) (82,83). In addition, angiogenesis and intermediate progenitor cell proliferation co-occur in mice (84). The evidence demonstrates that oxygen is an important component of the neurogenic niche (67).

Tissue specific oxygen concentration is highly dependent on vascularization (79). In insects, trachea is the gas exchange organ that delivers oxygen throughout the insect body through diffusion (85). A single tracheal branch enters the central brain from the medial side of the brain hemisphere and infiltrates the brain (86). It is possible that the *Drosophila* cerebral trachea is part of the NB stem cell niche, and supplies oxygen to NBs, glia and neurons for cellular respiration (87). Further understanding of the precise role that oxygen plays in the neurogenic niche is important for studying recovery from hypoxic brain injuries.

Source of Insulin in the Brain and Implications

Insulin receptor is widely expressed in a variety of cells in the brain, demonstrating the brain's capacity to respond to insulin/IGF signaling (88,89). Insulin/IGF signaling regulates neuronal development, energy homeostasis, cognitive function, mood, learning and memory (88,90,91). Understanding how brain cells respond to insulin, and how insulin is delivered to those cells is important for understanding normal brain development and therapeutic considerations in neurodegenerative disorders. Insulin is produced both peripherally in the pancreatic β cells, and locally in the brain (90). The majority of insulin present in the brain enters through active transport across the blood-brain barrier (90,92–94). Evidence of local insulin production in the brain includes the detection of insulin mRNA in the brain of rabbits (95). Recent evidence shows that GABAergic "neurogliaform" cells, located in the rodent cerebral cortex are also capable of producing insulin (96,97). Regardless of the origin, insulin/IGF signaling plays an important role in neurogenesis. In rodents, IGF-I induces neural stem cell proliferation in the striatum (98), and IGF-II promotes stemness of neural stem cells in the SVZ neurogenic niche (99). In these studies, the origin of the IGF remains unclear, as the experimental approaches relied on *in vitro* culture of neural progenitors, or peripheral infusion of IGF (99–102). In *Drosophila*, glial derived local source of *Drosophila* insulin-like peptide 6 (Dilp-6) in the CNS has been shown to activate insulin signaling of neural stem cells in response to dietary nutrients (48,55). Utilizing *Drosophila* as a model organism will further our understanding of the source of insulin/IGF that promotes neurogenesis.

There has been a rapid growth of literature on the correlation of neurodegenerative disorder such as Alzheimer's disease (AD) with insulin resistance. AD has also been referred to as "Type III" diabetes because of increased insulin resistance with decreased insulin and insulin receptor expression level observed in the AD patient brain (103,104). Reduction in circulating insulin contributes to AD pathogenesis, while improvements in cognitive function have been demonstrated following intranasal insulin treatment (105). Type 2 diabetes mellitus (T2DM) is also associated with cognitive deficits, and an increased risk of neurodegenerative dementias (104). Understanding the balance of insulin levels in the brain and in the periphery, and how local versus systemic insulin regulates neurogenesis may shed light on the pathogenesis of neurogenerative disease and diabetes.

In this dissertation, I aim to address the biological process of how dietary nutrients regulate NB reactivation from quiescence through the establishment of NB stem cell niche cellular architecture. Furthering our understanding of this process is important because nutrient regulation of neural stem cell niche development is under appreciated, and proper functional neural circuit establishment may not occur if NB reactivation fails to occur on time. I sought to answer the following questions: 1) What is the NB stem cell niche? 2) Is niche development nutrient-responsive? 3) Is NB niche development required for NB reactivation? 4) Is NB reactivation required for NB niche development? 5) Are the *Drosophila* insulin-like peptides required for NB reactivation and niche development? If so, which Dilp? 6) Lastly, what are the cellular sources of insulin that reactivate quiescent NBs? I address these knowledge gaps in this dissertation using elegant genetic tools available in *Drosophila*, confocal microscopy of fixed and live brains, and other molecular biology techniques. We were able to characterize growth morphology of various cell types using cell-type specific fluorescent expression. We also uncovered functional requirements of various cell types that are required to reactivate quiescent NBs. This work represents the first thorough investigation of NB stem cell - niche interactions in response to dietary nutrients, and uncovered a possible role of circulating insulin in neurogenesis.

Chapter II

Dilp-2 mediated PI3-kinase activation coordinates reactivation of quiescent neuroblasts with growth of their glial stem cell niche

In review as a research article in *PLOS Biology* 10/3/2019

Xin Yuan, Conor W. Sipe, Miyuki Suzawa, Michelle L. Bland, Sarah E. Siegrist

Abstract

Dietary nutrients provide macromolecules necessary for organism growth and development. In response to animal feeding, evolutionarily-conserved growth signaling pathways are activated, leading to increased rates of cell proliferation and tissue growth. It remains unclear how different cell types within developing tissues coordinate growth in response to dietary nutrients and whether coordinated growth of different cell types is necessary for proper tissue function. Here, we report that Drosophila neural stem cells, known as neuroblasts, reactivate from developmental quiescence in a dietary nutrient-dependent manner. Neuroblast reactivation requires non-cell autonomous activation of PI3-kinase signaling from cortex glia and tracheal processes, both of which are closely associated with neuroblasts. Furthermore, PI3-kinase activation in neuroblasts is required non-cell autonomously for glial membrane expansion and robust neuroblast-glial contact. Finally, PI3-kinase is required cell autonomously for nutrient-dependent growth of neuroblasts, glia, and trachea. Of the seven Drosophila insulin-like peptides (Dilps), we find that Dilp-2 is required for PI3-kinase activation and growth coordination between neuroblasts and glia. Dilp-2 induces cortex glia to initiate membrane growth and make first contact with quiescent neuroblasts. After contact,

neuroblasts increase in size and reenter S-phase. Once reactivated from quiescence, neuroblasts promote growth of cortex glia which in turn form a selective membrane barrier around neuroblasts and their newborn progeny. Our results highlight the importance of bi-directional growth signaling between neural stem cells and surrounding cell types in response to nutrition and demonstrate how coordinated growth among different cell types drives tissue morphogenesis and function.

Introduction

Organs must be appropriately sized and patterned to function properly and meet physiological needs of adult animals. To achieve proper organ size and function, a multitude of different cell types are produced over time and space. Yet, it remains unclear how different cell types with different molecular programs integrate their own growth with growth of their nearby neighbors, some of which have different developmental origins. This is particularly true for stem cells, many of which reside within specialized microenvironments composed of many different cell types. Hormones and other secreted growth factors and cytokines have clear and important roles in growth regulation from the single cell to tissue level and beyond (106–111). What is less understood is whether local growth decisions are coordinated in response to nutrient availability, what regulatory networks coordinate local growth, and whether coordinated growth is required for tissue function. Dietary nutrients also play important roles in growth regulation, as they provide the building blocks for biosynthesis of macromolecules (lipids, proteins, and nucleic acids) and serve as co-factors used in metabolic reactions.

Here we investigate how growth occurs in the Drosophila brain in response to dietary nutrients during development. In Drosophila, nutrient sensing pathways, including insulin/ phosphatidylinositol 3-kinase (PI3-kinase) and target of rapamycin (TOR)-kinase, are evolutionarily conserved, and genetic tools for cell type-specific manipulation of gene function are available (112–114). The Drosophila brain is well-suited for investigating how growth is regulated and coordinated among different cell types in response to dietary nutrients, because it contains a multitude of different cell types, including a heterogenous population of neural stem cells and progenitors, a diverse array of specialized glia, different neuron subtypes including neurosecretory neurons, and a tracheal network of branched epithelial tubules for oxygen exchange. Furthermore, in Drosophila, the time when animals receive their first dietary nutrients can be precisely controlled, and growth of molecularly- and functionally-distinct cell types assayed over time using available markers. Better understanding of how dietary nutrients regulate brain growth and development is fundamentally important given the incidence of human neurodevelopmental disorders and defects associated with poor nutrient quality and/or limited nutrient availability (101,115–118).

Drosophila receive their first dietary nutrients after consuming their first meal as freshly hatched larvae, which occurs about 22 hours (at 25˚C) after fertilization following completion of embryogenesis. Dietary amino acids stimulate TOR-kinase pathway activity in the fat body, a lipid storage organ with endocrine function similar to the mammalian liver (119,120). In response to dietary nutrients, fat body derived signals (FDS) are synthesized and secreted into the circulating

hemolymph, which stimulates tissue growth systemically (45,48,120–123). Sub-perineural (SPG) glia, a glial subtype that encapsulates the brain and ventral nerve cord to form a blood brain-like barrier, respond to the FDS by synthesizing and secreting Drosophila insulin-like peptide 6 (Dilp-6) locally within the brain (48,55,124). Local Dilp-6 activates the PI3-kinase pathway in neural stem cells, known as neuroblasts in Drosophila, leading to increased growth and their reactivation from developmental quiescence (48,55). This is the current model for how dietary nutrient conditions regulate neuroblast reactivation from developmental quiescence. What is lacking is a better understanding of how other cell types within the brain grow in response to dietary nutrients, whether their growth is coordinated in response to dietary nutrients, and whether their growth is required for neuroblast reactivation. Stem cells generally reside within specialized microenvironments, referred to as niches, that support and insulate them from outside factors (60). These specialized microenvironments integrate local and systemic cues to control stem cell proliferation decisions, cues that inform on nutrient status, tissue physiology and function, and perhaps even developmental time.

Here, we report, that in addition to neuroblast reactivation from developmental quiescence, animal feeding also initiates growth of glia and trachea. Moreover, growth of all three cell types occurs continuously and concomitantly, suggesting that common nutrient-sensing pathways regulate and coordinate growth among the different cell types in response to nutrition. We find that Drosophila insulin-like peptide 2 (Dilp-2) mediates PI3-kinase activation in

neuroblasts and glia, and that Dilp-2 mediated PI3-kinase activity is required to coordinate growth of neuroblasts with development of their cortex glia niche. Cortex glia, a subset of brain glia, ensheathe neuroblasts and their progeny with a selective membrane that provides barrier function to protect neuroblasts and their progeny from outside factors. Furthermore, we find that Dilp-6 is dispensable for neuroblast reactivation from quiescence, as well as growth of glia and trachea in the brain, compensated for by high dilp2 transcript and protein levels in response to feeding. This work highlights the importance of bi-directional signaling among different cell types in response to nutrition and sheds light on how dietary nutrients coordinate growth among different cell types within the developing Drosophila brain.

Results

Neuroblast reactivation from quiescence, glial growth, and tracheal morphogenesis are nutrient-regulated

To better understand how cell growth is coordinated with tissue growth in response to dietary nutrients, we assayed proliferation and growth rates of different cell types in the Drosophila brain in response to animal feeding. Freshly hatched larvae were fed a standard fly food diet for defined periods of time (4, 12, 16, 20, or 24 hours), and growth and proliferation of neuroblasts, glia, and trachea was assayed in the brain (Figure 1). Fly food was supplemented with EdU to assay S phase entry, and size was measured based on the average diameter of neuroblasts or total membrane surface area for glia and trachea (see Materials and Methods for details). After 4 hours of animal feeding, we observed that the four mushroom body

neuroblasts (MB neuroblasts, white arrows) and one lateral neuroblast were dividing based on their incorporation¬ of EdU and generation of EdU-positive progeny (Figure 1A,G,L). In contrast, the other central brain neuroblasts (~100 per brain hemisphere), referred to as non-MB neuroblasts, failed to incorporate EdU during this time (Figure 1A,G,L). EdU-positive MB and lateral neuroblasts were larger than the EdU-negative, non-MB neuroblasts, but all expressed the HES1 orthologue, Deadpan (Dpn), a pan-neuroblast marker (Figure 1B,C). After 12 hours of feeding, a few non-MB neuroblasts incorporated EdU, and EdU incorporation correlated with increased neuroblast size (Figure 1F,H,L). Over time, the fraction of EdU-positive, non-MB neuroblasts continued to increase, and at 24 hours, more than 60% of non-MB neuroblasts were EdU-positive (Figure 1D,I,J,L). Similar to earlier time points, EdU-positive non-MB neuroblasts were larger than EdU-negative non-MB neuroblasts (Figure 1F). To confirm that increases in neuroblast size and S-phase entry are nutrient-regulated, we fed animals a sucrose-only diet for 24 hours. Consistent with previous reports, no neuroblasts other than the four MB neuroblasts (white arrows) and the lateral neuroblast incorporated EdU (Figure 1E,K,L), and non-MB neuroblast size was reduced compared to both EdU-positive and -negative non-MB neuroblasts from 24 hour fed animals (Figure 1F). We conclude that neuroblasts reactivate from developmental quiescence in response to animal feeding and that reactivation occurs stepwise. Neuroblasts grow in size first and subsequently re-enter S phase and begin generating new progeny. This conclusion is in agreement with previously published work (45,46,48,55,125),

Next, we asked whether growth of other cell types within the brain is also nutrient-regulated. Nutrient-dependent growth of other cell types, including niche-like cortex glia, could play a role in regulating neuroblast reactivation from quiescence and contribute to the substantial increases in brain size observed after 24 hours of animal feeding (~1.76X, S1A Figure). After 24 hours of feeding, we found ~45% glia, identified based on expression of the homeodomain transcription factor Repo, incorporated EdU (S1B,C Figure). This was unexpected and suggested that either new glia are being produced or that existing glia endoreplicate in response to feeding. To distinguish between these possibilities, we counted glia nuclei before animal feeding (0 hours fed, freshly hatched) and after 24 hours of animal feeding. We found ~95 Repo-positive glia per brain hemisphere before feeding and ~100 after feeding, suggesting that EdU incorporation is not followed by glial cell division (S1D Figure). Next, we expressed UAS-dupRNAi in glia (using repoGAL4) to inhibit DNA replication and block endoreplication (76). After 24 hours of feeding, essentially no dupRNAi expressing glia were EdU-positive (<1%, n=5 brain hemispheres), and glial number was unchanged compared to controls, indicating that glia endoreplicate in response to feeding (S1E,F Figure). Next, we expressed a membrane-tagged GFP in glia (repoGAL4, UAS-mCD8GFP) to assay glial surface area over time. Between 12 and 24 hours of animal feeding, glial membrane surface area increased nearly 3 fold (Figure 1M-P,Q). To determine whether glial membrane growth and S-phase entry are nutrient regulated, animals were fed a sucrose-only diet. After 24 hours, no EdU-positive glia or increases in glia membrane surface area were found,

demonstrating that glial membrane growth and S-phase entry are nutrient-regulated (Figure 1Q,R and S1C). We conclude that glia endoreplicate and their membrane surface area increases in response to dietary nutrients.

Next, we assayed growth of brain trachea in response to feeding. Trachea are a network of epithelial-derived tubules that supply oxygen and exchange gas throughout the animal. In the brain, during later larval stages, trachea extend along glia forming a peri-neuropilar tracheal plexus, analogous to cerebral vasculature in mammals (86). During mammalian cortical development, intermediate neural progenitors divide near blood vessel branch points, suggesting that cerebral vasculature provides niche-like support, similar to Drosophila glia (126). To determine whether tracheal morphogenesis in the Drosophila brain is nutrient regulated, we assayed tracheal growth over time in response to feeding. Before animal feeding, a single tracheal branch enters the medial brain region (86). After 24 hours of feeding, we observed one to four EdU-positive tracheal nuclei, located at the base of secondary branches, in each brain hemisphere (S1G,H Figure), and we found an overall 3-fold increase in tracheal surface area (Figure 1S-V,X). Tracheal branching became more elaborate over time with brain hemispheres being infiltrated from the inside out in a stereotypic pattern. In contrast, when animals were fed a sucrose-only diet, no EdU-positive tracheal nuclei were observed and tracheal surface area and branching was reduced (Figure 1W,X and S1H). Together, we conclude that growth (S phase entry and size) of neuroblasts, glia, and trachea is nutrient-regulated. Moreover, growth of all three cell types

occurs continuously and concomitantly, raising the possibility that nutrient-sensing pathways coordinate growth among different cell types.

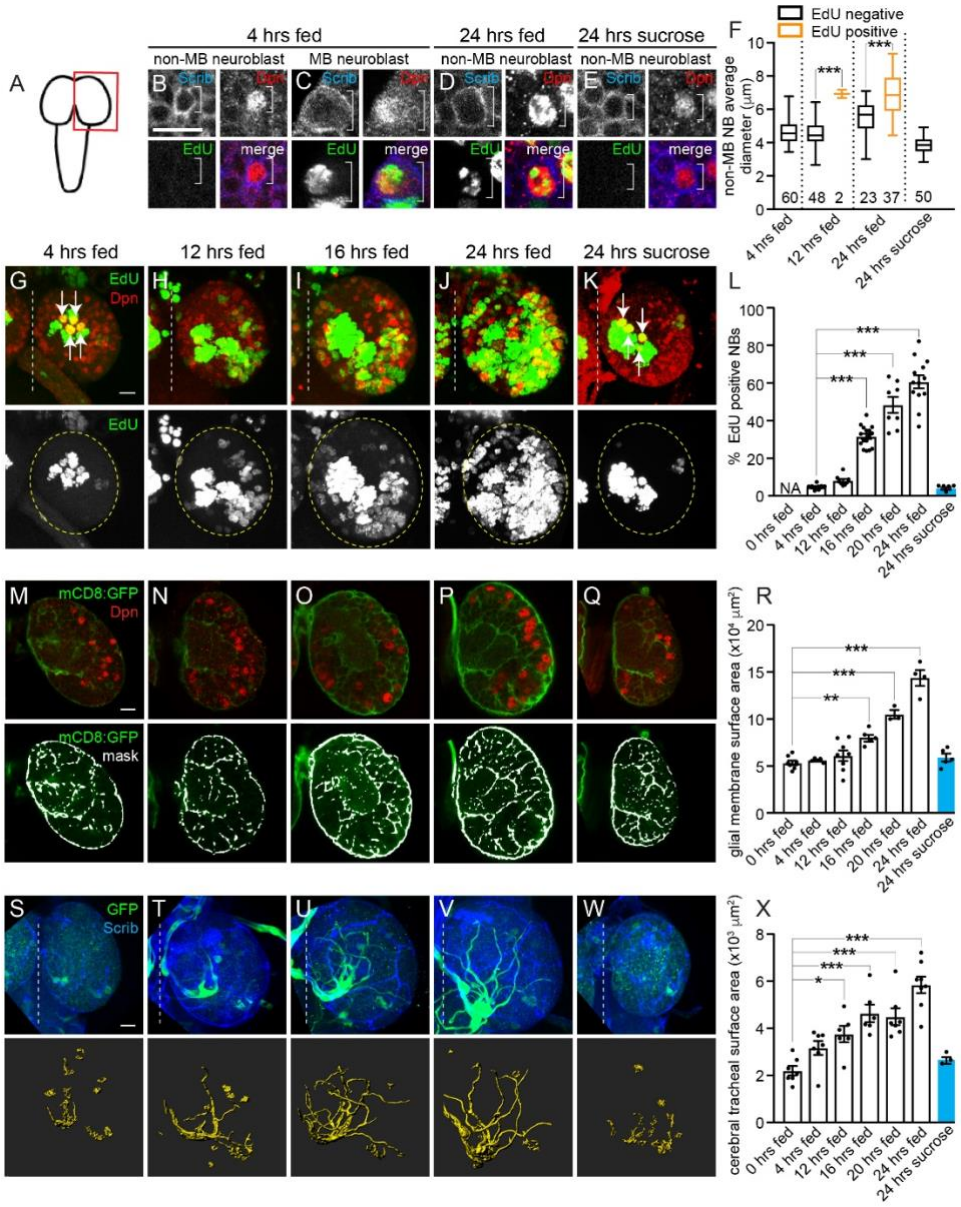

Figure 1. Neuroblast reactivation from quiescence, as well as glial and tracheal growth are nutrient-regulated.

(A) Larval brain cartoon with red box indicating the brain region imaged in this and subsequent figures. (B-E) Single confocal Z images of non-MB and MB neuroblasts (NBs), top and bottom left panels are single-channel grayscale images, with colored overlay, bottom right. Molecular markers are denoted within

panels and white brackets indicate NBs in this and all figures. (F) Box and whisker plots of NB diameter of EdU-negative (black) and EdU-positive (orange) NBs. The number of NBs analyzed is indicated below plots. Student's two-tailed t test, ***p<0.001. (G-L) EdU-positive NBs over time. (G-K) Maximum intensity projections of brain hemispheres. Top panels are colored overlays with single-channel grayscale images below. Brain hemispheres are outlined and the dotted vertical line indicates the midline. White arrows in (G,K) indicate MB neuroblasts. (L) Quantification of EdU-positive neuroblasts over time shown as scatter plots with dots representing individual brain hemispheres. Columns indicate mean and error bars indicate SEM in this and all subsequent figures. (M-R) Increases in glial membrane surface area over time in animals expressing mCD8:GFP using *repoGAL4*. (M-Q) Single optical sections of brain hemispheres. Top panels are colored overlays, and bottom panels are single-channel images with mask overlays used in quantification (R) of total glial membrane surface area over time (see Materials and Methods). (S-X) Cerebral tracheal morphology over time in animals expressing GFP using *btlGAL4*. (S-W) Maximum intensity projections of brain hemispheres with rendered trachea below and quantified in (X). (L,R,X) One-way ANOVA with Tukey's post hoc analysis, *p<0.05, **p<0.01, ***p< 0.001. (B,G,M,S) Scale bar equals 10 μm in this and all subsequent figures. Genotypes of panels listed in S5 Table.

Nutrient-dependent growth of neuroblasts, glia, and trachea requires cell autonomous and cell non-autonomous activation of PI3-kinase

Increases in cell growth in response to dietary nutrients are typically due to increased PI3-kinase pathway activity, an evolutionarily conserved growth signaling pathway that activates TOR kinase and other growth pathways(101,106,108,112,114). To determine whether PI3-kinase is required for nutrient-dependent growth of neuroblasts, glia, and trachea, we expressed UAS-dp60 to reduce PI3-kinase activity using cell type-specific GAL4 lines and assayed EdU incorporation (S2A-D Figure) and cell size or membrane surface area after 24 hours of feeding (Figure 2A-D) (127). When levels of PI3-kinase activity were reduced in neuroblasts (worGAL4, UAS-dp60), neuroblast EdU incorporation was reduced and neuroblast size reduced as previously reported (Figure 2B and S2A) (46,48,55). When levels of PI3-kinase activity were reduced in all glia (repoGAL4, UAS-dp60), EdU incorporation was essentially absent in glia and membrane surface area reduced (Figure 2C and S2B,C). Reduction of PI3-kinase activity in trachea (btlGAL4, UAS-dp60), eliminated EdU incorporation and tracheal surface area and branching were reduced (Figure 2D and S2D). Therefore, PI3-kinase is required for cell autonomous nutrient-dependent growth of neuroblasts, glia, and trachea.

To determine whether PI3-kinase is also required to coordinate growth among neuroblasts, glia, and trachea in response to nutrition, levels of PI3-kinase activity were reduced in one cell type (neuroblasts, glia, or trachea) alone and growth of the other two cell types was assayed. When PI3-kinase levels were

reduced in neuroblasts (worGAL4, UAS-dp60), a modest, but significant reduction in glial membrane surface area was observed after 24 hours of feeding (Figure 2E,F,H). To further support that neuroblast growth is required for glial growth, we expressed raptorRNAi in neuroblasts (worGAL4, UAS-raptorRNAi) to knock down TOR activity. Again, a significant reduction in glial membrane surface area was found after 24 hours of feeding (Figure 2E,G,H). Reductions in glial membrane surface area could be due to reductions in glia number, as some worGAL4-expressing neuroblast lineages generate glia. Indeed, glia number was reduced compared with controls in raptorRNAi knock down animals (worGAL4, UAS-raptorRNAi) but remained unchanged when PI3-kinase activity was reduced in neuroblasts (worGAL4, UAS-dp60) (Figure 2I). Next, we assayed tracheal surface area when levels of PI3-kinase activity were reduced. No change in tracheal surface area was detected (S2E-G Figure). We conclude that activation of PI3-kinase signaling in neuroblasts is required for glial membrane growth but not for growth of trachea.

Next, we reduced PI3-kinase activity in glia and assayed growth of neuroblasts and trachea. When PI3-kinase levels were reduced in glia (repoGAL4, UAS-dp60), significant reductions in both neuroblast EdU incorporation and neuroblast size were found after 24 hours of feeding (Figure 2J-M). Yet, tracheal surface area remained relatively unchanged compared to controls (S2H,I Figure). Finally, we reduced PI3-kinase activity in trachea and assayed growth of neuroblasts and glia. When PI3-kinase activity levels were reduced in trachea (btlGAL4, UAS-dp60), we found a modest, but significant reduction in neuroblast

EdU incorporation after 24 hours of feeding (Figure 2N,O), but no change in glia membrane surface area (S2J,K Figure). We conclude that activation of PI3-kinase signaling in glia and trachea both contribute to neuroblast reactivation, revealing that both cell types provide niche-like stem cell support. In addition, activation of PI3-kinase in neuroblasts is required for glial growth, but not tracheal growth (summary panel S2L Figure). Altogether, we conclude that PI3-kinase signaling functions in a cell autonomous and non-autonomous manner to coordinate growth among different cell types within the developing Drosophila brain.

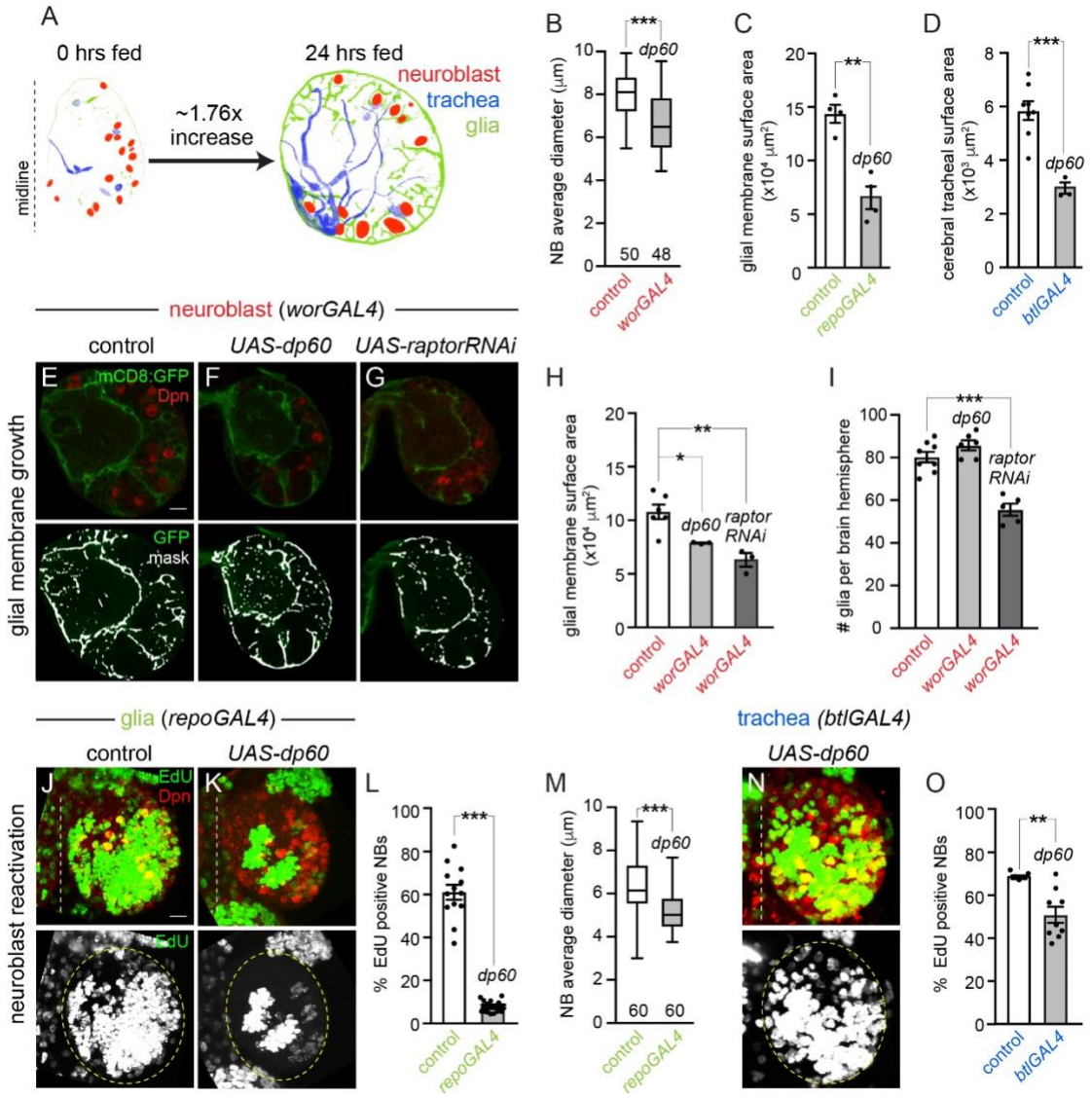

Figure 2. Nutrient-dependent growth of neuroblasts, glia, and trachea requires autonomous and non-autonomous PI3-kinase activation.

(A) Single Z images of segmented brain hemispheres with cell types colored as indicated. Quantification of NB size (B) **(Conor Sipe),** glial surface area (C), and tracheal surface area (D) per brain hemisphere from the indicated genotypes after 24 hours of feeding. (E-I) Glial membrane morphology and glial number at 24 hours after feeding in animals expressing dp60 or *raptorRNAi* in neuroblasts

and mCD8GFP in glia. (E-G) Single Z images of brain hemispheres. Top panels are colored overlays, and bottom panel are single-channel images overlayed with the mask used for quantification (H) (see Materials and Methods). Quantification of glial number (I). (J-M) EdU-positive NBs after 24 hours of feeding in animals expressing dp60 in glia. (J-K) Maximum intensity projections of brain hemispheres from the indicated genotypes. Top panels are colored overlays, and single-channel grayscale images are below. Brain hemispheres outlined, and the dotted vertical line to left indicates the midline. Quantification of EdU-positive neuroblasts (L) and NB size (M). (N-O) Cerebral tracheal morphology over time in 24 hour fed animals expressing dp60 in trachea. Maximum intensity projection of brain hemispheres with a rendered trachea image below, quantified in (O). (B,C,D,L,M,O) Student's two-tailed t test, *$p<0.05$, **$p<0.01$,***$p< 0.001$, error bars, SEM. (H,I) One-way ANOVA with Tukey's post hoc analysis. Genotypes of panels listed in S5 Table.

Growth of cortex, subperineural, and neuropil glia is nutrient-regulated and PI3-kinase dependent

The glial population in the Drosophila brain is composed of several different subtypes, including cortex glia, that ensheathe neuroblasts and their newborn neuron progeny, subperineural glia (SPG), that encapsulate the central nervous system (CNS) forming a "blood brain-like barrier", and neuropil glia, that separate neuron cell bodies from their axon projections (Figure 3A). To better understand how PI3-kinase dependent growth is coordinated between neuroblasts and glia, we assessed numbers and types of glia, based on location, before and after animal feeding. Before feeding, ~95 Repo positive glia were found in each brain hemisphere. Of these, ~18 were cortex glia (19%), ~34 neuropil glia (35%, which include ensheathing glia of the neuropil and astrocytes), and the rest, ~46% SPGs and optic lobe-associated glia combined. After 24 hours of feeding, glial number and subtype distribution, based on location remained relatively unchanged (S3 Figure). We conclude that glial number and type are not specified by dietary nutrient uptake.

Next, we screened existing glial GAL4 lines to identify lines that drive GAL4 reporter expression specifically in different glia subsets in 24 hour fed animals (S4 Table). We found that NP0577GAL4 drove UAS-histoneRFP reporter expression in all cortex glia, identified based on location and Repo co-expression, as well as in some other glia (Figure 3B,C). MoodyGAL4 drove UAS-histoneRFP in most SPGs, almost half of neuropil glia, but no other glia (Figure 3D,E). Of the glial GAL4 lines screened, NP0577GAL4 and moodyGAL4 exhibited the most restricted and

specific patterns of glia GAL4 expression in brains of 24 hour fed animals. Therefore, we used these lines for subsequent analyses.

We expressed a membrane-tagged GFP in cortex glia (NP0577GAL4, UAS-mCD8GFP) to assay membrane growth in this glial subtype. After 24 hours of feeding, cortex glial membrane surface area increased nearly 3-fold and cortex glial began to ensheathe neuroblasts with new glial membrane (Figure 3F,I). In contrast, animals fed a sucrose-only diet or a normal diet with reduced PI3-kinase levels in cortex glia (NP0577GAL4, UAS-dp60) showed no increases in cortex glia membrane surface area after 24 hours (Figure 3G,H,I). Furthermore, we found no evidence of glial membrane ensheathment of neuroblasts under these conditions (Figure 3G,H, right panels). Next, we carried out a similar set of experiments in moodyGAL4, UASmCD8GFP animals. In animals fed a sucrose-only diet or those fed a normal diet but with reduced PI3-kinase levels in glia (moodyGAL4, UAS-dp60), we observed reductions in SPG and neuropil glial membrane surface area compared to animals fed a normal diet for 24 hours (Figure 3J-M). We noted that neither SPG or neuropil glia ensheathe neuroblasts (Figure 3J). We conclude that cortex glia, SPG, and neuropil glia require dietary nutrients and PI3-kinase activity for growth. Importantly, using glial subtype-specific GAL4 lines, we can now further dissect non-autonomous growth regulation between neuroblasts and specific glia subtypes in response to nutrition and PI3-kinase activity levels.

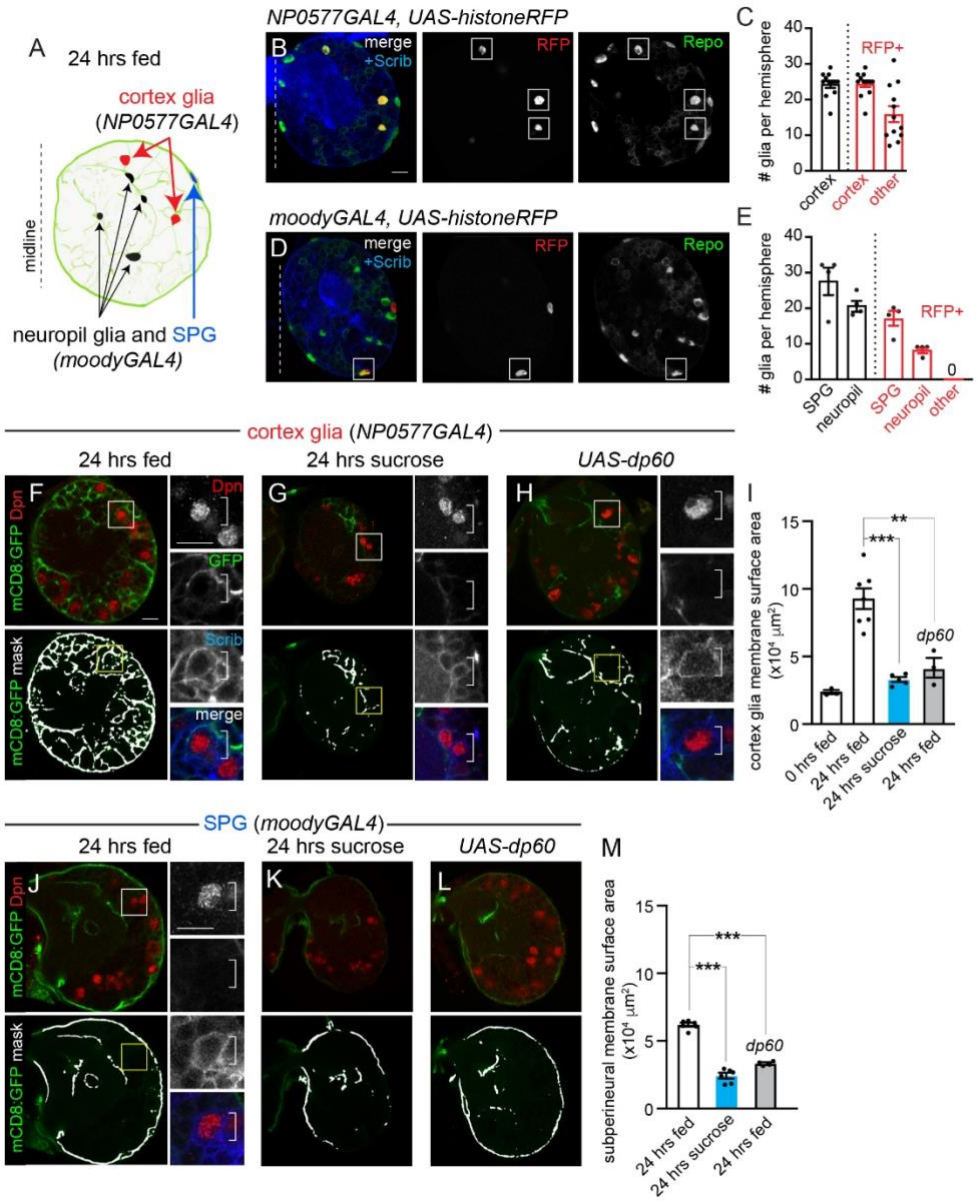

Figure 3. Growth of cortex glia and SPG is nutrient-regulated and PI3-kinase dependent.

(A) Single Z image of a segmented brain hemisphere with glia subtypes and corresponding GAL4 lines denoted in color. (B and D) Left panels, colored overlays of a single Z plane from a brain hemisphere of the indicated genotype, with grayscale images on the right. Quantification of glial populations are shown

in C and E. Red columns, mean of histoneRFP expressing glia and black columns, mean of glia identified based on position. Whites boxes indicate RFP-expressing cortex glia in (B) and SPG in (D). (F-I) Cortex glial membrane morphology after 24 hours of feeding standard food (F and H) or sucrose (G). (F-H) Single Z planes of brain hemispheres. Top panels are colored overlays, and bottom panels are single-channel images with the mask overlays used for quantification of cortex glia membrane surface area (I). Boxed Deadpan-positive neuroblasts are shown at higher magnification to the right. (J-M) SPG and neuropil glial membrane morphology after 24 hours of feeding on standard food (J and L) or sucrose (K). (J-L) Single Z images of brain hemispheres. Top panels are colored overlays, and bottom panels show single-channel images with the mask overlay used for quantification of SPG and neuropil membrane surface area (M). Deadpan-positive neuroblasts denoted in box shown at higher magnification to the right. One-way ANOVA with Tukey's post hoc analysis, **$p<0.01$, ***$p< 0.001$. Error bars, SEM. Genotypes of panels listed in S5 Table.

Cortex glia are required to reactivate neuroblasts from developmental quiescence

We found that reduction of PI3-kinase activity in all glia inhibited neuroblast reactivation from quiescence (refer back to Figure 2J-M). Using glial subtype-specific GAL4 lines, we reduced PI3-kinase levels in a glial subtype-specific manner and assayed neuroblast EdU incorporation and size after 24 hours of feeding. When PI3-kinase levels were reduced in cortex glia (NP0577GAL4, UAS-dp60), we found that neuroblast EdU incorporation and size were reduced after 24 hours of animal feeding (Figure 4A,B,D,E). The same effect was observed when phosphatidylinositol (3,4,5)-triphosphate (PIP3) levels were reduced by overexpressing the lipid phosphatase, Pten (NP0577GAL4, UAS-Pten) (Figure 3D). However, when PI3-kinase activity levels were reduced in SPG/neuropil glia (moodyGAL4, UAS-dp60), no difference in neuroblast EdU incorporation was found compared to controls (Figure 4F-H). To confirm that cortex glia are required for neuroblast reactivation, the pro-apoptotic gene, grim was expressed (NP0577GAL4, UAS-grim) to ablate cortex glia genetically (Figure 4I-K). After 24 hours of feeding, neuroblast EdU incorporation was essentially absent, and neuroblast size reduced (Figure 4C-E). We conclude that neuroblast growth and reactivation from quiescence requires activation of PI3-kinase in cortex glia, the glia subtype that ensheathe neuroblasts and their newborn progeny, but not SPG or neuropil glia.

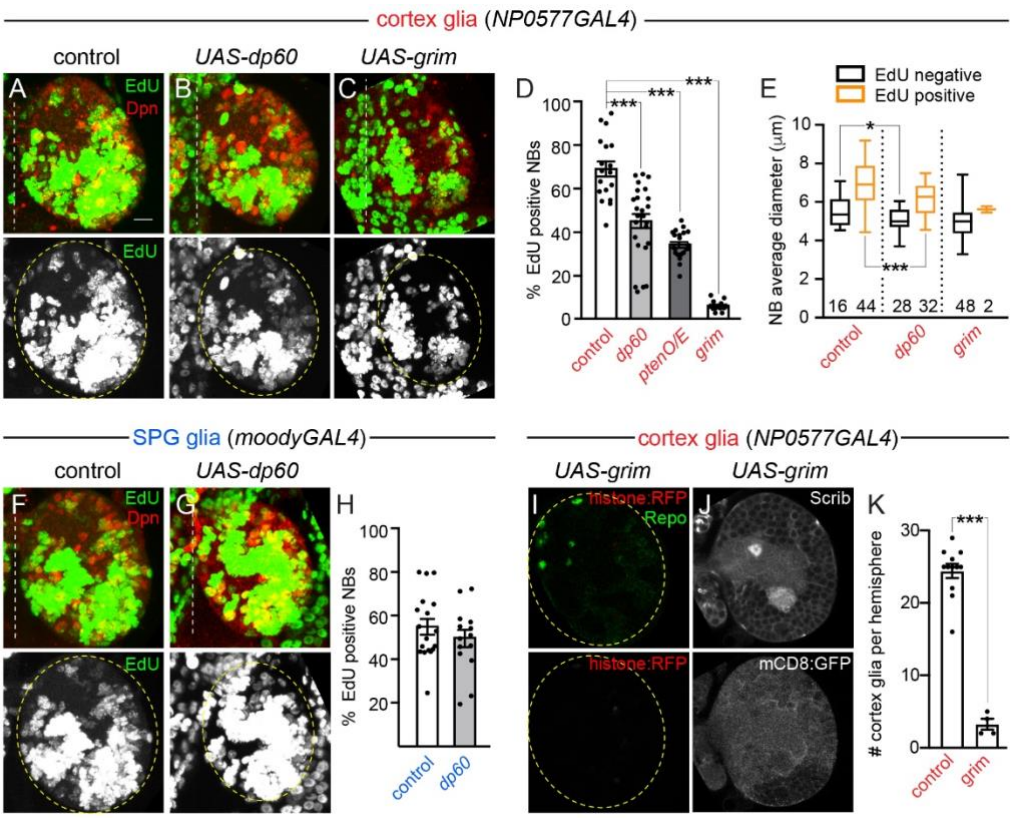

Figure 4. Cortex glia are required for nutrient-dependent neuroblast reactivation from quiescence.

(A-E) EdU-positive NBs in animals with genetic manipulations in cortex glia at 24 hours after feeding. (A-C) Maximum intensity projections of brain hemispheres. Top panels are colored overlays, and bottom panels show single-channel grayscale images. Brain hemispheres are outlined, and the dotted vertical lines indicate the midline. Graphs show quantification of EdU positive neuroblasts per brain hemisphere (D) and NB size split based on EdU incorporation (E). Numbers in E indicate the number of NBs analyzed. (F-H) EdU-positive NBs in animals with genetic manipulations in SPG and neuropil glia at 24 hours after feeding. (F-G) Maximum intensity projections of brain hemispheres. Panels are

colored overlays (top), with single-channel grayscale images below. Brain hemispheres are outlined, and dotted vertical lines indicate midline. Quantification of EdU-positive neuroblasts per brain hemisphere (H). (I) Single Z-plane images, top panel colored overlay with single-channel grayscale image below, brain hemispheres outlined. (J) Two (top and bottom) grayscale images of same Z plane, with cortex glia number following genetic ablation quantified in (K). (D) One-way ANOVA with Tukey's post hoc analysis and (E,H,K) Student's two-tailed t test, *$p<0.05$, **$p<0.01$, ***$p< 0.001$. Genotypes of panels listed in S5 Table.

Dilp-2 regulates neuroblast reactivation and cortex glia membrane growth, but not growth of trachea

PI3-kinase is activated in response to feeding, after any one of Dilps 1 through 7 bind to and activate the single insulin-like tyrosine kinase receptor (InR). While a role in neuroblast reactivation has been attributed to Dilps, a systematic analysis of all dilp mutants is lacking. To better understand how PI3-kinase coordinates growth among different cell types within the developing brain, we assayed neuroblast EdU incorporation in each of the seven dilp null mutants. Compared to controls and other dilp mutants, neuroblast EdU incorporation was reduced in dilp1, dilp2, and dilp7 null mutants (Figure 5D). Of these, dilp2 mutants displayed the most severe and penetrant reductions in neuroblast EdU incorporation and neuroblast size (Figure 5A,B,D-F,H). Somewhat surprisingly, neuroblast EdU incorporation in dilp6 null mutants was not changed compared with controls, dilp3, dilp4, or dip5 mutants, nor was neuroblast size affected by loss of dilp6 (Figure 5C,D,G,H). We conclude that Dilp-1, Dilp-2, and Dilp-7 regulate neuroblast reactivation from quiescence in the brain.

In dilp2 mutants, cortex glial membrane surface area was reduced by half compared to controls after 24 hours of feeding (Figure 5I-K), whereas tracheal surface area remained unchanged (Figure 5L-N). We conclude that Dilp-2 is required for cortex glial membrane growth, but not tracheal growth. Furthermore, because Dilp-2 is also required for neuroblast growth and reactivation, it suggests that growth coordination between cortex glia and neuroblasts is Dilp-2 dependent.

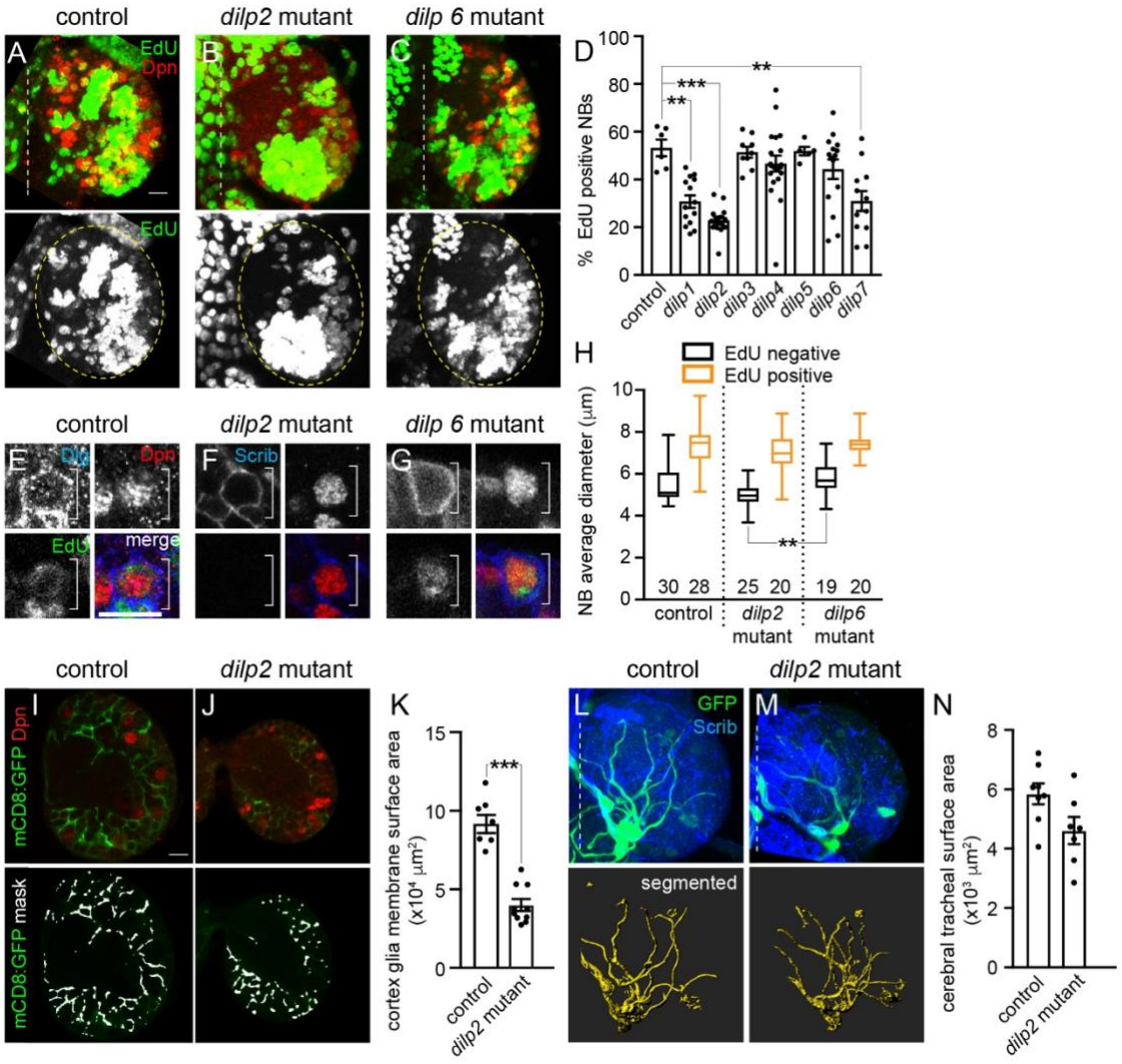

Figure 5. Dilp-2 regulates neuroblast reactivation and cortex glia membrane growth.

(A-D) EdU positive NBs after 24 hours of feeding in *dilp* single null mutant animals, (A-C) maximum intensity projections of brain hemispheres, top panel colored overlay with single-channel grayscale image below, brain hemispheres outlined and dotted vertical lines to left indicate midline, with quantification (D) shown as scatter plot with dots indicating brain hemispheres, bars indicating means, and error bars SEM. (E-H) Single Z images of non-MB NBs at high

magnification in 24 hour fed animals. Top and bottom left panels are single-channel grayscale images, with colored overlays at bottom right. (H) Plots of NB diameter of EdU-negative (black) versus EdU-positive (orange) NBs. Column numbers indicate number of NBs analyzed **(Conor Sipe).** (I-K) Cortex glial membrane morphology after 24 hours of feeding in controls and *dilp2* mutants. (I-J) Single Z images of brain hemispheres. Top panels are colored overlays, and bottom panels are single-channel images with the mask overlays used for quantification in (K). (L-N) Cerebral tracheal morphology after 24 hours of feeding in controls and *dilp2* mutants. (L-M) Maximum intensity projections of brain hemispheres with rendered trachea below and quantified in (N). (D) One-way ANOVA with Tukey's post hoc analysis and (H,K,N) Student's two-tailed t test, *$p<0.05$, **$p<0.01$, ***$p< 0.001$. Genotypes of panels listed in S5 Table.

Dilp-2 regulates CNS Dilp-6 protein levels, but not dilp6 transcript levels

We found that Dilp-2 regulates neuroblast growth and reactivation from quiescence in the central brain but that Dilp-6 does not. This was unexpected, because Dilp-6 is reported to be expressed in glia and is thought to be required for neuroblast reactivation in the ventral nerve cord (VNC). Next, we asked whether Dilp-6 regulates cortex glial growth or growth of trachea in the brain in response to feeding. In dilp6 mutants, both glia membrane (Figure 6A-C) and tracheal surface area (Figure 6D-F) were not different compared to controls. Together, this suggests that Dilp-6 is not required for PI3-kinase dependent growth of neuroblasts, glia or trachea in the central brain. However, neuroblasts located within different regions of the CNS (brain versus VNC) could have different requirements for reactivation. Alternatively, Dilp-2 could mask Dilp-6 function in the brain. To address this possibility, EdU incorporation and size was assayed in dilp2, dilp6 double mutant neuroblasts. After 24 hours of feeding, neuroblast EdU incorporation was reduced in dilp2, dilp6 double mutants (~15% EdU-positive neuroblasts) compared to dilp2 single mutants (~22% EdU-positive neuroblasts), although the reduction was not statistically different (Figure 6G,H). Next, we assayed dilp2 and dilp6 transcript levels (Figure 6I,J), and endogenous ¬Dilp-2 and Dilp-6 protein levels (Figure 6K) in the CNS of wild type animals after feeding (Figure 6I-K). We found that Dilp-2 transcript and protein levels were ~80 times higher than Dilp-6 transcript and protein levels, consistent with the notion that Dilp-2 is the predominant Dilp in the central brain. Furthermore, in dilp2 mutants, we found that dilp6 transcript levels were not different than wild type controls, although Dilp-6 protein levels were

significantly reduced in 24 hour-fed dilp2 mutants compared to wildtype animals (Figure 6J,L). We conclude that Dilp-2 is the primary Dilp regulating PI3-kinase dependent growth of neuroblasts, glia, and trachea in the brain and that Dilp-2 directly or indirectly regulates Dilp-6 protein levels.

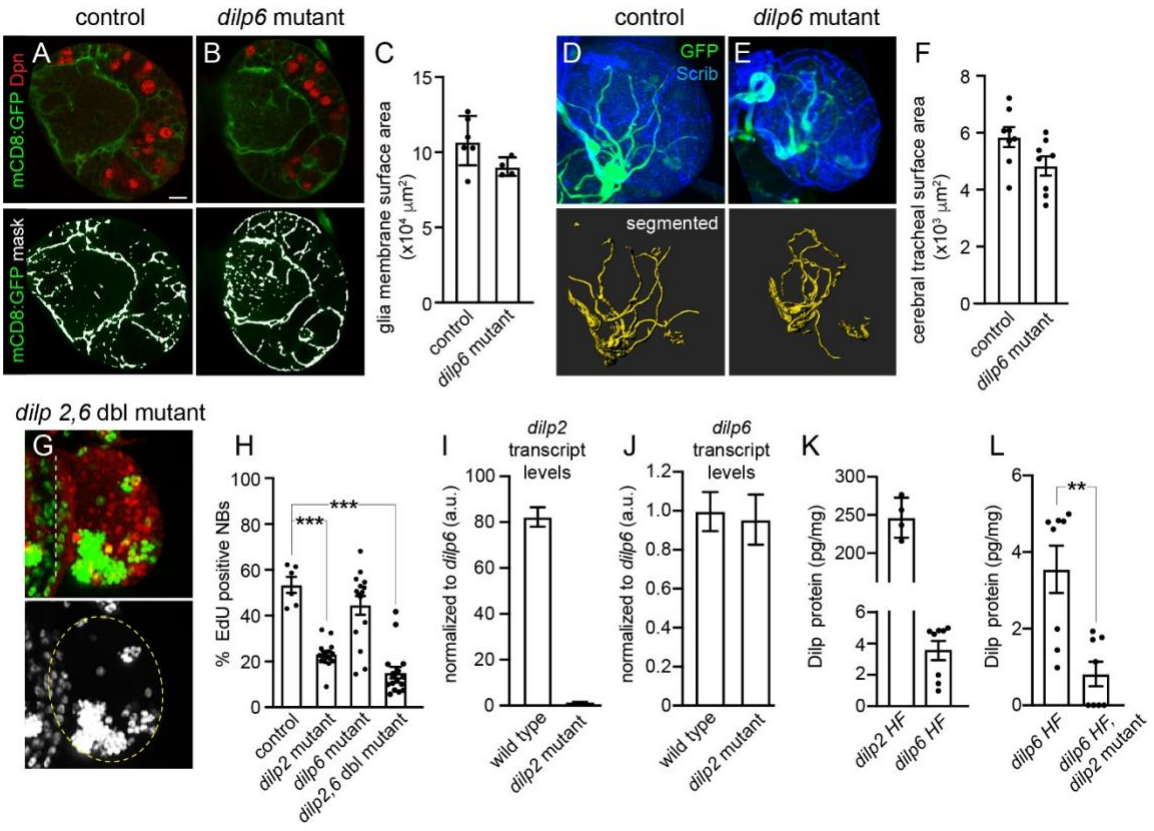

Figure 6. Dilp-2 regulates Dilp-6 CNS protein levels.

(A-C) Glial membrane morphology after 24 hours of feeding in controls and *dilp6* mutants. (A,B) Single Z images of brain hemispheres. Panels are colored overlays (top) and single-channel images with mask overlays (bottom) used for quantification of total glial membrane surface (C). (D-F) Cerebral tracheal morphology after 24 hours of feeding in controls and *dilp6* mutants. (D-E) Maximum intensity projections of brain hemispheres with rendered trachea below and quantified in (F). (G-H) EdU-positive NBs after 24 hours of feeding in *dilp2, dilp6* double mutants. (G) Maximum intensity projection of a brain hemisphere. Top panel is a colored overlay, and the bottom panel is a single-channel grayscale image below with quantification in (H). Brain hemispheres are outlined,

and the dotted vertical line indicates the midline. (I,J) RT-qPCR analysis of *dilp2* and *dilp6* transcript levels in the CNS of wild type and *dilp2* mutant animals after 24 hours of feeding. Transcript levels of *dilp2* and *dilp6* are normalized to *Gapdh1* and then to *dilp6* levels in wild-type animals. (K,L) Brain Dilp-2 and Dilp-6 protein levels, normalized to total brain protein, in wild-type and *dilp2* mutant animals after 72 hours of feeding. **(Miyuki Suzawa)** (H) One-way ANOVA with Tukey's post hoc analysis and (K) Student's two-tailed t test, **p<0.01, ***p< 0.001.

Coordination of growth between neuroblasts and cortex glia promotes formation of a selective membrane barrier for niche stem cell support

During later stages of larval development, neuroblasts and their progeny reside within characteristic glial membrane-bound pockets (Figure 7A,B). One or two cortex glia that lie nearby or adjacent to neuroblasts and their progeny provide the membrane that comprises each pocket. We injected a fluorescently-conjugated 10 kDa dextran directly into the brain to test the permeability of glia membrane-bound pockets. We found fluorescent dextran co-localized with cortex glia membrane along the outside of each pocket, but no fluorescence within the pocket (Figure 7A). This suggests that cortex glia form a membrane barrier that selectively regulates passage of factors based on size.

Next, we investigated whether Dilp-2 mediated PI3-kinase activation in neuroblasts and glia is required for glia pocket formation. First, we measured the fraction of neuroblast membrane in contact with glia membrane (% neuroblast membrane with glial contact, see Materials and Methods) over time in control animals (Figure 7B, schematic at bottom). From 0 hour freshly-hatched stages until 8 hours after feeding, we found that the fraction of neuroblast membrane in contact with glial membrane increased ~3.5 fold (Figure 7C-F). At 24 hours after feeding, glia ensheathe ~44% of the neuroblast membrane and at 72 hours after feeding, ~72% (Figure 7B-D,G). Next, we assessed the temporal relationship between neuroblast and glial membrane contact with changes in neuroblast size. We found that neuroblast size increased after the fraction of neuroblast glial contact increased (Figure 7C-G). Next, we measured fraction of neuroblast membrane in

contact with glia membrane in 24-hour fed dilp2 mutants (Figure 7I,K). We found significant reductions in neuroblast membrane glia contact that correlated with reductions in neuroblast size. A similar result was found when levels of PI3-kinase activity were reduced in glia, but not in neuroblasts (Figure 7H,J,K). In neuroblasts, when PI3-kinase activity levels were reduced, neuroblast size remained reduced compared to controls, but increases in neuroblast membrane in contact with glial membrane were found. We conclude that Dilp-2 mediated PI3-kinase activation is required to initiate glial pocket formation. Importantly, increases in neuroblast membrane with glia contact precede increases in neuroblast size, consistent with the notion that cortex glia membrane contact triggers neuroblast growth and reactivation.

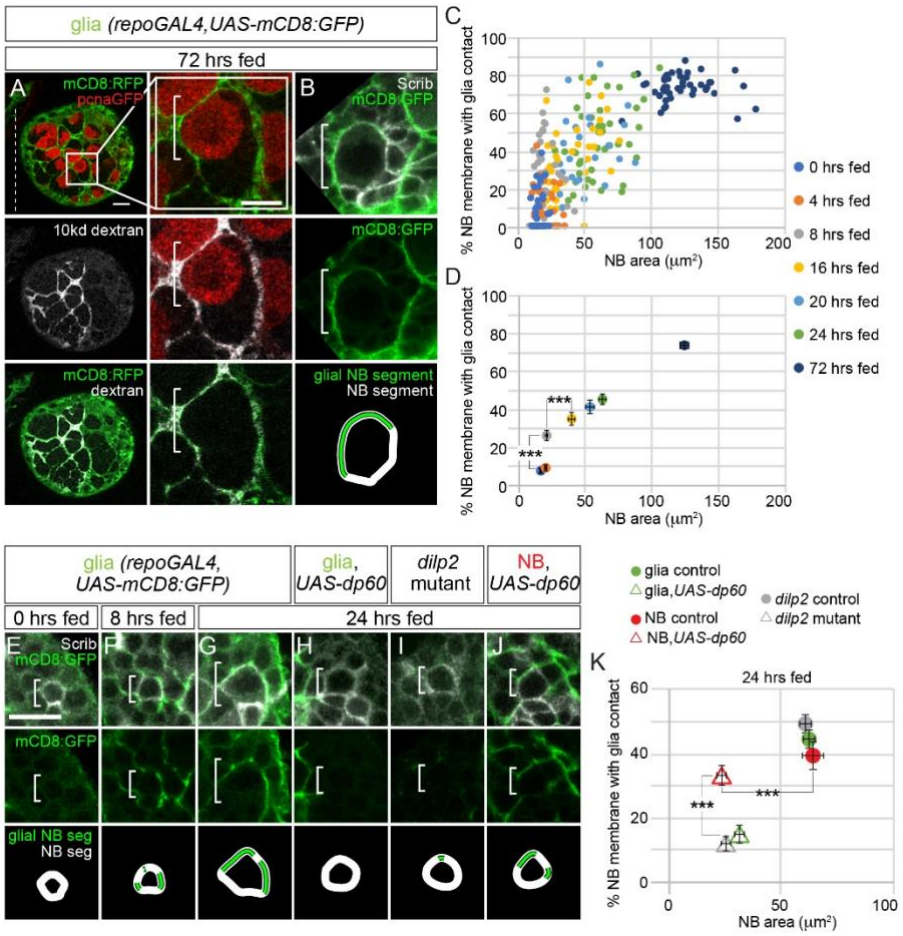

Figure 7. Cortex glia ensheathe neuroblasts and their progeny and provide a niche-like barrier function.

(A) Top panel, colored overlay of 10 kDa dextran. Middle panel, single channel grayscale image, with GFP marking *pcnaGFP* expressing NBs. Bottom panel, colored overlay with 10kd dextran and RFP marking glial membranes. To the right, high magnification images of the boxed NB, with double-labeled glial membrane in a 72 hour fed animal after dextran injection (see Materials and Methods). (B) Cortex glia ensheathe NBs (white bracket) and their newborn progeny, which express high levels of Scrib. Top panel, colored overlay. Middle

panel, single-channel image. Bottom panel is a depiction of the glial and NB segments used for quantification in (C,D,K) **(Sarah Siegrist)** (see Materials and Methods). (C,D) Percentage of NB membrane in contact with glial contact over time. Colored circles in (C) indicate individual NBs and colored circles in (D) indicate averages for the indicated time points. Both are plotted relative to NB area. (E-G) Increasing surface contact between NBs and glia membrane over time. Single Z of representative NBs at different time points after feeding. Top panels are colored overlays, middles panels are single-channel image, and bottom panels depict the glial NB segment and NB segment used in quantification (C-D). (H-K) Top panel colored overlay, middle panel single-channel image, bottom panel glial NB segment and NB segment used in quantification of animals at 24 hours of feeding with genotypes listed above. (D,K) One-way ANOVA with Tukey's post hoc analysis, ***$p < 0.001$. Genotypes of panels listed in S5 Table.

Discussion

Here we report that different cell types in the brain utilize the same evolutionarily-conserved cell signaling pathway, PI3-kinase, to promote growth in response to dietary nutrients. PI3-kinase is a lipid kinase that converts PIP2 to PIP3 at the plasma membrane when active, leading to downstream Akt activation and nuclear exclusion of Foxo, a transcription factor and negative regulator of growth(128–131). We found that active PI3-kinase not only regulates cell growth autonomously in the brain, but also regulates growth of other cell types in a non-autonomous manner. For example, glial growth is reduced when PI3-kinase levels are reduced in neuroblasts. The molecular basis for this reduction is not yet known, but reactivated and proliferating neuroblasts with active PI3-kinase may express or secrete factors on their cell surface that promote glial growth non-autonomously. These could include PVF, a secreted growth factor, or components of the Hippo or Notch cell signaling pathways, that would not normally be expressed in quiescent neuroblasts having low to no PI3-kinase activity (52,132,133). We also found that PI3-kinase-dependent growth of cortex glia is required for neuroblast reactivation and that cortex glia membrane ensheathes neuroblasts before they increase in size. The glial process that makes first contact with a neuroblast could deliver signaling molecules to stimulate neuroblast reactivation from quiescence, similar to cytonemes or nanotubules, or simply supply a foreign membrane that stimulates growth(134,135). We also found that neuroblasts rely on PI3-kinase-dependent growth of trachea for reactivation. Trachea allow for oxygen exchange, but are also important sources of cell signaling molecules, including EGF-R and FGF-R. Whether neuroblast quiescence versus proliferation decisions are regulated by

oxygen levels has yet to be determined, but quiescent adult stem cells in other organisms are thought to reside within hypoxic microenvironments(136,137).

Of all the Dilps, we found that Dilp-2 plays a predominant role in mediating PI3-kinase-dependent growth of neuroblasts and glia as well as neuroblast reactivation. This was not expected based on previous reports, however neuroblasts with different intrinsic programs located within different regions of the CNS (brain versus VNC) could reactivate in a different manner. In the brain, Dilp-2 is synthesized and secreted in a dietary nutrient-dependent manner from 14 neurosecretory neurons located along the anterior midline (138,139). Axons of these neurosecretory neurons, known as the insulin-producing cells (IPCs) terminate on the dorsal vessel, which pumps hemolymph and thus, Dilp-2, systemically throughout the body(139). Dilp-2 is also released locally in the brain through IPC connections with other neurosecretory neurons, including the centrally-located Dilp-recruiting neurons (DRNs) (140). Whether local or systemic Dilp-2 activates PI3-kinase in the different brain cell types remains an open question. Once released, Dilp-2 could activate PI3-kinase in the different cell types in a simultaneous or sequential manner. Furthermore, Dilp-2 could stimulate synthesis and secretion of other Dilps and other factors that could promote autonomous or non-autonomous growth, either locally within the brain or systemically. Such factors include Dilp-6, which is reported to be expressed in glia, and other Dilps that are expressed in neurosecretory neurons including the IPCs (48,55,139–141).

In the brain, different cell types coordinate growth in response to dietary nutrients. Growth among different tissue types is also coordinated and relies on systemic factors, including the relaxin-like hormone, Dilp-8 (141–143). For example, in response to tissue damage, Dilp-8 is expressed and secreted systemically, inducing developmental arrest, which allows time for tissue damage to self-repair. Once complete, Dilp-8 levels decrease, development resumes and adults emerge with appropriately sized and proportioned appendages(141–145). Systemic growth is also regulated by 20-hydoxyecdysone, an ecdysteroid hormone that promotes growth globally and couples increases in cell and tissue size with developmental progression (107,110,111). Dietary nutrient conditions play a key role in both ecdysone production and developmental timing, as PI3-kinase regulates growth of the prothoracic gland that synthesizes and secretes ecdysone. Accumulated nutrient biomass is monitored by a "critical weight" check point in development; before critical weight, development delays if dietary nutrients are limited, but once animals reach "critical weight," commitment to metamorphosis commences without delay regardless of dietary nutrients (106–111) . It will be important to determine whether coordinated cell growth occurs during tissue repair in periods of limited nutrient availability, and whether coordinated cell growth continues after "critical weight" is reached.

In mammals, cell growth decisions in response to nutrient availability are regulated by PI3-kinase and TOR-kinase signaling as well. However, how growth decisions are made and whether they are coordinated in response to dietary nutrients among stem cells within their local microenvironments is not well

understood. Adult mammals, unlike flies, maintain a population of proliferative neural stem cells in the brain, some of which reside within rosette-like structures located along the lateral wall of the ventricle(146,147). Multi-ciliated ependymal cells form the rosette with the stem cell and its primary cilium at the center (64). Both ependymal cells and stem cells receive signals through their cilia, which project into the ventricles filled with cerebral spinal fluid (CSF). The choroid plexus produces CSF and with it, a host of factors, including IGF (148). Whether IGF regulates levels of PI3-kinase signaling in neural stem cells within their niche remains unclear, but loss of the rosette-like pinwheels correlates with decreased adult neurogenesis and premature progenitor differentiation (64). In the future, it will be interesting to determine whether dietary nutrients regulate choroid plexus IGF levels and how stem cells and their niche respond to IGF during homeostasis and aging.

Materials and methods

Drosophila stocks

Genotypes of fly stocks used in this study and their source are listed in S6 Table.

Drosophila maintenance and feeding methods

Larvae were collected immediately after hatching and placed on either Bloomington fly food diet or in a sucrose-only solution. Freshly hatched larvae were maintained at 25˚C on a 12 hour light/dark cycle for defined periods of time. Fly food or sucrose solution were supplemented with 0.1mM EdU, and EdU

incorporation was detected using commercially available Click-iT EdU Proliferation Kits for Imaging as described previously (46).

Immunofluorescence, dextran injections, and confocal imaging

Larval brains were fixed and stained as previously described (46). In brief, early staged larval brains were dissected and fixed in 4% EM grade formaldehyde in PEM (Pipes, EGTA, Magnesium chloride) buffer with 0.1% Triton-X for 20 mins. Tissues were washed in 1X PBT with 0.1% TritonX-100 and blocked overnight at 4˚C in 1X PBT with 10% normal goat serum. Primary antibodies used in this study include: chicken anti-GFP (1:500, Abcam), rat anti-Deadpan (1:100, Abcam), rabbit anti-Scribble (1:1000), mouse anti-Repo (1:5, DSHB, 8D12). Primary antibodies were detected using Alexa Fluor-conjugated secondary antibodies. For dextran dye experiments, 10 kDa dextran conjugated to Alexa Fluor 647 was injected into L3 brains maintained in culture using micro-manipulators. Brains were then fixed and stained as described above. Brains were imaged using a Leica SP8 laser scanning confocal microscope equipped with a 63X, 1.4 NA oil-immersion objective. For glia and trachea surface measurements, Z stacks were acquired at 0.5 μm steps using same confocal settings. All other confocal data were collected at 1.0 μm steps. Images were processed using the Imaris and Fiji software packages.

Cell counts and quantification of glia and tracheal membrane surface area

For neuroblast EdU quantification, the number of EdU-positive, Dpn-positive neuroblasts were counted using the “cell counter” plugin in Fiji and divided by the total number of Dpn-positive neuroblasts. For quantification of glia, the total number of Repo-positive nuclei were counted in each brain hemisphere, and cortex, SPG, and neuropil glia distinguished based on their location and morphology. Neuroblast diameter was calculated based on the average length of two perpendicular lines drawn through center of the neuroblast at its widest point. To quantify glial and trachea surface area, GFP-expressing membranes were segmented and analyzed using the Surface module in Imaris 9.0.2 (Bitplane). Imaris Surface generates a volumetric surface object based on fluorescence intensity and creates a 3D surface mesh based on voxel intensity. After segmentation, a mask was generated and confirmed by manual visual inspection using Imaris slice mode. All confocal images used for surface area measurements were acquired using the same settings. For measurement of percentages of neuroblast membrane with glia contact, we used a Fiji plug-in as described previously (72). Brains were mounted with their dorsal side closest to coverslip, and all non-MB neuroblasts within 30 microns of the coverslip were assayed.

Whole brain Dilp-2 and Dilp-6 measurements

Brains were dissected at 72 hours after larval hatching and lysed by sonication in extraction buffer (1X PBS with protease inhibitor). Lysed samples were cleared by centrifugation and dual-epitope tagged Dilp2 (Dilp2-HF) or Dilp6 (Dilp6-HF) was measured by ELISA (149). Protein concentration for normalization was measured

using a bicinchoninic assay (BCA) (Pierce). To convert molar concentrations to pg Dilp/mg protein, we used a molecular weight of 7828.86 daltons for mature Dilp2HF protein (A-chain and B-chain with HA and FLAG tags) and 10303.62 daltons for mature Dilp6HF protein (A-chain, C-peptide and B-chain with HA and FLAG tags).

Quantitative RT-PCR

Total RNA was extracted from 24 hour fed larval brains. For each experimental sample, 40 brains were pooled in TRIzol, and isolated RNA was reverse transcribed into cDNA using SuperScript IV First-Strand Synthesis System kit (Thermo Fisher). Quantitative PCR was performed using the iQTM SYBR Green Supermix system (Bio-Rad). Gapdh1 expression was used as a control. Relative dilp2 and dilp6 mRNA levels for each sample were calculated using the 2-DCt method after normalizing to Gapdh1expression. The following primers were used: dilp6 (40), Gapdh1(22), dilp2 forward: ACGAGGTGCTGAGTATGGTGTGCG, and dilp2 reverse: CACTTCGCAGCGGTTCCGATATCG.

Statistical analysis

Student's t-tests and one-way ANOVAs were performed using Prism 8. For box plots, the boundary of the box closest to zero indicates the 25th percentile, a line within the box marks the median, and the boundary of the box farthest from zero indicates the 75th percentile. Whiskers (error bars) above and below the box

indicate the maximum and minimum, respectively. The data in plots and the text are presented as means ± SEM.

ACKNOWLEDGEMENTS

We thank Andrea Brand, Marc Freeman and the Bloomington and Kyoto stock centers for fly stocks and reagents. We especially thank Susan Doyle, Chhavi Sood, and Nahid Ausrafuggaman for help in tissue dissections. We thank Chris Doe, Susan Doyle, and Karsten Siller for providing comments on the manuscript. This work was funded by NIH/NICHD R00-HD067293 and by NIH/NIGMS R01-GM120421.

Supplemental Information

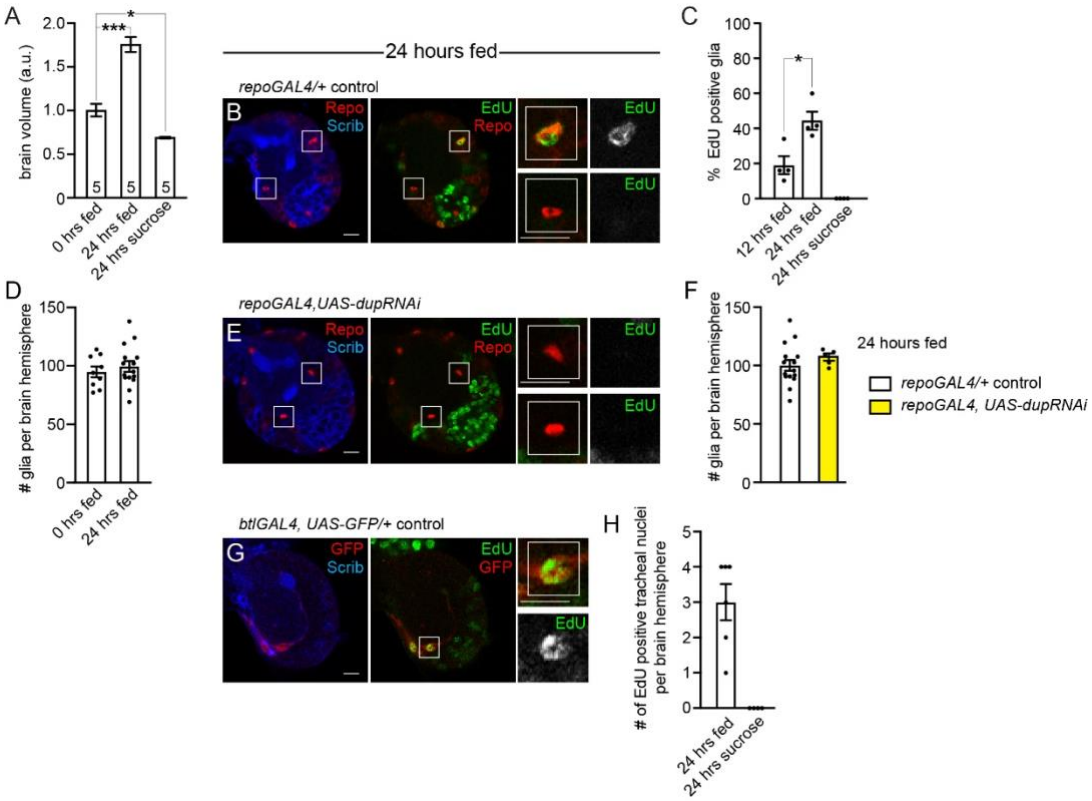

S1 Figure: Glia and trachea endoreplicate in response to animal feeding.

(A) Fold changes in brain volume per hemisphere in response to animal feeding (see Materials and Methods). Column numbers indicate number of brain hemispheres scored. Values are normalized to 0 hour fed animals. (B,C) Single Z planes of brain hemispheres. Left and middle panels are color overlays of a control brain after feeding. High magnification of two Repo-positive glia are shown to the right, one EdU-positive and one EdU-negative (white boxes). (C) Quantification of EdU-positive glial cells per brain lobe in response to feeding. (D) Number of Repo-positive glia cells per brain hemisphere before and after animal feeding. (E,F) Single Z image of a brain hemisphere from a *dupRNAi* knockdown animal. Left and middle panels are color overlays with high magnification of two Repo-positive

glia shown to the right (white boxes). (F) Quantification of glia number in *dupRNAi* knockdown animals compared to control. (G-H) Single Z image of a brain hemisphere. Left and middle panels are color overlays of control brain after feeding. A high magnification image of a tracheal nucleus is shown to the right (white boxes). (H) Quantification of EdU in trachea from animals fed standard food or sucrose. (A) One-way ANOVA with Tukey's post hoc analysis and student's two-tailed t test, *p<0.05, **p<0.01, ***p< 0.001. Genotypes of panels listed in S5 Table.

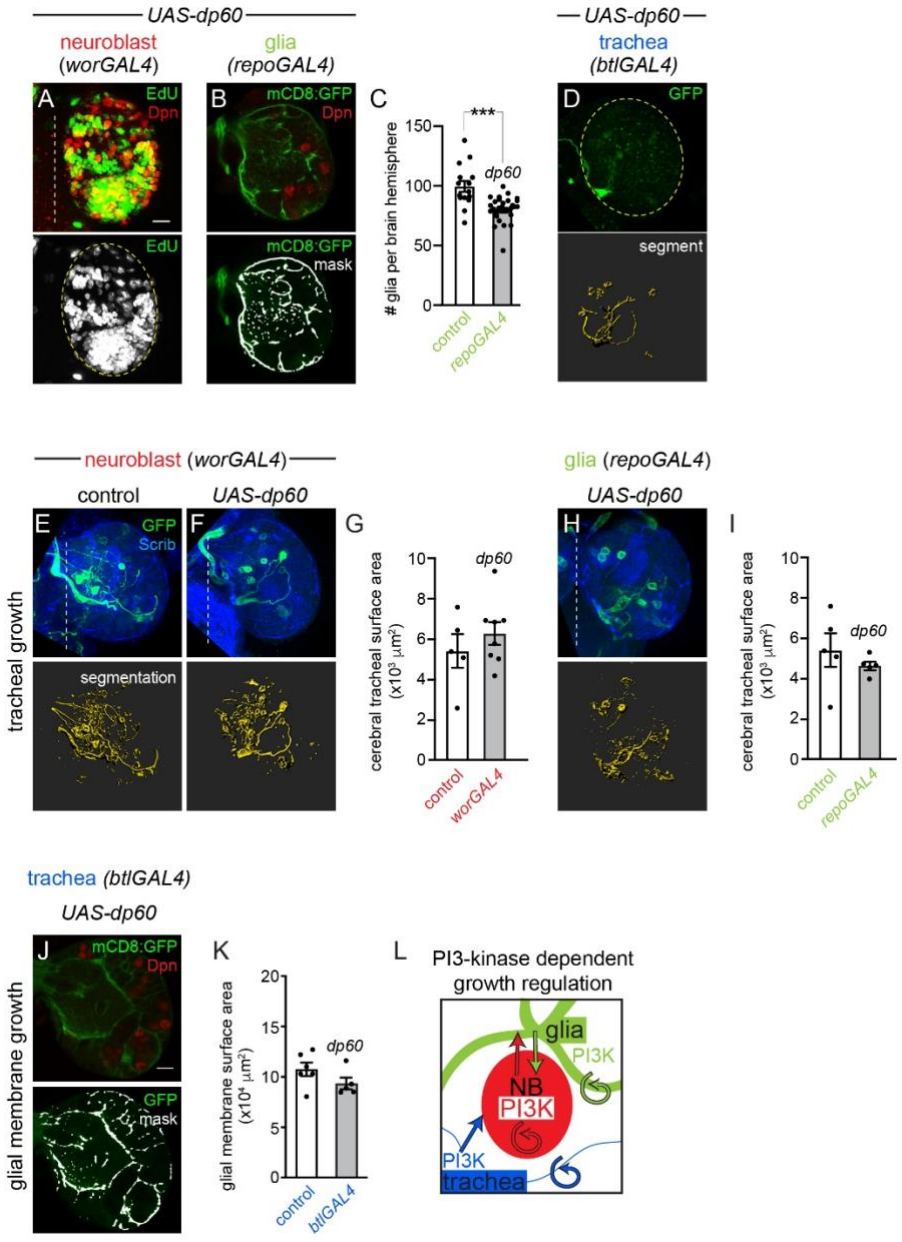

Figure S2: PI3-kinase-dependent growth regulation in the developing brain.

(A) EdU labeling of single brain hemisphere **(Conor Sipe).** (B) Glial and (D) tracheal morphology when PI3-kinase is reduced in neuroblasts with quantification of glial number in (C). (A,D) Maximum intensity projections. Top panels are colored overlays, with single channel grayscale images below (A) and rendered maximum

intensity projection of trachea below (D). (B) Single Z image. Top panel is a color overlay, with single channel and mask below, (D) bottom panel, rendered maximum intensity projection of trachea. (E,F,H) Maximum intensity projections of cerebral trachea when levels of PI3-kinase are reduced, with tracheal segmentation in bottom panels with quantification of tracheal surface area (G,I). (J) Single Z plane of brain hemisphere of glial morphology, color overlay with single channel image below with glia mask used in quantification of glial membrane surface area (K). (L) Summary of PI3-kinase growth regulation between different cell types in the brain, circle arrows indicate requirement for autonomous PI3-kinase growth signaling and straight arrows, indicate non-autonomous growth signaling. Genotypes of panels listed in S5 Table.

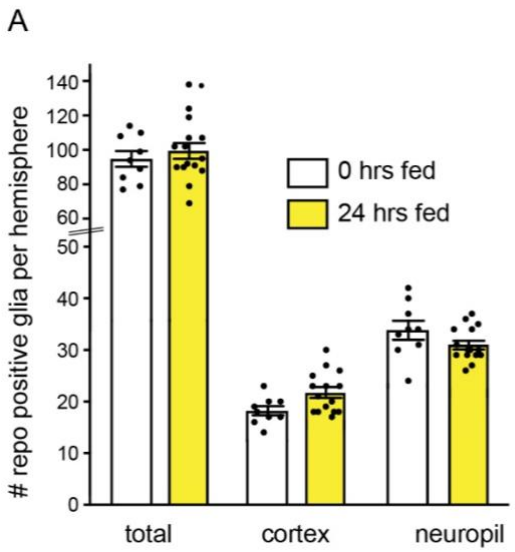

S3 Figure: Distribution of glia based on location before and after animal feeding.

Total number of glia subtypes before and after animal feeding. Glia type was identified based on location. Error bars, S.E.M. Black circles indicate single brain hemispheres. Genotypes of panels listed in S5 Table.

S4 Table: Classification of glial GAL4 expression in the larval brain after 24 hours of feeding.

	Glia expression				
GAL 4 line	cortex glia	SPG	neuropil glia	astrocytes	other expression
repoGAL4	+++	+++	+++	+++	none
NP0577Gal4	+++	+	+	-	few neurons
NP2222Gal4	++	-	-	-	trachea and IPCs
moodyGal4	-	++	+	-	NA
spinGal4	-	++	-	-	few neurons and semi-viable
wunGal4	+++	-	+++	+++	NA

+++ expressed in all glia

++ expressed in some glia

+ expressed in few glia

- expressed in no glia

NA, not assayed

S5 Table: Genotypes listed by figure panel

FIGURE	GENOTYPE	
Figure 1B-L	*repoGal4/+ (OregonR)*	
Figure 1M-R	*UAS-mCD8GFP, repoGal4/+ (OregonR)*	
Figure 1S-X	*btlGal4, UAS-GFP/+ (OregonR)*	
Figure 2B	*worGal4/+ (OregonR)*	control
	worGal4/UAS-dp60	
Figure 2C	*UAS-mCD8GFP, repoGal4/+ (OregonR)*	control
	UAS-mCD8GFP, repoGal4/UAS-dp60	
Figure 2D	*btlGal4, UAS-GFP/+ (OregonR)*	control
	btlGal4, UAS-GFP/UAS-dp60	
Figure 2E,H,I	*repoQF2, QUAS-mCD8GFP/+ (OregonR)*	control
Figure 2F,H,I	*worGal4, UAS-dp60/repoQF2,QUAS-mCD8GFP*	
Figure 2G,H,I	*worGal4; repoQF2,QUAS-mCD8GFP/UAS-raptorRNAi*	
Figure 2J,L,M	*repoGal4/+ (OregonR)*	control
Figure 2K,L,M	*repoGal4/UAS-dp60*	
Figure 2N,O	*btlGal4, UAS-GFP/UAS-dp60*	
Figure 2O	*btlGal4, UAS-GFP/+ (OregonR)*	control
Figure 3B,C	*NP0577Gal4/UAS-histoneRFP*	
Figure 3D,E	*moodyGal4/UAS-histoneRFP*	
Figure 3F,G,I	*NP0577Gal4, UAS-mCD8GFP*	
Figure 3H,I	*NP0577Gal4, UAS-mCD8GFP, UAS-dp60*	

Figure 3J,K,M	*moodyGal4, UAS-mCD8GFP*	control
Figure 3L,M	*moodyGal4, UAS-mCD8GFP/UAS-dp60*	
Figure 4A,D,E	*NP0577Gal4/+(OregonR)*	control
Figure 4B,D,E	*NP0577Gal4/UAS-dp60*	
Figure 4C-E	*NP0577Gal4/UAS-grim*	
Figure 4F,H	*moodyGal4/+(OregonR)*	control
Figure 4G,H	*moodyGal4/UAS-dp60*	
Figure 4I,K	*NP0577GAL4, UAS-histoneRFP/UAS-grim*	
Figure 4K	*NP0577Gal4/UAS-histoneRFP*	control
Figure 4J	*NP0577GAL4, UAS-mCD8GFP/UAS-grim*	
Figure 5A,D,E,H	*OregonR/w^{1118}*	control
Figure 5B,D,F,H	*$dilp2_1$/$dilp2_1$*	
Figure 5C,D,G,H	*$dilp6_{68}$/$dilp6_{68}$*	
Figure 5D	*$dilp1_1$/$dilp1_1$ and $dilp3_1$/$dilp3_1$ and $dilp4_1$/$dilp4_1$ and $dilp5_1$/$dilp5_1$* and *$dilp7_1$/$dilp7_1$*	
Figure 5I,K	*NP0577Gal4, UAS-mCD8GFP*	control
Figure 5J,K	*NP0577Gal4, $dilp2_1$/UAS-mCD8GFP, $dilp2_1$*	
Figure 5L,N	*btlGal4, UAS-GFP/+ (OregonR)*	control
Figure 5M,N	*btlGal4, UAS-GFP, $dilp2_1$/$dilp2_1$*	
Figure 6A,C	*repoQF2, QUAS-mCD8GFP/+ (OregonR)*	control

Figure 6B,C	*dilp6$_{68}$; repoQF2, QUAS-mCD8GFP*	
Figure 6D,F	*btlGal4, UAS-GFP/+ (OregonR)*	control
Figure 6E,F	*dilp6$_{68}$; btlGal4, UAS-GFP*	
Figure 6G,H	*dilp6$_{68}$/dilp6$_{68}$; dilp2$_1$/dilp2$_1$*	
Figure 6H	*OregonR/w$_{1118}$* and *dilp2$_1$/dilp2$_1$* and *dilp6$_{68}$/dilp6$_{68}$* and *dilp6$_{68}$/dilp6$_{68}$; dilp2$_1$/dilp2$_1$*	
Figure 6I,J	*Oregon R* and *dilp2$_1$/dilp2$_1$*	
Figure 6K	*dilp2$_{HA}$* and *dilp6$_{HF}$ and dilp6$_{HF}$;dilp2$_1$/dilp2$_1$*	
Figure 7A	*pcnaGFP; repoGAL4, UAS-mCD8RFP*	
Figure 7B-E,G,K	*UAS-mCD8GFP, repoGal4/+ (OregonR)*	
Figure 7H,K	*UAS-mCD8GFP, repoGal4/+*	control
	UAS-mCD8GFP, repoGal4/UAS-dp60	
Figure 7I,K	*NP0577Gal4, UAS-mCD8GFP/+ (OregonR)*	control
	NP0577Gal4, dilp2$_1$/UAS-mCD8GFP, dilp2$_1$	
Figure 7J,K	*repoQF2, QUAS-mCD8GFP/+ (OregonR)*	control
	worGal4, UAS-dp60/repoQF2, QUAS-mCD8GFP	
S1 Figure A-D	*repoGal4/+ (OregonR)*	
S1 Figure E,F	*repoGal4/UAS-dupRNAi*	
S1 Figure G,H	*btlGal4, UAS-GFP/+ (OregonR)*	
S2 Figure A	*worGAL4/UAS-dp60*	
S2 Figure B,C	*UAS-mCD8GFP, repoGal4/+ (OregonR)*	control
	UAS-mCD8GFP, repoGal4/UAS-dp60	

S2 Figure D	*btlGal4, UAS-GFP/UAS-dp60*	
S2 Figure E,G	*btlLexA, LexAOP-mCD8GFP*	control
	worGal4/UAS-dp60; btlLexA, LexAOP-mCD8GFP	
S2 Figure H,I	*btlLexA, LexAOP-mCD8GFP*	control
	UAS-dp60; repoGal4/btlLexA, LexAOP-mCD8GFP	
S2 Figure J,K	*repoQF2, QUAS-mCD8GFP/+ (OregonR)*	control
	btlGAL4/UAS-dp60, repoQF2, QUAS-mCD8GFP	
S3 Figure A	*repoGal4/+ (OregonR)*	

S6 TABLE: DROSOPHILA STOCK LIST AND SOURCE	
OregonR	Bloomington Drosophila Stock Center #5
worGal4	(150)
UAS-mCD8GFP on II	Bloomington Drosophila Stock Center #5137
UAS-mCD8GFP on III	Bloomington Drosophila Stock Center #5130
repoGal4	Bloomington Drosophila Stock Center #7415
btlGal4, UAS-GFP	Bloomington Drosophila Stock Center #8807
btlGal4 on III	Bloomington Drosophila Stock Center #78328
UAS-dp60	(127)
repoQF2	Bloomington Drosophila Stock Center #66477
QUAS-mCD8GFP	Bloomington Drosophila Stock Center #30003
btlLexA	Bloomington Drosophila Stock Center #66620
LexAOP-mCD8GFP	Bloomington Drosophila Stock Center #32203
NP0577Gal4	Kyoto Stock Center #112228
UAS-histoneRFP	(151)
pcnaGFP	(152)
moodyGal4 on II	(153)
moodyGal4 on III	(153)
UAS-grim	isolated from Bloomington Drosophila Stock Center #52016
UAS-Pten	Bloomington Drosophila Stock Center #82170
w1118	Bloomington Drosophila Stock Center #3605
dilp1$_1$	(40)

dilp2$_{1}$	(40)
dilp3$_{1}$	(40)
dilp4$_{1}$	(40)
dilp5$_{1}$	(40)
dilp6$_{68}$	(40)
dilp7$_{1}$	(40)
dilp6HF	(149)
dilp2HF	(154)
UAS-dupRNAi	Bloomington Drosophila Stock Center #29562
UAS-raptorRNAi	Bloomington Drosophila Stock Center #34814
UAS-mCD8RFP	Bloomington Drosophila Stock Center
NP2222GAL4	Kyoto Stock Center #112830
spinGAL4	Kyoto Stock Center #112853
wunGAL4	Kyoto Stock Center #103953

Chapter III

Investigation of Local versus Circulating Insulin that Drives Neural Stem Cell Reactivation from Quiescence

Abstract

While known to express the insulin receptor (InR), the brain was long thought to be insensitive to insulin signaling. This view has recently been challenged, and emerging evidence suggests that the brain is an insulin-responsive organ. Insulin that is produced both peripherally from the pancreas, and centrally in the brain, regulates neuronal activity. Proper regulation of insulin signaling in the brain is important for the prevention of neurodegenerative disorders such as Alzheimer's disease. We previously demonstrated that *Drosophila* insulin-like peptide 2 (Dilp-2) is required for neural stem cell reactivation from quiescence, and development of the stem cell niche cytoarchitecture in response to dietary nutrients. In this chapter, I present evidence that the *Drosophila* insulin producing neurons (IPCs), which are analogous to mammalian pancreatic β cells, are the cellular source of Dilp-2 that reactivates quiescent neuroblasts (NBs). IPCs are known to release Dilp-2 both systemically into the insect blood hemolymph, and locally within the brain. Here, we show evidence that circulating Dilp-2 in the hemolymph is required for neural stem cell reactivation from quiescence. Additionally, Dilp-recruiting neurons (DRNs), known to make neuronal contact with IPCs, are required for NB reactivation and may act as the local source of insulin in the brain. This work furthers the understanding of how dietary nutrients regulate neurogenesis through

insulin signaling, and highlights the strength of using *Drosophila* as a model to study how brain cells respond to local or circulating insulin.

Introduction

Insulin signaling, mediated by wide spread insulin receptor expression within the brain, regulates neuronal development, energy homeostasis, cognitive function, mood, and learning and memory (88,90,91). The majority of insulin delivered to the brain occurs through active transport across the blood-brain barrier (90,92–94). Recent evidence shows that GABAergic “neurogliaform” cells are also capable of producing insulin (96,97). Understanding how brain cells respond to insulin, and how insulin is delivered to those cells is important for understanding normal brain development and the progression of neurodegenerative diseases such as Alzheimer’s disease (104).

Insulin and insulin-like growth factor (IGF) signaling promote tissue growth in response to dietary nutrients (155). Insulin-like growth factor binding proteins (IGFBPs) bind IGFs with high affinity in mammals to modulate insulin signaling (156,157). *In vitro* evidence demonstrates a dual function of IGFBPs; whereby circulating IGFBPs in the blood antagonize IGF and act as potent growth inhibitors, whereas cells that have membrane-bound IGFBPs, or secrete IGFBPs into the extracellular matrix, create a higher insulin/IGF availability locally to the InR which result in higher InR signaling (156).

Drosophila have an insulin production and secretion system where the insulin producing cells (IPCs) reside in the medial region of the brain (120,138,158,159). The IPCs are secretory neurons in nature and release *Drosophila* insulin-like peptides (Dilps) in response to dietary nutrients (120,122,159,160). Dilp-1, Dilp-2, Dilp-3 and Dilp-5 are produced in the IPCs (139,161,162). Additionally, IPCs release Dilp-2 into the hemolymph in response

to dietary amino acids to promote systemic growth (159,163). IPCs also make contact with neurons in the brain and the suboesophageal ganglion (SOG) to release Dilp-2 locally (140). Because these neurons do not produce Dilp-2 mRNA, but recruit Dilp-2 protein from the IPCs, they are called Dilp-recruiting neurons (DRNs) (164). To recruit Dilp-2, the DRNs must express Imp-L2, and be in direct contact with the IPCs (140). Imp-L2 is a IGFBP7 homolog (165) that may share a dual function with respect to InR signaling like other IGFBPs (140).

We recently discovered that Dilp-2, the most potent growth regulator of all Dilps (139), plays a significant role in both neuroblast (NB) reactivation and NB niche development (Yuan et al., in review *PLOS Biology*). Researchers have demonstrated that IPCs, DRNs, and surface glia of the ventral nerve cord are all positive for Dilp-2 antibody labeling (55,120,140), making the identity of the cellular Dilp-2 source that reactivates quiescent NBs unclear. Here we confirm that IPCs produce Dilp-2 and release it locally within the brain to the DRNs during early larval stages (140). Genetic ablation of IPCs results in a failure of NB reactivation, similar to what we have observed in Dilp-2 null mutant animals. Taking advantage of the dual function of Imp-L2, over-expression of Imp-L2 in the fat body inhibits NB reactivation, possibly through counteracting circulating Dilp-2 in the insect blood hemolymph. Since the IPCs are neurons, we explored a possible Dilp-2-mediated neural circuit that regulates NB exit from quiescence. The DRNs that make physical contact and recruit Dilp-2 from the IPCs, are required for NB reactivation. In mice, GABAergic, dopaminergic and serotonergic neural circuits are proposed to be involved in neural progenitor proliferation (69). Uncovering an insulin-

mediated neural circuitry that regulates neural stem cell proliferation will shed light on a potentially evolutionarily conserved mechanism describing how brain insulin modulates neurogenesis.

Results

Insulin producing neurons are necessary to reactivate quiescent neuroblasts

We previously uncovered that Dilp-2*,* among the seven Dilps in *Drosophila*, plays a prominent role in reactivating quiescent NBs and promoting growth of the niche glia (Yuan et al., in review in *PLOS Biology*). However, it remains unclear which cells are producing Dilp-2, and how Dilp-2 is delivered to the NBs and cortex glia. To address these unknowns, we performed immunostaining of insulin receptor (InR) to identify the cellular targets of Dilp-2. We found that InR is abundantly expressed in the larval brain at the freshly hatched stage and 24 hours after feeding (Supp figure 1 A-D), demonstrating the brain's ability to respond to insulin signaling during early stage of larval development. Following this observation, we sought to identify the cellular source of insulin in the brain. IPCs have been demonstrated to release Dilp-2 into the hemolymph to promote growth systemically (163,166). In addition, surface glia in the ventral nerve cord are also known to express Dilp-2 (55). To investigate the cellular source of Dilp2 during early larval stages in the brain, we assayed the transcriptional expression pattern of Dilp-2 using *dilp2-Gal4* (167), and performed anti-Dilp2 immunofluorescence (Jan Veenstra). Aside from the 7 previously described IPCs, we observed 3 additional neurons in each brain hemisphere that were positive for Dilp-2 staining, although at a markedly reduced level compared to the IPCs (Figure 1B).

It has been previously described that a select few neurons in the brain, and in the suboesophageal ganglion (SOG) of the ventral nerve cord, make physical contact with the IPCs (140). These neurons are Dilp-2 positive, however, they do

not produce Dilp-2 transcriptionally (139). Instead, they recruit Dilp-2 via Imp-L2 expression (140). Thus they are named Dilp-recruiting neurons (DRNs) (164). Since NBs fail to reactivate in the *dilp2$_1$* mutant (Yuan et al., in review *PLOS Biology*), we postulated that lack of Dilp-2 produced from the IPCs was the cause. To test whether the IPCs were required for NB reactivation, we drove a pro-apoptotic gene Grim in IPCs to genetically ablate them. Because the Dilp-2 expression in DRNs is dependent on the IPC expression of Dilp-2 (140), it is presumed that ablating IPCs will also diminish the Dilp-2 expression in the DRNs. Indeed, when we drove *UAS-grim* to ablate the IPCs, we observed that NBs fail to reactivate from quiescence (Figure1 E, F and G). Because the IPCs are neurosecretory neurons and release peptides through neuron depolarization (120), we also drove *UAS-kir2.1*, a constitutively active potassium channel that causes neuron hyperpolarization to inactivate the IPCs without ablating them. Similar to the genetic ablation of the IPCs, when their neuronal activity was blocked, a significant delay of NB reactivation was observed (Supp figure 1 E and H).

Since the IPCs produce multiple Dilps including Dilp-1, Dilp-2, Dilp-3 and Dilp-5 (138,168), we asked whether the phenotype we observed when manipulating IPCs was specific to a reduction in Dilp-2 level. To accomplish this, we knocked down Dilp-2 in the IPCs using an RNAi line, and confirmed that majority of Dilp-2 expression was abolished by Dilp-2 antibody labeling (Supp figure 1G). Surprisingly, we observed a marginal increase in NB reactivation following the RNAi knockdown (Supp figure 1 F and H). Broughton et al have shown that Dilp-3 and Dilp-5 mRNA levels increase when Dilp-2 is knocked down

using an RNAi (169). Despite the evidence that Dilp-3 is not expressed in the IPCs during early larval stages (139), it is possible that by knocking down Dilp-2 using an RNAi line, Dilp-3 and Dilp-5 are upregulated in the IPCs as a compensatory mechanism, and thus masking the phenotype of NB failure of reactivation caused by the absence of Dilp-2. From these data, we conclude that IPCs are required for NB reactivation, possibly through controlling the release of Dilp-2.

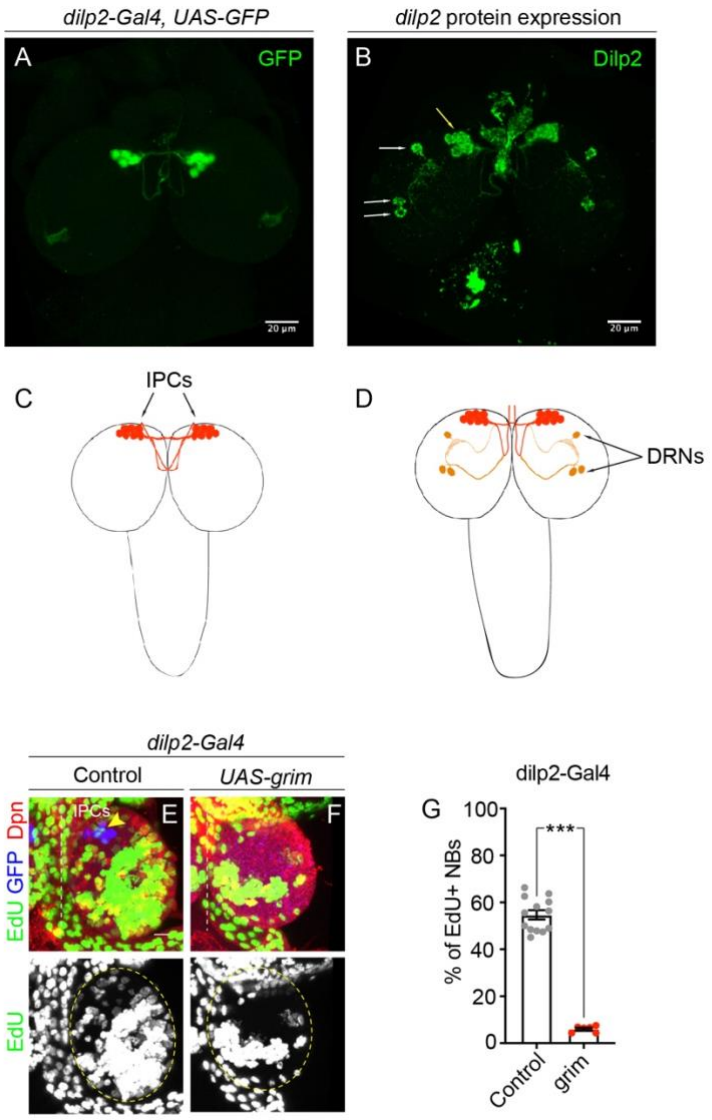

Figure 1. Neuroblasts fail to reactivate when ablating the cellular source of Dilp2. (A) Maximum intensity projection image of a brain showing *dilp2-Gal4* driving a cytoplasmic GFP, 24 hours fed. (B) Maximum intensity projection image of a brain showing Dilp-2 Ab staining, 24 hr fed. Yellow arrow: cluster of 7 IPCs in the left hemisphere. White arrows: 3 DRNs. (C). Cartoon illustration of the 14 IPCs

and their axon projections. (D). Cartoon illustration of the 3 DRNs (orange) in each brain hemisphere making physical contact with the IPCs (red). (E). Maximum intensity projection image of EdU incorporation in control animals. Genotype: *dilp2-Gal4* x *UAS-GFP*/OR. Arrow head points to the cluster of IPCs. (F). Maximum intensity projection image of EdU incorporation in *grim* animals. Genotype: *dilp2-Gal4* x *UAS-GFP*/*UAS-grim*. Scale bar: 10 μm. (G). Quantification of reactivated NBs in E and F. Control genotype: *dilp2-Gal4* x OR. Control: mean = 54.7. grim: mean = 6.06. Student's two-tailed t-test, *** $p < 0.001$. Data are represented as mean ± SEM.

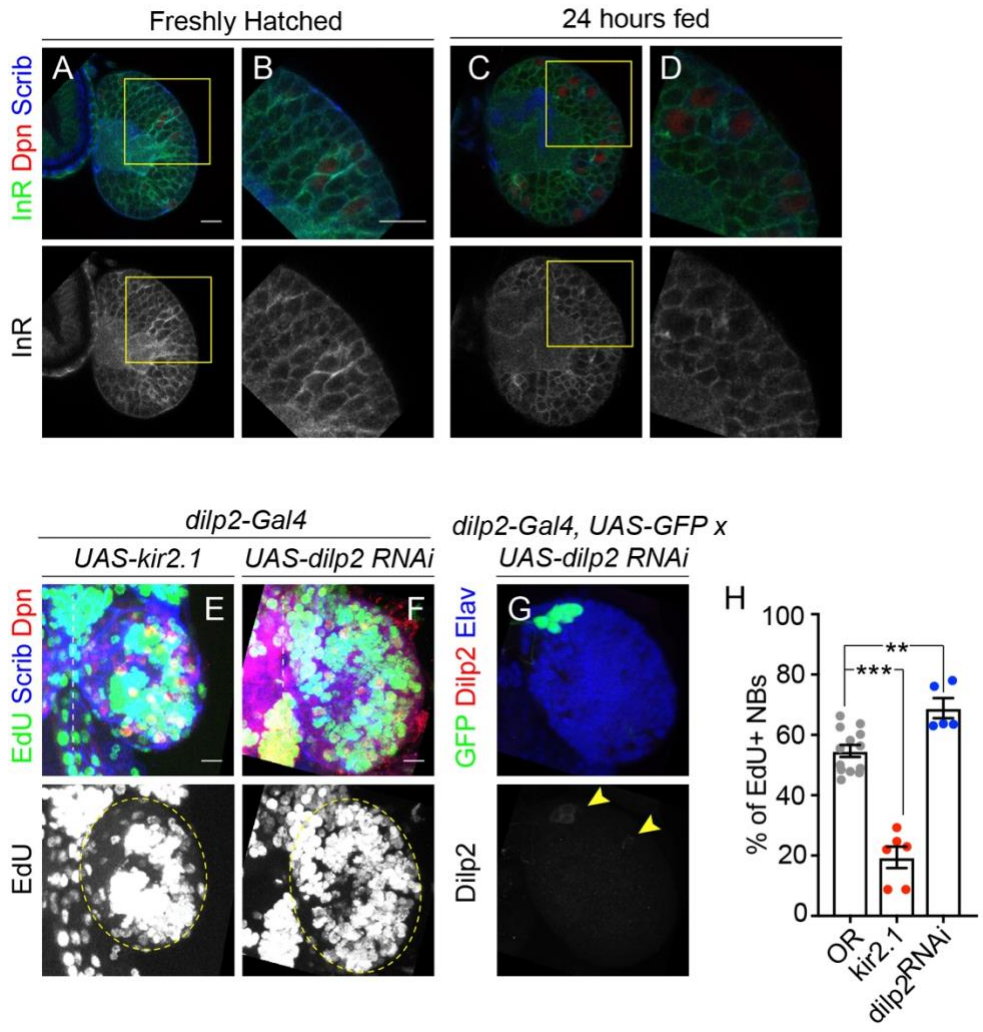

Supplemental figure 1. (A) and (C). Single Z plane image showing InR Ab staining (B) and (D). Magnified image of the yellow square in A and C, respectively. (E) and (F). Maximum intensity projection image with merged channels on top and greyscale image of EdU channel on the bottom. White dashed lines indicate the midline of the brain hemispheres. Yellow dashed lines circle the brain hemispheres. (G). Dilp-2 Ab staining in the IPCs of *dilp2-Gal4* x *UAS-dilp2 RNAi* larvae. Yellow arrowheads point to residual Dilp-2 Ab. (H). Quantification of percentage of reactivated NBs in E and F. *dilp2-Gal4* was crossed to OR as the control. OR: mean = 54.7; kir2.1: mean = 19.42 dilp2RNAi: mean = 68.88. One-way ANOVA

with post-hoc Tukey test, ** $p < 0.005$, *** $p < 0.001$. Data are represented as mean ± SEM. All scale bars are 10 μm.

Circulating insulin is required for neuroblast reactivation from quiescence

Since we observed two distinct Dilp-2-expressing neuronal populations, we postulated that either the systemic release of Dilp-2 to the hemolymph, or local release within the brain is required to reactivate quiescent NBs. To distinguish between these two possibilities, we first tested whether increased levels of circulating Dilp-2 in the hemolymph would accelerate NB reactivation. We used *r4-Gal4* to overexpress Dilp-2 from the fat body, which can secrete Dilp-2 upon feeding, and measured rate of NB reactivation. Surprisingly after 24 hours of feeding, we observed a decrease in the number of proliferating NBs when over-expressing Dilp-2 in the fat body(Figure 2A, 1B and 1E). This may be caused by a Dilp-2 induced growth competition between the peripheral tissue and the brain when ectopically high levels of Dilp-2 are present in the hemolymph. To identify the consequence of reducing Dilp-2 levels in the hemolymph, we blocked circulating Dilp-2 by overexpressing Imp-L2, an IGFBP7 homolog that binds to Dilp-2 and counteracts its activity (165). Dilp-2 promotes tissue growth systemically (139,158), and overexpression of Imp-L2 in the fat body strongly reduces body size, whereas Imp-L2 mutant animals show increased body size (165). Indeed, when we over-expressed Imp-L2 in the fat body, despite maintenance of animal feeding, NBs failed to reactivate after 24 hours (Figure 2C and 2E). From these data, we suspected that ImpL2 in the hemolymph could enter the brain and interfere with the local source of Dilp-2. To test this possibility, we performed Dilp-2 antibody labelling in the brain of Imp-L2 overexpression animals. We observed high levels of Dilp-2 expression in the IPCs, in both cell bodies and axons (Figure

2D) indicating that the ability of IPCs to produce, and perhaps release, Dilp-2, remains normal in the Imp-L2 over-expression animals.

Next, we asked whether peripheral insulin was sufficient to reactivate quiescent NBs in the absence of food consumption. To test this hypothesis *in vivo*, we needed to remove Dilp-2 that is released locally in the brain, and provide a source of circulating Dilp-2 in the hemolymph. Dilp-2 secretion from the IPCs is controlled by dietary nutrients (159,163). We attempted to test this hypothesis *in vivo* through overexpression of Dilp-2 in the fat body while depriving larvae of dietary nutrients. Under this condition, endogenous Dilp2-release is inhibited, and only Dilp2-secreted from the fat body is provided ectopically. This perturbation under nutrient deprivation resulted in lethality, and we were unable to proceed with the examination of NB reactivation (data not shown). To overcome this, we explored an alternative *ex vivo* method that incubates larval brains in bovine insulin as an alternative of circulating Dilp-2. Freshly hatched (FH) brains were dissected, incubated in Schneider's media with insulin, antibiotics, and EdU for 12 hours, and then examined for EdU incorporation in the brain (Figure 2F). We observed reactivated NBs from FH larval brains after 12 hours of incubation with Schneider's media supplemented with insulin (Figure 2G). To test whether the reactivation of NBs occurred because circulating insulin activated the local source of Dilp-2, we incubated brains from Dilp-2 mutant larvae in the same culture media. No endogenous Dilp-2 is present in these larvae, including the local source of Dilp-2 in the brain. Similar to control larvae, we observed reactivated NBs in these Dilp-2 mutant brains (Figure 2H). This result demonstrates that bovine insulin is sufficient

to reactivate *Drosophila* NBs when present outside the brain, and that no endogenous source of Dilp-2 is required.

The caveat of this experiment is that we utilized a high concentration of bovine insulin (1.74 x 10_5 pM), which is 872 times higher than the concentration of circulating Dilp-2 in an adult animal (assuming the concentration of circulating Dilp-2 is around 200 pM, (170)). When we tested media with a low concentration of bovine insulin, one that reflects a similar concentration to circulating Dilp-2 levels in *Drosophil*a, the brain structural integrity was compromised from those cultural media after 12 hours of incubation (data not shown) and difficult to evaluate. Taken together, these results suggest that circulating Dilp-2 is required to reactivate quiescent NBs, possibly through active transport by the blood-brain barrier similar to mammals (90,93,94). Whether circulating Dilp-2 alone is sufficient for the reactivation requires further experimentation.

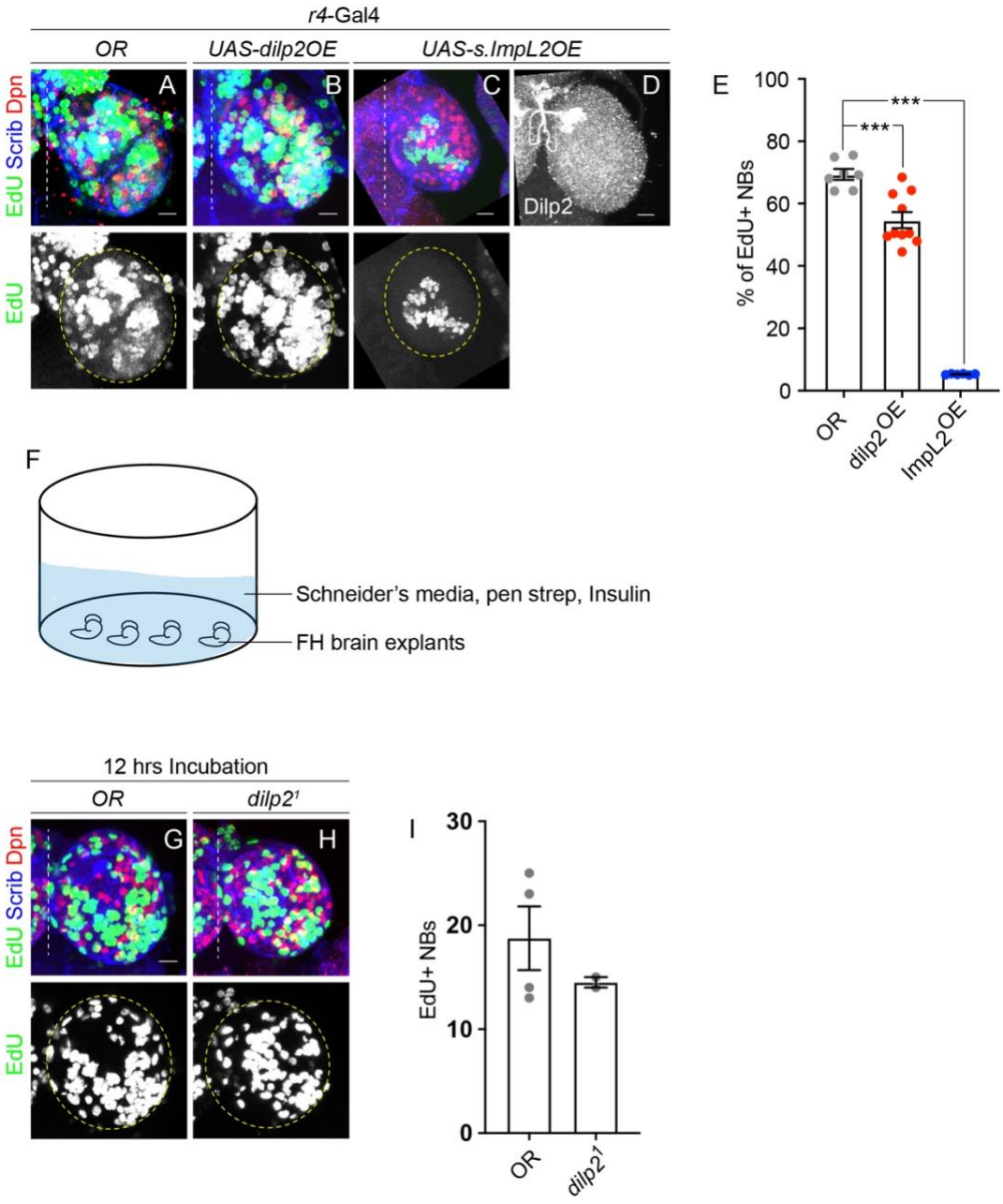

Figure 2. Blocking Circulating Dilp-2 inhibits NB reactivation.

(A) (B) (C). Maximum intensity projection images of 24 hr fed larval brains. Top panels show merged channels, bottom panels show greyscale EdU channel. Genotypes are shown above the panels. (D). Maximum intensity projection of

greyscale image of Dilp-2 staining in *ImpL2* OE larval brain. (E). Quantification of A, B and C. OR: mean = 69.37; dilp2 OE: mean = 54.73; ImpL2 : mean = 5.27. One-way ANOVA with post-hoc Tukey test, *** $p < 0.001$. Data are represented as mean ± SEM. (F). Cartoon demonstrating incubation media of *ex vivo* brain culture. (G) and (H). Maximum intensity projection images of FH larval brains after 12 hrs of incubation in Schneider's media supplemented with bovine insulin. Genotypes are indicated above the panels. (I). Quantification of G and H. OR: mean = 18.75. $dilp2_1$: mean = 14.5. Student's two-tailed t-test. Data are represented as mean ± SEM. All scale bars are 10 μm.

DRNs are required to reactivate quiescent neuroblasts

IPCs have been shown to release Dilp-2 both systemically into the hemolymph and locally within the brain (120,123,140,164). Next, we explored whether the DRNs act as a local source of Dilp-2 to reactivate quiescent NBs. *ImpL2-RA-Gal4* in combination with *repo-Gal80* was used to label the Imp-L2 positive neurons, and inhibit glial expression of *ImpL2-RA-Gal4* through expression of *repo-Gal80*. Imp-L2 is expressed in the blood-brain barrier glia and a subpopulation of neurons in the brain, and *ImpL2-RA-Gal4* faithfully reflects Imp-L2 protein expression pattern (171). Imp-L2 can be secreted both into hemolymph to counteract Dilp-2*,* or into the extracellular matrix to create a higher local concentration of Dilp-2 to activate the InR on the cell membrane (140,164,165,172). To address this, we first assayed whether the DRNs are specified and become Dilp-2 positive before larval begin feeding. We found that in the FH larval brain, the three DRNs that make neuronal contact with the IPCs are present based on expression of *ImpL2-RA-Gal4*. However, most of them are Dilp-2 negative (Figure 3A and 3C). In the FH larval brains, the IPCs (7 per brain hemisphere) contribute to the majority of the Dilp-2 positive neurons. After 24 hours of larval feeding, we observed an increased number of neurons that are either Imp-L2 positive, Dilp-2 positive or Imp-L2, Dilp-2 double positive (Figure 3B and 3C), demonstrating that additional neurons become Dilp-2 positive after feeding. All the Dilp2 positive neurons except for the IPCs are also Imp-L2 positive, suggesting that expression of Imp-L2 recruits Dilp-2 protein to the neuron cell surface as described previously (140).

Next, we assayed whether the DRNs, labeled by *ImpL2*, are required for NB reactivation. Inhibition of DRN activity via expression of *UAS-kir2.1*, resulted in inhibition of NB reactivation (Figure 3D, E and F). Since DRNs' neuronal activity is required for NB reactivation, and DRNs potentially act as a local source of Dilp-2 for the NBs, we sought to counteract only the local source of Dilp-2. Overexpression of Imp-L2 in glia in the CNS could possibly counteract Dilp-2 present in the brain via direct binding to decrease the bioavailability of Dilp-2 to InR. When we performed this experiment, we observed no reactivated NBs (Figure 3G and 3I). To test whether this experiment interfered with systemic Dilp-2 release from the IPCs, we performed Dilp-2 antibody labeling, and observed low levels of Dilp-2 present in the IPCs (Figure 3H). These experiments suggest that IPC production of Dilp-2 is compromised when we overexpressed Imp-L2 in glia, and that systemic Dilp-2 release is possibly reduced as well. We conclude that the DRNs are required for NB reactivation, possibly through modulation of the IPCs to control Dilp-2 release. Whether the DRNs reactivate quiescent NBs through Dilp-2 release locally in the brain requires further investigation.

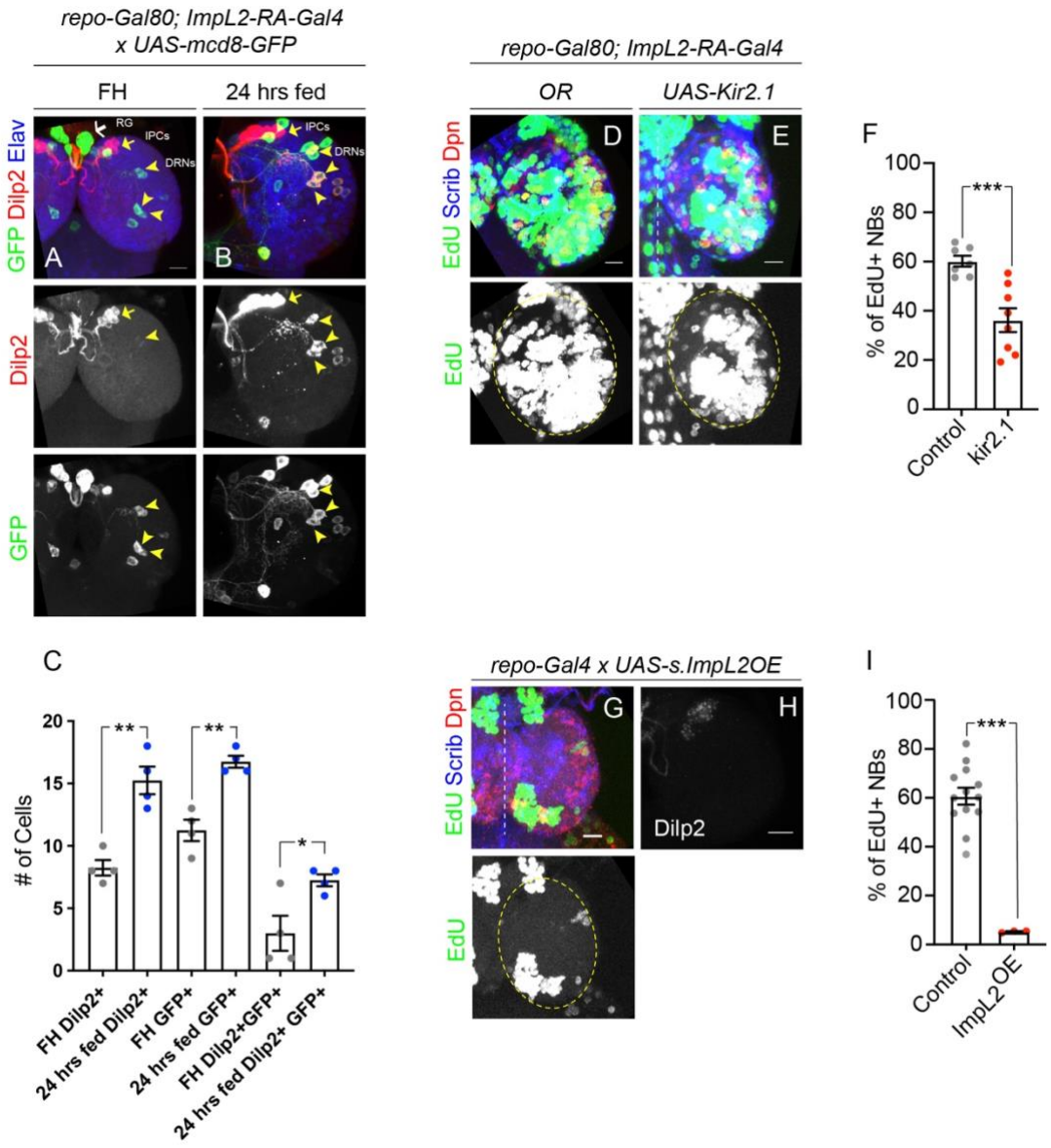

Figure 3. Neuronal activity of the DRNs is required for NB reactivation.

(A) and (B). Maximum intensity projection images showing Dilp-2 positive and ImpL-2 positive neurons. Merged channel images on top and greyscale single channel images on the bottom. Yellow arrows point to the IPCs, and yellow arrowheads point to the DRNs. (C). Quantification of A and B. Number of FH Dilp-2+ neurons: mean = 8.25; number of 24 hr fed Dilp2+ neurons: mean = 15.25; **

p = 0.002. Number of FH GFP+ neurons: mean = 11.25; number of 24 hr fed GFP+ neurons: mean = 16.75; ** p = 0.001. Number of FH Dilp-2+GFP+ neurons: mean = 3; number of 24 hr fed Dilp-2+GFP+ neurons: mean = 7.25; * p = 0.03. Student's two-tailed t-test. Data are represented as mean ± SEM. (F). Quantification of D and E. Control genotype: *repo-Gal80; ImpL2-RA-Gal4* x OR. Control: mean = 60.16; Kir2.1 = 36.23. Student's two-tailed t-test, *** p < 0.001. Data are represented as mean ± SEM. (G) Maximum intensity projection image with merged channels on top and greyscale image on the bottom. (I). Control genotype: *repo-Gal4 x OR*. Control: mean = 60.66; ImpL2 = 5.21. Student's two-tailed t-test, *** p < 0.001. Data are represented as mean ± SEM. All scale bars are 10 μm.

Discussion

Drosophila are an incredible model organism to study how dietary nutrients reactivate quiescent NBs to achieve proper neurogenesis. The current model of NB reactivation starts with larval food consumption, followed by release of an unknown fat body-derived signal (FDS) from the fat body. This FDS initiates local insulin secretion within the brain enabling NB exit from quiescence (48,55,56). Here we demonstrate that both local and circulating Dilp-2 are required for the reactivation of quiescent NBs. Additionally, we identify two populations of Dilp-2 positive neurons, the IPCs and the DRNs, which are both required for NB reactivation. Blocking circulating Dilp-2, or brain Dilp-2 via expression of Imp-L2 leads to failure of reactivation.

The DRNs make physical contact with the IPCs (140). However, whether this contact is axonal or dendritic in nature remains to be investigated. Understanding how the DRNs and the IPCs communicate and transport peptides between each other might shed light on how neural circuitry influences neurogenesis.

To further demonstrate that circulating insulin is sufficient to reactivate quiescent NBs *ex vivo*, and avoid using ultra high level of bovine insulin in the incubation, one could collect larval hemolymph and use that as an incubation media. In addition, one could incubate brains with synthetic Dilp-2 (173). This methodology could demonstrate an active transport of peripheral insulin into the brain and drives insulin signaling in brain cells.

In this chapter, we investigated whether NB reactivation requires Dilp-2 locally produced in the brain, or circulating Dilp-2 entering the brain through blood-

brain barrier transport. Clinically, individuals with type 2 diabetes mellitus (T2DM) are associated with cognitive deficits, and are at increased risk of neurodegenerative dementias (104) Conversely, in Alzheimer's disease and related dementias (ADRDs) patients, brain tissue exhibits abnormal insulin signaling including decreased insulin and insulin receptor expression levels (104). Understanding how insulin signaling in various cell types in the brain is coordinated with each other, as well as how systemic insulin signaling coordinates with insulin signaling in the brain will shed light on the relationship of T2DM and cognitive function in humans. Also, insulin and adipocyte-derived leptin target the hypothalamus to control energy homeostasis (174). A recent study showed that reduction in circulating leptin levels restores insulin sensitivity in obesity (175). As the functional homolog of leptin in flies has been uncovered (121), one could also utilize *Drosophila* as a model to study the interplay between insulin and leptin, which will provide significant insight into how nutritional status influences cognition and energy homeostasis.

Materials and Methods

Fly Husbandry

Animals were raised in uncrowded conditions at 25°C under a 12 hour light/dark cycle. Fly stocks used in this chapter are listed in appendix table.

Immunofluorescence

Larval brains were fixed and stained as previously described (176) (177) (46). Briefly, larval brains were dissected in 1xPBT. L1 and L3 brains were fixed with 4% paraformaldehyde in PEM buffer for 20 mins and 30 mins, respectively. After thorough washing in 0.1% Triton-x/PBS, antibody staining was performed according to standard methods. Primary antibodies used in this study were: chicken anti-GFP (1:500, Abcam, Cambridge, MA), rat anti-Deadpan (1:100, Abcam), rabbit anti-Scribble (1:1000; gift of C. Doe). Rabbit anti-DsRed (1:1000 Clontech), mouse anti-Repo (1:5 DSHB), guinea pig anti-InR (1:300; C.Doe) Secondary antibodies were conjugated to Alexa Fluor dyes (Molecular Probes).

Feeding Assay

Freshly hatched larvae were picked and transferred on standard Bloomington fly food. Flies were raised at 25 °C throughout.

EdU Treatment

0.1mM EdU was supplemented to Bloomington Fly food. The following EdU Click-iT kits were used: EdU Click-iT Alexa 488 Imaging Kit, and EdU Click-iT Alexa 647 Imaging Kit (Invitrogen).

Confocal microscopy

Larval brains were mounted in Antifade Gold (Invitrogen), and imaged using a Leica SP8 laser scanning confocal microscope equipped with a 63×/1.4 NA oil-immersion objective.

Percentage of Proliferating Neuroblasts

Quantifying percentage of proliferating Neuroblasts and number of glial cell nuclei: Number of Dpn+ cells and Dpn+ EdU+ cells in the entire central brain were manually counted using the “cell counter” plugin in Fiji (178). To quantify the total number of Dpn+ cells, Dpn and Scribble channels were merged together, and Dpn+ NBs were marked throughout the z stack using one color in the “cell counter” plugin. This plugin automatically recorded cell counts. Dpn, EdU and Scribble channels were merged together to count Dpn+ EdU+ cells with a second color. Dpn+ intermediate progenitors and optic lobe NBs were identified based on distinct brain regions outlined by Scribble, and excluded from the analysis. The number of repo+ nuclei in the central brain were also manually counted using Fiji “cell counter” (Kurt De Vos).

***Ex Vivo* Brain Culture**

Larval brains from freshly hatched larvae were dissected in Schneider's media (Gibco), and transferred into 1 ml of the Schneider's based incubation media that consists of 4.9 ml of Schneider's media, 100 μl Pen-Strep (Sigma, P4458), 5 μl 10 mg/ml Insulin from bovine pancreas, in 25 mM HEPES, pH 8.2 (Sigma, I0516). 10 μl of 0.1 mM EdU was then added to the media and brains were cultured for 12 hours in a 25 °C incubator. Brains were then fixed and stained as described above. The concentration of bovine insulin in the incubation media is approximately 872 times higher than circulating Dilp-2 level (170).

Statistical analysis

Student's t-test and one-way Anova were done in Graphpad Prism 8. Data in scatter plots with bar are presented as ± SEM.

Chapter IV

Discussion and Future Directions

Dietary nutrients regulate stem cell proliferation, however, the molecular and cellular underpinnings of how dietary nutrients impact stem cell niche development is understudied. In this dissertation, I presented evidence that dietary nutrients induce Dilp-2 release from the insulin-producing cells (IPCs), both systemically into the hemolymph, and locally in the brain. Dilp-2 drives cell-autonomous PI3-Kinase activation resulting in cell growth within NBs and cortex glia. Cerebral tracheal growth is nutrient and PI3K dependent, however not regulated by Dilp-2 signal. Activated PI3K is also required non-autonomously in cortex glia and the trachea to reactivate quiescent NBs. Reactivation and growth of NBs is also required for glial membrane growth, demonstrating the importance of bi-directional signaling between NBs and their cortex glial niche. Finally, insulin/PI3K signaling promotes robust cortex glia and NB contact (see summary figure).

While we have addressed how nutrients regulate cellular interactions between NBs, glia and trachea, and investigated the cellular source of Dilp-2, several questions in the field remain unanswered. For example, we observed inhibition of NB reactivation in the Dilp-1 and Dilp-7 null mutant animals as well. These observations reveal the following questions: are Dilp-1 and Dilp-7 also required for cell growth of cortex glia and trachea? What are the cellular sources of Dilp-1 and Dilp-7 during early stage of larval development? It is reported that the IPCs produce Dilp-1 transiently during pupal phases (179). Perhaps Dilp-1 is released to ensure reactivation of NB occurs as a backup mechanism. Dilp-7 is

expressed in dMP2 neurons in the abdominal region of the ventral nerve cord, which are efferent neurons that project onto the hindgut (180). Another pair of Dilp-7 neurons, the DP neurons, terminate close to the protocerebral region of the IPCs (34,180,181). It is possible Dilp-7 regulates NB reactivation through regulation of nutrient absorption or activity of the IPCs.

The current model of how NBs reactivate from quiescence requires the drosophila fat body (FB) to secrete un unknown mitogen to the brain in response to nutrient intake (45,48). Future investigation must address how IPCs sense nutritional status to release Dilp-2 and reactivate NBs to promote development of the NB stem cell niche. Many secreted peptides from the FB have been uncovered to regulate IPCs in the brain, such as Unpaired (Upd2) (121), CCHamide-2 (182), Stunted (159), Growth-blocking peptides (GBP1 and GBP2) (122,160). Whether the IPCs receive nutritional information through one of the known fat body derived signals (FDS), or a novel FDS, to reactivate quiescent NBs remains unsolved. In addition, the IPCs can also directly sense extracellular leucine via receptor minidiscs to regulate Dilp-2 expression (183). It is possible that IPCs release Dilp-2 through direct amino acid sensing present in the hemolymph. Many neural circuits have been demonstrated to couple nutritional information with insulin secretion through regulation of IPCs (160,162). In this dissertation I presented evidence that dilp-recruiting neurons (DRNs) are required for NB reactivation. Whether the neuronal activity of DRNs are nutrient responsive, and in turn regulate the activity of IPCs in response to dietary nutrients will be the topic of future

investigation. Taken together, these studies identify possible avenues for further understanding of how IPCs sense nutritional status.

Nutrient regulation of the neural stem cell niche has been well studied in *Drosophila* germline stem cells and intestinal stem cells. Nutrient availability and insulin signaling heavily influence stem cell proliferation, maintenance and their niche function (36,184). The *Drosophila* neural stem cell niche could be the next best studied model to help us understand how change in niche cytoarchitecture regulates stem cell proliferation and quiescence in response to dietary nutritional cues. One could utilize the ease of conducting feeding assays in *Drosophila* to explore various nutrient deficient diets, and assay morphological or transcriptional changes in both NBs and their niche cells. Future work in the *Drosophila* NB stem cell niche will shed light on how neurogenesis occurs in other organisms through conserved cell types and signaling pathways.

Summary

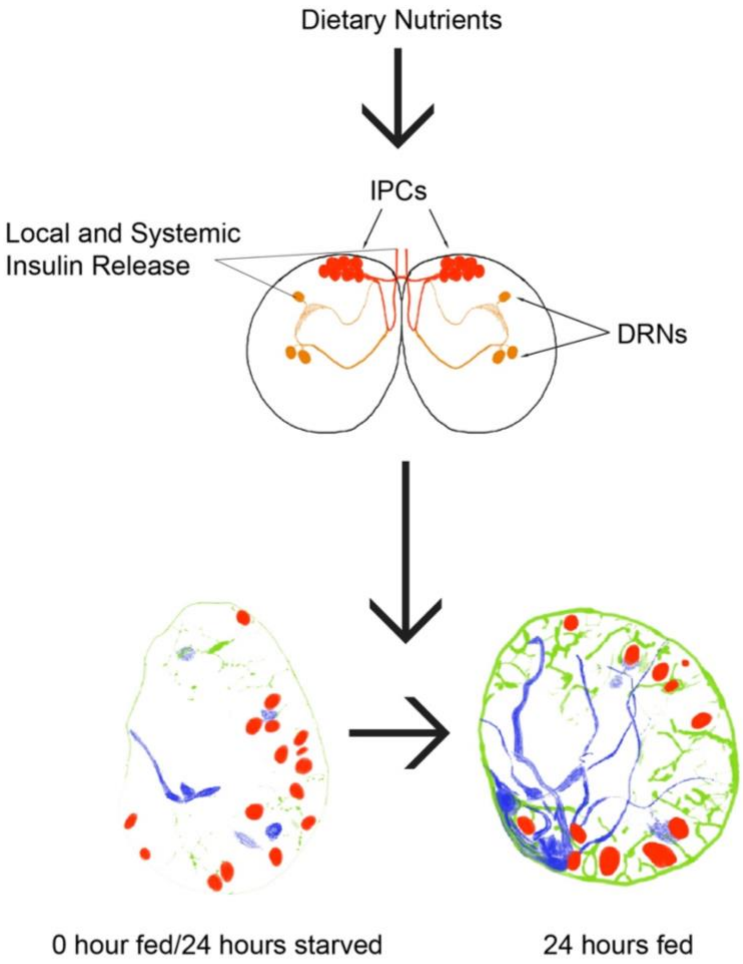

Glia: endoreplication and membrane growth, ensheathment of the neural stem cells
Neural Stem Cell: cell size increase and reactivation from quiescence
Trachea: trachea increase in surface area, branching and infiltration of the brain

Appendix I

Live Imaging Techniques of Whole Larvae and Brain Explants

Live imaging techniques are important for the visualization of dynamic biological processes. To visualize and capture the dynamic glial membrane processes interacting with proliferating neuroblasts in response to dietary nutrients, I explored time-lapse imaging techniques of live larvae to visualize cellular activities in the larval brains. In addition, to live image brains that reside in pigmented pupal cuticles, I utilized *ex vivo* brain culture live imaging techniques adapted for both upright and inverted confocal microscopes. Imaging intact, live larvae *in vivo* would provide the most accurate information that reflects animal physiology after ingesting dietary nutrients. However, the imaging window for intact, live larvae is limited due to a disruption of larval feeding while the animal is immobilized for imaging. The imaging window for *in vitro* or *ex vivo* cultures allows for longer time-lapse recordings to capture multiple neuroblast division events; however, growth media present in the culture could potentially interfere with the endogenous cellular activities. With pros and cons of both methods in mind, here I present two immobilization and mounting methods developed to image live larvae, as well as two mounting methods for imaging *ex vivo* brain cultures.

Live Larvae techniques:

To explore the effect of dietary nutrients on larval neuroblast proliferation and the dynamics of their glial niche, we explored methods of imaging straight through the larval cuticle. *Drosophila* larvae present an advantage for whole animal, live

imaging, due to their translucent cuticle. We tested two whole-larvae immobilization techniques for live imaging methods; a microfluidics method and a gluing method. The microfluidics larva chip immobilization method is best suited for experiments that require the recovery of the imaged larvae; where the Elmer's glue method is best suited for screening of gene expression patterns in the whole larvae.

Microfluidics Chip

To immobilize *Drosophila* larvae, we tested the published method "larva chip," a microfluidics apparatus that was developed for live imaging (185). We modified this method for use with an upright confocal microscope. In brief, a polydimethylsiloxane (PDMS) chip is placed on a glass microscope slide (Fisherfinest Premium Microscope slides superfrost, 25 x 75 x 1mm), adhered by double-sided tape (Scotch brand) (Figure 1A). A 1ml syringe attached to a 3-way valve regulator was used to create a vacuum plunger. A 25-gauge needle was inserted into the polyethylene tubing. The other end of the tubing was connected to the vacuum port on the PDMS chip (Figure 1C). The larva with a drop of halocarbon oil was then placed in the microchamber, and the coverslip was placed on top of the larva. Then the syringe was pulled to remove the air from the apparatus and bring the larva up against the coverslip (Figure 1D).

The advantage of this method is that this is nontoxic and maintains the structural integrity of the larval body wall and well-being of the imaged larva, which remains alive throughout the mounting and imaging process. This technique is best suited for longitudinal experiments that require multiple time points and several

days of analysis. For example, as stated in Mishra et al., one could induce nerve crush injury of the segmental nerves on the body wall muscles of the larva, recover the larva on a grape juice agar plate, then observe and conduct time-lapse imaging of Wallerian degeneration at different time intervals of the same larva (185).

The disadvantage of this method is that the exposure of the larval CNS to the laser of a laser scanning microscope can induce violent movement, possibly due to the laser damaging the larval visual system, which is located near the CNS (186). Because we are interested in cellular dynamics in the brain, this method is not suited for stable time-lapse of the brain for our purposes. It is a good method to live image time-lapse movies of the PNS, or take snapshots of the brain. However, due to the violent movement of the larval head area, stable time-lapsing of the brain is difficult.

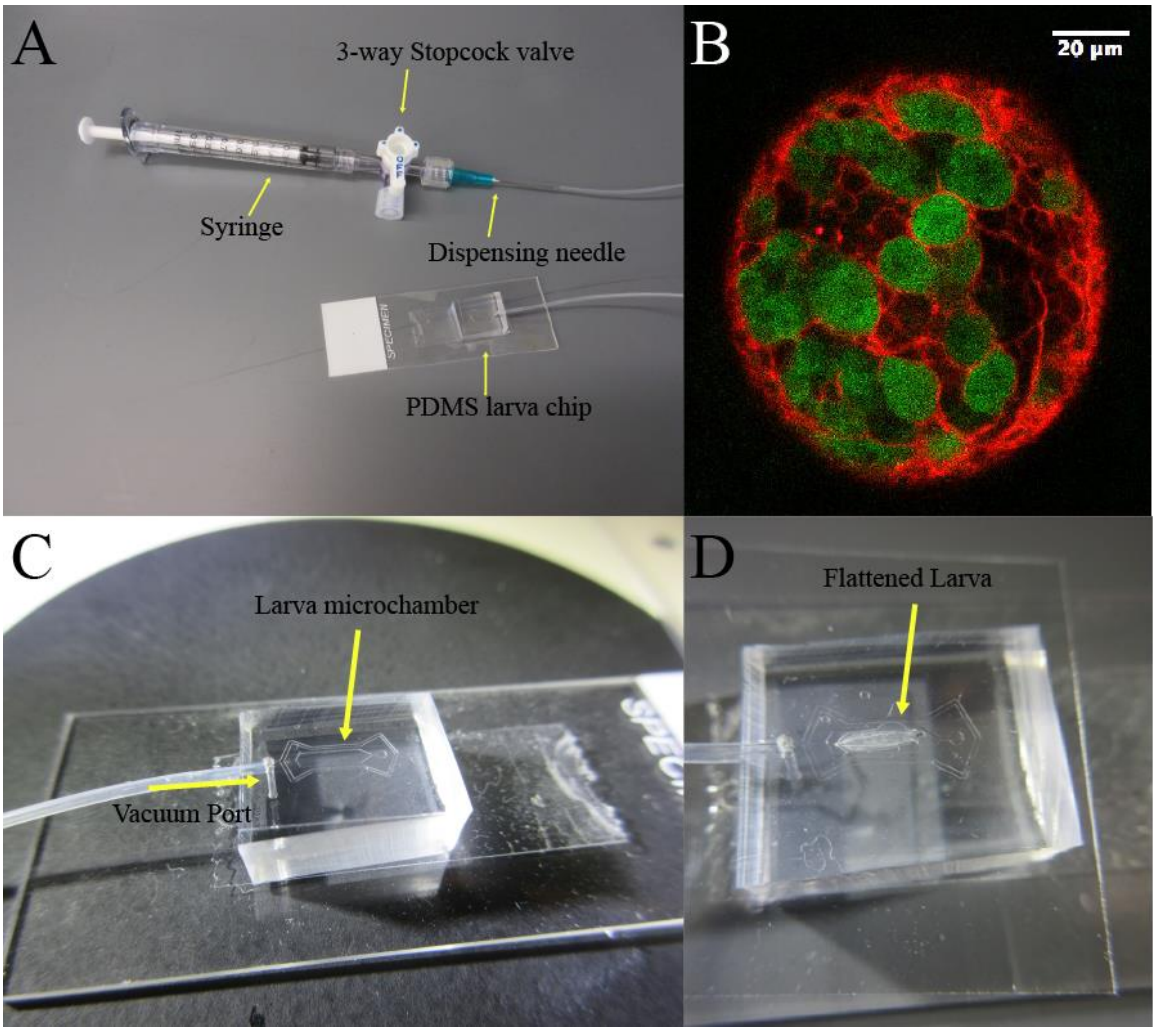

Figure 1. Microfluidics "larva chip" apparatus for immobilization of L2/L3 larvae for live imaging

(A). Ensemble of the microfluidics chip apparatus. (B). Confocal image of larval brain mounted on the larva chip. Genotype: pcna-GFP; repo-Gal4, pcna-GFP x UAS-mcd8-mRFP. GFP is in green, and RFP is in red. (C). Larva microchamber and vacuum port on the larva chip pointed out by arrows. (D). A L2 larva flattened in the microchamber after vacuum is applied through the syringe.

Elmer's Glue:

The larva chip is customized to immobilize very specific larval stages. For example, it would require a different larval chip with a bigger microchamber to image an L3 larva compare to a smaller L2 larva. To immobilize larvae during all stages of larval development for imaging, I sought to identify an adhesive product that would immobilize larvae between the glass slide and the coverslip. We tested different glues, including: Krazy glue (Elmer's products, Inc.), Gorilla Super glue (The Gorilla glue company) and Elmer's clear liquid glue (Elmer's products, Inc.). I determined that Elmer's clear liquid glue was the most effective product tested. It appropriately flattens the larva against the coverslip, and provides sufficient support to the larva from its viscous gooey texture and prevents explosion of the larva under pressure. To glue the larva, first, a drop of Elmer's glue (approximately 0.5 cm in diameter) was applied on the glass slide. The amount of glue applied is dependent on the size of the larva (more Elmer's glue is required to immobilize bigger larvae). Then a single larva was placed onto the center of the glue, and the larva's position was adjusted with a stainless steel probe (Fine Science Tools No. 10140-01, tip diameter 0.25 mm) for a relative straight body orientation and dorsal side facing up. Finally, a cover slip was placed on top of the larva in the glue. When lowering the coverslip over the larvae, it is important to allow the coverslip itself to slowly press down into the glue. This allows the coverslip to be carefully rolled horizontally to adjust the position of the larva and to ensure that the dorsal side of the larva is facing up (Figure 2A). Fluorescence as well as DIC images were then obtained to provide both fluorescence and anatomical information of the organ

imaged (Figure 2B). This method is best suited for taking a snapshot of transgenic labeling in the anatomical context of whole larvae since larvae would survive for only a short period of time after mounting.

Gluing live larvae on a microscope slide using Elmer's glue provides a fast and user friendly method to immobilize larvae from all developmental stages for live imaging. Compared to the larva chip method, larvae are consistently and stably mounted in the Elmer's glue, which provides stable imaging of different areas throughout the larval body. One could screen gene expression patterns in transgenic larvae using this immobilization method as soon as larvae reach a desired stage and at relatively low cost. The disadvantage of this method is that larvae are irrecoverable after mounting, possibly due to lack of oxygen as well as hardening of the glue. Therefore, the live imaging window is limited to less than an hour.

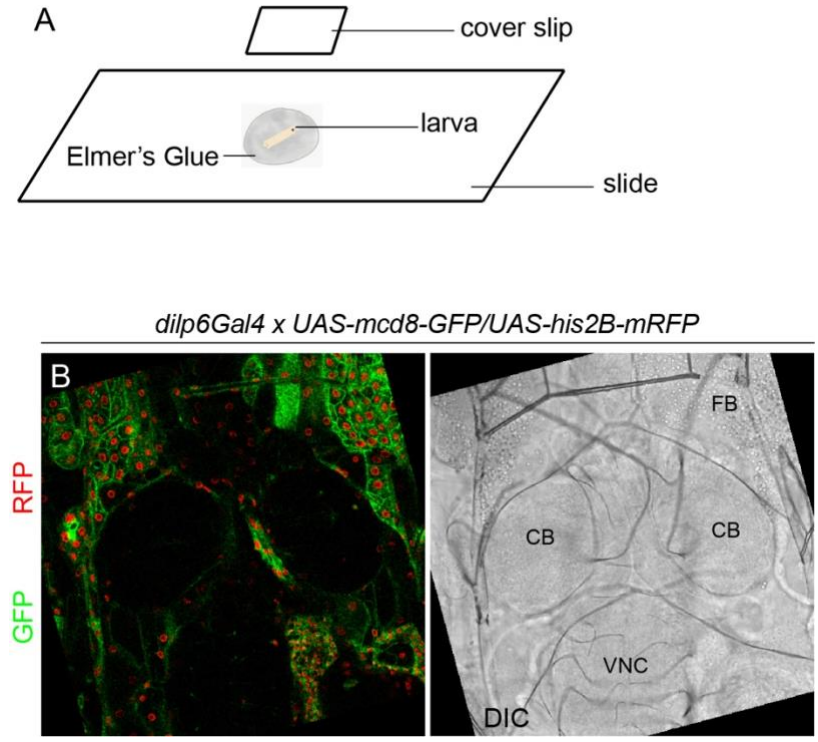

Figure 2. Whole larva immobilization by Elmer's glue and live imaging.

(A). Schematic of immobilizing a single larva on a glass slide using Elmer's glue. (B). Single plane confocal image of an L1 larval brain obtained from this immobilization method. Left, membrane GFP and nuclear mRFP signal from live fluorescence. Right, DIC image providing anatomical information of the brain on the left. FB: fat body. CB: central brain. VNC: ventral nerve cord. Genotype listed above panel B.

Ex vivo brain culture techniques:

As larvae explore their environment and feed on food, they use their mouths to propel their bodies while digging into the food (187). The larval brain is connected to the mouth hook through other tissues (188). As the larvae remain alive and feeding, larval exploratory movements will cause back and forth movement of the brain through movements of the head and mouth hook. To ensure immobilization of the brain during time-lapse imaging for brief periods, we developed an approach of imaging brain explants in culture, as separating brains from the mouth hooks eliminates the pulling motion. In addition, imaging the brain cultures *ex vivo* is especially advantageous for visualizing biological processes in the *Drosophila* pupal brains, since pupae reside in pigmented pupal cases that make it difficult for fluorescent imaging. The culturing apparatuses also keep the brains in place, therefore minimizing movement of the brains during the imaging window.

The fat bodies in *Drosophila* are known to secrete an unknown mitogen to the brain to stimulate neural stem cell proliferation (45,159). Therefore, to image mitotic neural stem cells, larval or pupal brains were dissected, and then co-cultured with the fat bodies dissected from third instar larvae, a stage when larvae reach peak growth and neurogenesis with potentially most mitogen secreted from the fat bodies (45,50). We explored two commonly used insect medias that mimic the hemolymph (insect blood), a D22 (189) (HIMEDIA) based media and a Schneider's (Schneider and Blumenthal, 1978) (Gibco) based media. To make 10 ml of D22 based culture media, I combined 9.25 ml D22 media with 750 μl Bovine

Growth Serum (BGS) and 5 μl 1M ascorbic acid (72,190). Schneider's media was used on its own to culture the larval brains.

Imaging ex vivo brain culture on an inverted microscope:

In order to image our *ex vivo* brain cultures on an inverted confocal microscope, I adapted a mounting method from Lewis and Kucenas (191). First, larval brains were dissected in Schneider's media at room temperature. A single brain with approximately 10 μl media was then pipetted onto the center of the coverslip of a glass-bottomed 35 mm Petri dish (Electron Microscopy Sciences) (Figure 3A). A drop of liquefied and cooled 1% low-melting point agarose (Invitrogen) was then applied onto the brain (Figure 3B and 3C). I picked 1% agarose to ensure that the firmness of the agarose is sufficient to stabilize the brain once it is hardened. Before the agarose solidified, a stainless steel probe was used to quickly adjust the position of the brain in agarose so that the dorsal side of the brain was pressed against the coverslip. 1 ml of Schneider's media was then applied to cover the brain mounted in agarose (Figure 3D). Fat bodies dissected from fed L3 larvae were then added into the Schneider's media in the dish to co-culture with the brain. The glass-bottomed petri dish was put onto an inverted microscope and a time-lapse was begun. Figure 3F and 3G shows still images from a time-lapse movie (movie 1) of a 48 hrs fed larval brain using this mounting method.

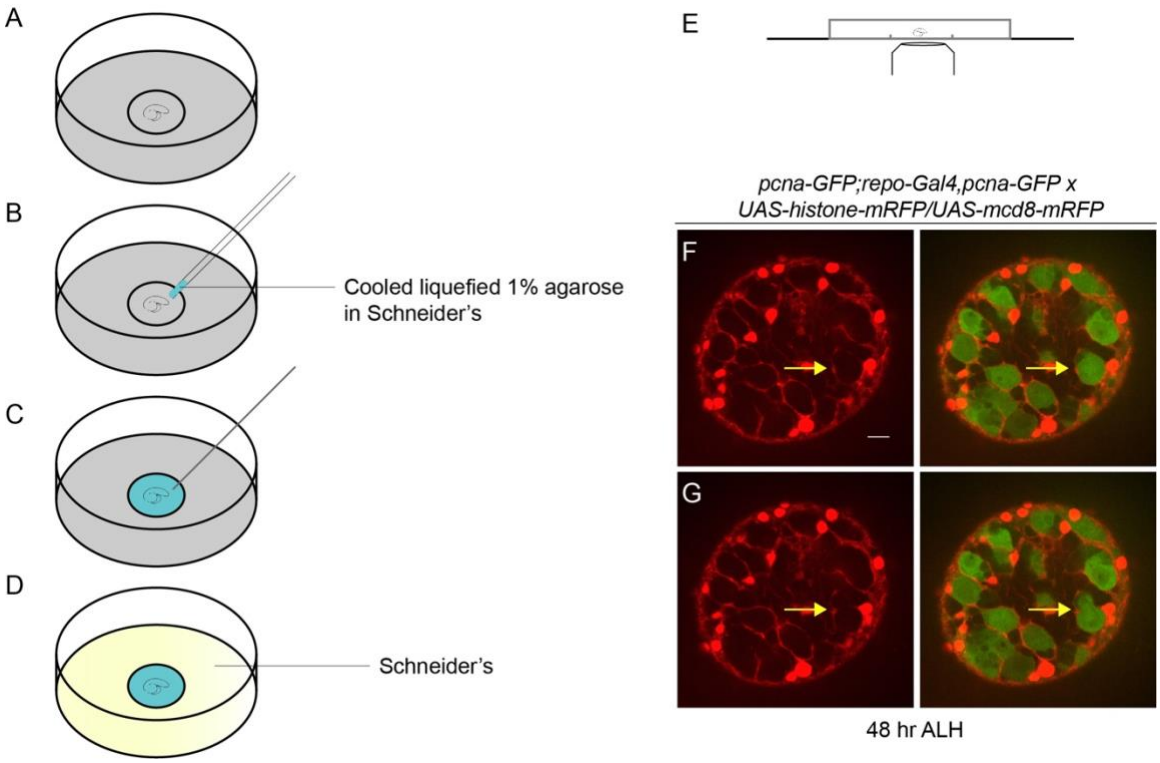

Figure 3. Mounting larval brains for live imaging on an inverted microscope. (A) – (D). Larval brain mounting method using a glass-bottomed petri dish. (E). Glass-bottomed petri dish mounted on the inverted microscope. (F) and (G). Still images of a time-lapse movie. *pcna-GFP* labels proliferating NBs, and RFP labels glial cell nuclei and membrane. Panels on the left show RFP channel only; panels on the right are GFP and RFP merge channels. Genotype: *pcna-GFP; repo-Gal4, UAS-mcd8-mRFP* x *UAS-histone-mRFP*. Yellow arrows point to a NB in mitosis in a glial pocket.

Imaging *ex vivo* brain culture on an upright confocal microscope:

To image *ex vivo* brain cultures on an upright microscope, I used a metal cell culture slide as the base of the mounting apparatus and a silicone base, a breathable membrane (YSI model 5793 standard membrane kit) and a silicone gasket (with a center hole) to create a well of culturing space (Figure 4A). 80 μl of D22 media based mixture with pupal brains and larval fat bodies were then placed onto the center of the membrane. Fat bodies and brains were then arranged so the dorsal side of the brain lobes were facing up and the fat bodies were not covering the brains. A coverslip then was placed on top and excess liquid outside of the coverslip was absorbed with a Kim wipe until brains were just touching the coverslip. Warm Vaseline was then used to seal the edges of the coverslip so that culture liquid did not evaporate during imaging (method and figure 4A adapted from Lindsay Ardiff, personal communication). Movie 2, 3 and 4 were recorded using this mounting method. Figure 4C shows a still image from a time-lapse movie (movie 2) of a brain 78 hr after pupal formation (APF), and an apoptotic mushroom body neuroblast (MB NB) from an 85 hr APF brain in Figure 4D (movie 3). Figure 4E show still images from a time-lapse movie (movie 4) of a 72 hr ALH larval brain.

In summary, it is important to not be restricted to one method, and to explore and adapt multiple methods to meet the needs of the experiment. For my dissertation research, I examined cell growth in the brain during early larval development in response to dietary nutrients. Continuous larval feeding is required in order to study the effect of dietary nutrients on cell growth. This makes time-lapsing the brain in whole larvae challenging due to the movements in the brain

from larval feeding. Neither larva chip or the gluing method for time-lapsing purposes is suited for my topic of interest. To separate the brains from larval feeding motions, dissection and *ex vivo* brain cultures are required. Because first instar larval brains are much smaller compare to second/third instar larval brains and pupal/adult brains, the biggest challenge to time-lapse a first instar larval brain in culture is to find a method that keeps the tiny first instar larval brain still. Through trial and error, I have found that applying liquefied and cooled agarose onto a dissected first instar larval brain works the best (data not shown). In addition, the imaging window of *ex vivo* brain cultures is limited to a few hours before brains show signs of distress; visible deterioration of tissue quality and health. Therefore, the best method is to re-create the environment first instar larval brains reside in in culture, perhaps extracting hemolymph from larvae of the same stage as the culturing media, and time-lapse those brains *ex vivo*.

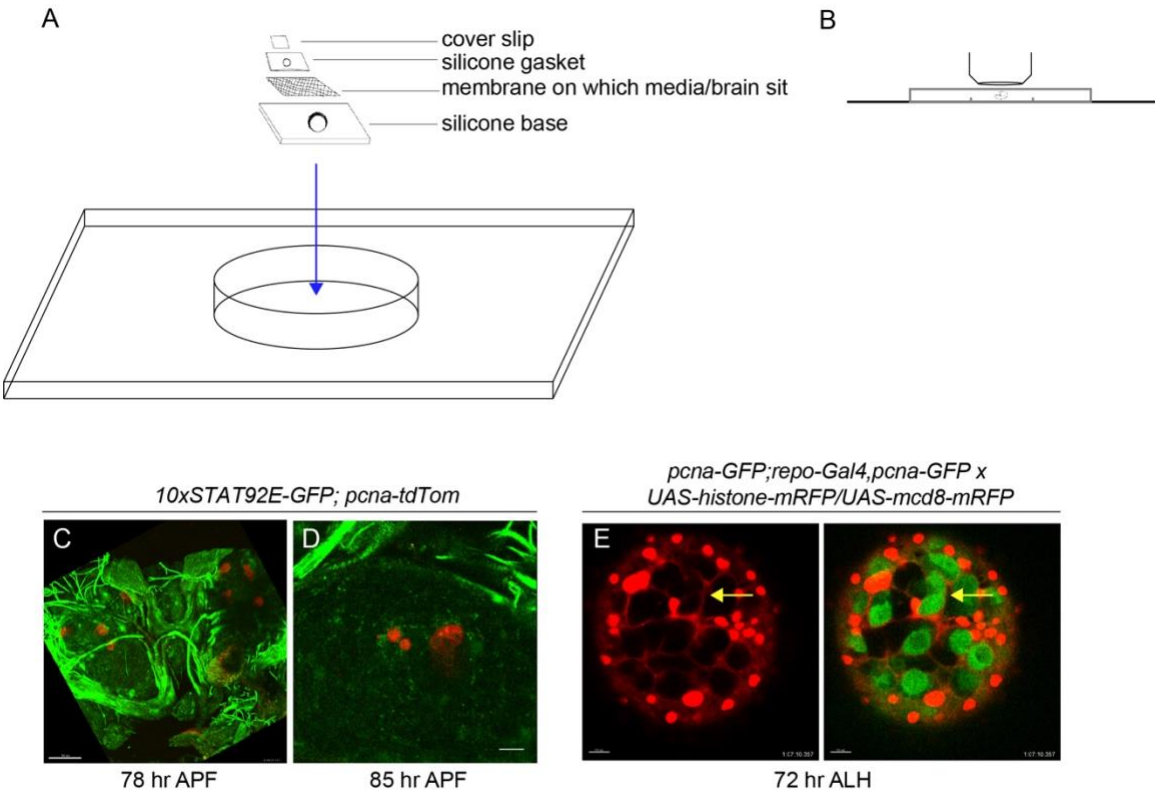

Figure 4. Mounting larval brains for live imaging on an upright microscope.

(A). Pupal brain mounting method (B). Live imaging apparatus under the objective of an upright microscope. (C). a 78 hr APF brain. (D). an apoptotic MBNB from 85 hr APF brain. Green: GFP labels STAT positive glia as well as trachea. Red: tdTom labels proliferating NB. Genotype listed above panel C and D. (E). Still images of a time-lapse movie. *pcna-GFP* labels proliferating NBs, and RFP labels glial cell nuclei and membrane. Panels on the left show RFP channel only; panels on the right are GFP and RFP merge channels. Genotype listed above panel E. Yellow arrows point to a NB in cytokinesis in a glial pocket.

Appendix II

Local JAK/STAT Signaling Regulates Mushroom Body Neuroblast Termination

Mushroom body neuroblasts (MB NBs) generate neurons important for memory and learning and persist late into pupal stages of development. Prior to eclosion, MB NBs are eliminated by programmed cell death (129,177,190). Janus kinase/signal transducers and activators of transcription (JAK/STAT) signaling is involved in cell proliferation, differentiation, migration and apoptosis from flies to mammals (192). *Drosophila* has a much simplified JAK/STAT signaling network compared to mammals, with one JAK (*Hopscotch* in flies*, Hop* in short), and one STAT (Stat92E in flies) (193). Simplified in the model figure (Figure 3D), Unpaired (Upd), Upd2, and Upd3 are the ligands of the receptor Domeless (Dome). Upd binding to *Dome* causes dimerization of *Dome*, and subsequent activation of Hop. Activated Hop phosphorylates Stat92E dimers. Stat92E dimers translocate into the nucleus and leads to downstream transcription activation (194). In *Drosophila*, JAK/STAT signaling has been demonstrated to be a key player in stem cell self-renewal and stem cell niche maintenance in the germline stem cell niche and the intestinal stem cell niche (195). We aim to decipher whether JAK/STAT signaling pathway also plays a role in the *Drosophila* neural stem cell niche regulating neural stem cell proliferation/maintenance. Using a 10xSTAT92E-GFP reporter (196), I observed that during late stage pupal development from 48 hr after pupal formation (APF) to 80 hr APF, the ensheathing glia of MB NBs and their recently born progeny have elevated levels of JAK/STAT cytokine signaling activity (Figure 1B, 1C, 1D). To trace the source of the ligand Upd, we use a previously published

method, G-TRACE, a Gal4 based cell lineage analysis tool (197). An *Upd-Gal4* driver is used to drive *UAS-RFP* and *UAS-FLP* (flipase). The flipase will subsequently flip out a “stop” sequence and results in GFP expression. In this experiment, RFP+ cells are cells that express Upd at the moment of dissection, and GFP+ cells are cells that had earlier Upd expression. I observed that, Upd, the ligand for JAK/STAT activation, was expressed in the MB neurons, differentiated progenies generated by the MB NBs themselves during pupal phases (Figure 2A and 2B). Upd expression in the MB neurons diminished in FE adults (Figure 2C). To determine whether Upd expression in the MB neurons play a role in MB NB survival, we knocked down Upd in MB neurons using an RNAi fly line (Figure 3A and 3B). In this experiment, I observed a marginal increase in the number of persisting MB NBs when we knocked down Upd in the MB neurons (mean = 0.84), although not statistically different from control (mean = 0.2) (Figure 3C). We propose that the glia that ensheath the MB NBs, and the MB neurons are two cell types that constitute the MB NB niche. Our working model is that MB NBs continuously generate MB neurons during pupal development. The increase in number of the MB neurons causes an accumulation of secreted Upd that activates JAK/STAT signaling in glia adjacent to the MB NBs. JAK/STAT signaling is then utilized as a negative feedback signal to instruct MB NBs to undergo apoptosis. (Figure 3D)

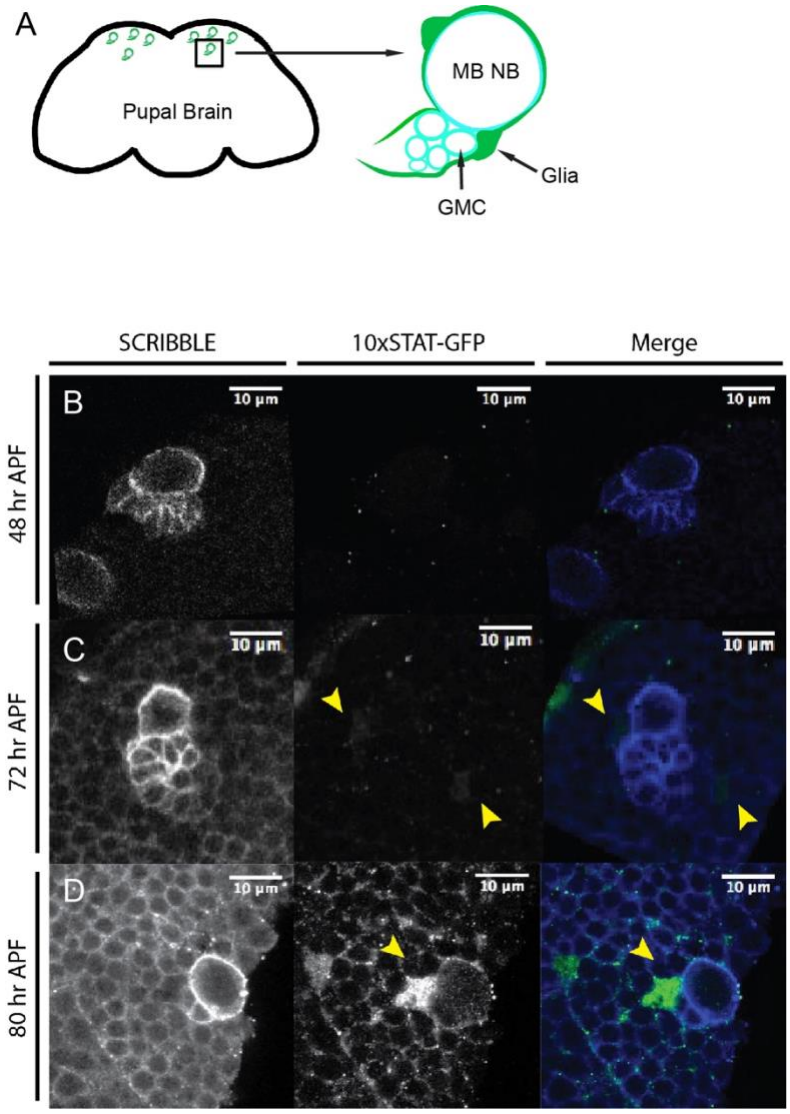

Figure 1. Ensheathing glia of MB NBs show elevated STAT expression.

(A). Illustration of MB NBs' anatomical position. MB NBs reside in a glial niche on the dorsal surface of the brain. Glial cells ensheath the MBNBs and their new born daughters. (B). (C). (D). Scribble staining outlines MB NBs and their new born daughters. 10xSTAT92E-GFP reporter labels the glia ensheathing NBs. Arrowheads indicate STAT-positive glia.

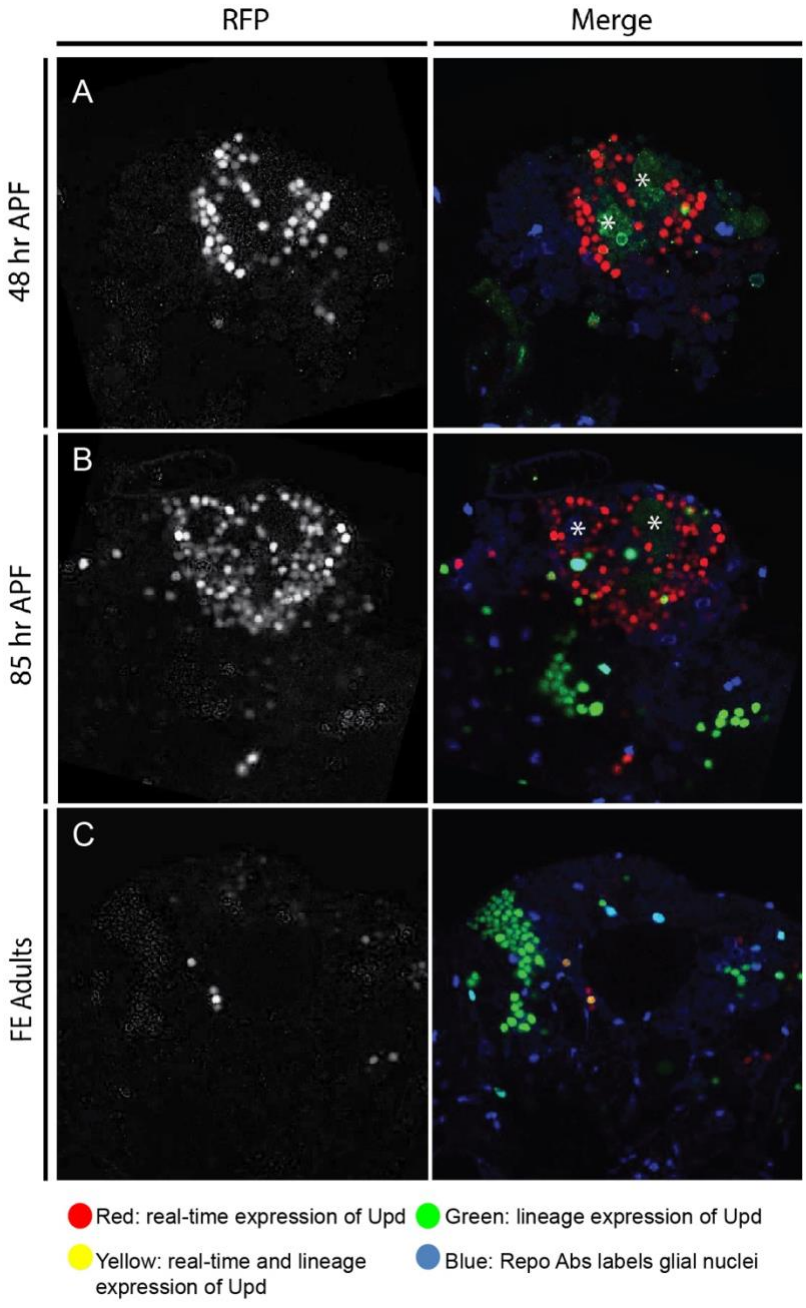

Figure 2. **G-TRACE method for tracing the cellular source of Upd.**

(A-C). The MB neurons surrounding the MB NBs express Upd throughout pupal development and cease Upd expression in adulthood. Asterisks indicate the

position of MB NBs. The timing of Upd expression coincides with MB NB persistence.

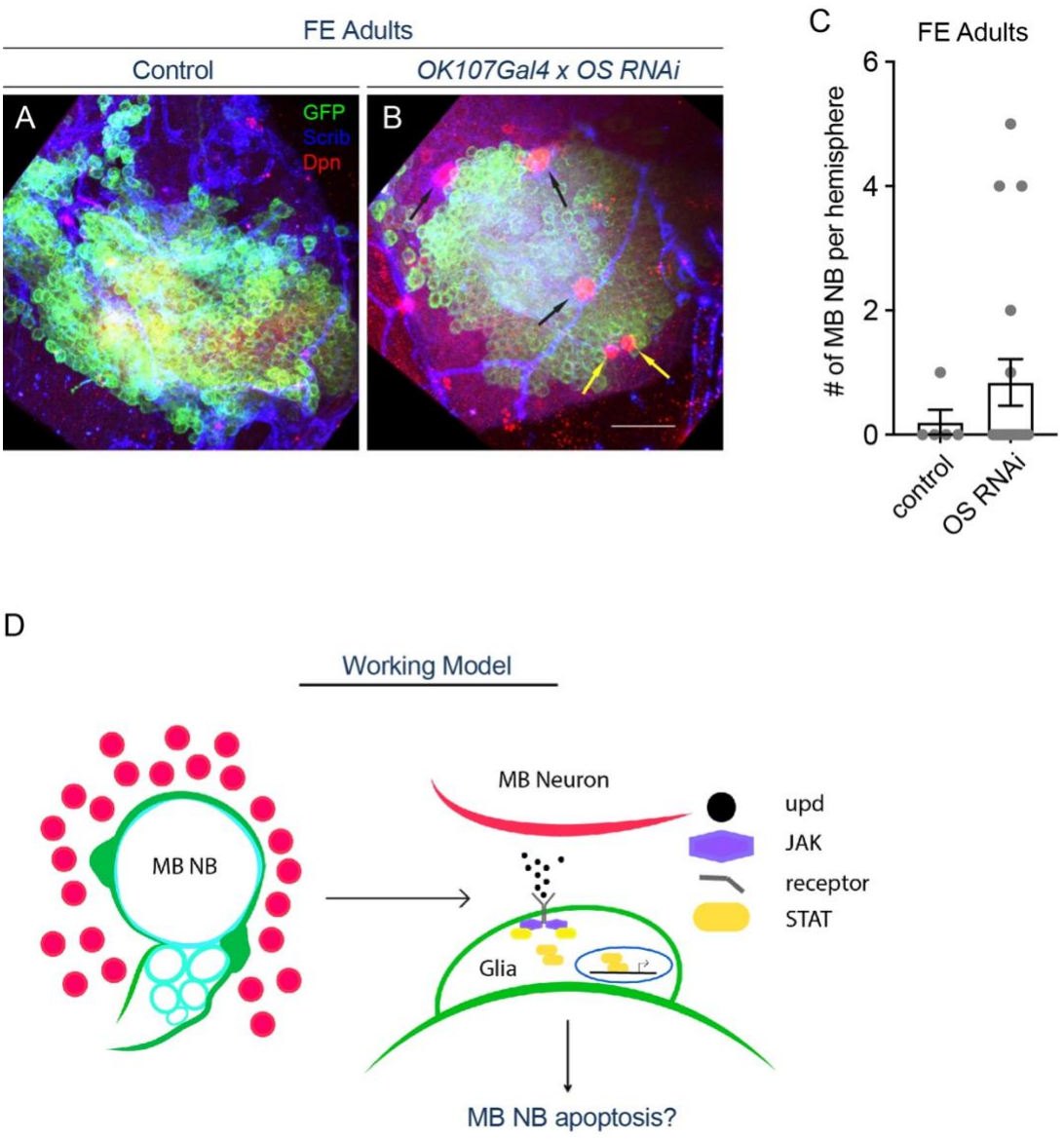

Figure 3. Model of JAK/STAT signaling in MB NB apoptosis.

(A) and (B). Maximum intensity projection of the MB NBs and MB neurons. Genotype of A: *OK107-Gal4, UAS-mcd8-GFP* x OR Genotype of B: *OK107-Gal4, UAS-mcd8-GFP* x OS_{RNAi}. Arrows point to persisting MB NBs. (C). Quantification of number of MB NBs persisting in FE adults of A & B. D. Working model.

To continue the investigation of the mechanism of how JAK/STAT signaling activity in the MB NB stem cell niche regulates MB NB apoptosis, one would further characterize the molecular underpinnings of the pathway, and identify cellular sources of the components of the JAK/STAT signaling pathway. For instance, the cellular expression patterns of Hop and Dome during late stage pupal development are yet to be identified. Additionally, one would further explore whether two other ligands for the JAK/STAT pathway, Upd2 and Upd3, are involved in activation of the pathway during late pupal stages that lead to MB NB apoptosis. Finally, the STAT expression we observed in the ensheathing glia of the MB NBs via the 10xSTAT92E-GFP should be further investigated. One could knock down Stat92E in glial cells and assay for aberrant persistence of MB NBs in adulthood or premature loss during early pupal stages.

Appendix Table

dilp2-Gal4 on II	Bloomington Drosophila Stock Center	Stock # 37516
UAS-kir2.1	Bloomington Drosophila Stock Center	Stock # 6596
ImpL2-RA-Gal4	Gift from Hugo Stocker	(171)
repoGal80	Gift from Takeshi Awasaki	(198)
dilp6-Gal4	Kyoto Stock Center	Stock # NP1079
pcna-tdTom	Sarah Siegrist	Personal communication
pcna-GFP		(152)
UAS-mcd8-mRFP	Bloomington Drosophila Stock Center	Stock # 27399
10xSTAT92E-GFP	Bloomington Drosophila Stock Center	Stock # 26197
upd-Gal4		(199)
GTRACE on II	Bloomington Drosophila Stock Center	Stock # 28280
OK107-Gal4	Bloomington Drosophila Stock Center	Stock # 854

References

1. Morrison SJ, Spradling AC. Stem Cells and Niches: Mechanisms That Promote Stem Cell Maintenance throughout Life. Cell. 2008;132(4):598–611.
2. Fillippis L De, Binda E. Concise Review : Limbal Stem Cell Deficiency , Dysfunction , and Distress. Stem Cells Transl. 2012;298–308.
3. O'Brien LE, Bilder D. Beyond the Niche: Tissue-Level Coordination of Stem Cell Dynamics. Annu Rev Cell Dev Biol. 2013;29(1):107–36.
4. Malta TM, Sokolov A, Gentles AJ, Burzykowski T, Poisson L, Weinstein JN, et al. Machine Learning Identifies Stemness Features Associated with Oncogenic Dedifferentiation. Cell. 2018;173(2):338-354.e15.
5. Rumman M, Dhawan J, Kassem M. Concise Review: Quiescence in Adult Stem Cells: Biological Significance and Relevance to Tissue Regeneration. Stem Cells. 2015;33(10):2903–12.
6. Wang YAZ, Plane JM, Jiang P, Zhou CJ, Deng W. Concise review: Quiescent and active states of endogenous adult neural stem cells: Identification and characterization. Stem Cells. 2011;29(6):907–12.
7. BioRad. Understanding the Eukaryotic Cell Cycle — a Biological and Experimental Overview. BioRad [Internet]. 2017;(4):1–8. Available from: https://www.bio-rad-antibodies.com/static/2017/brdu/understanding-the-eukaryotic-cell-cycle-a-biological-and-experimental-overview.pdf
8. Nakamura-Ishizu A, Takizawa H, Suda T. The analysis, roles and regulation of quiescence in hematopoietic stem cells. Dev.

2014;141(24):4656–66.

9. Otsuki L, Brand AH. Dorsal-Ventral Differences in Neural Stem Cell Quiescence Are Induced by p57KIP2/Dacapo. Dev Cell [Internet]. 2019;49(2):293-300.e3. Available from: https://doi.org/10.1016/j.devcel.2019.02.015
10. Yao G. Modelling mammalian cellular quiescence. Interface Focus. 2014;4(3).
11. Otsuki L, Brand AH. Cell cycle heterogeneity directs the timing of neural stem cell activation from quiescence. Science (80-). 2018;360(6384):99–102.
12. Kwon JS, Everetts NJ, Wang X, Wang W, Della Croce K, Xing J, et al. Controlling Depth of Cellular Quiescence by an Rb-E2F Network Switch. Cell Rep [Internet]. 2017;20(13):3223–35. Available from: https://doi.org/10.1016/j.celrep.2017.09.007
13. Cheung T, Rando T. Molecular regulation of stem cell quiescence. Nat Rev Mol Cell Biol [Internet]. 2013;14(6):1–26. Available from: http://www.nature.com/nrm/journal/v14/n6/abs/nrm3591.html
14. Li J. Quiescence regulators for hematopoietic stem cell. Exp Hematol [Internet]. 2011;39(5):511–20. Available from: http://dx.doi.org/10.1016/j.exphem.2011.01.008
15. Martins R, Lithgow GJ, Link W. Long live FOXO: Unraveling the role of FOXO proteins in aging and longevity. Aging Cell. 2016;15(2):196–207.
16. Wang Y, Ezemaduka AN, Tang Y, Chang Z. Understanding the

mechanism of the dormant dauer formation of C. elegans: From genetics to biochemistry. IUBMB Life. 2009;61(6):607–12.

17. Kriegstein A, Alvarez-Buylla A. The Glial Nature of Embryonic and Adult Neural Stem Cells. Annu Rev Neurosci. 2009;32(1):149–84.
18. Weiss S, Reynolds BA, Vescovi AL, Morshead C, Craig CG, Van Der Kooy D. Is there a neural stem cell in the mammalian forebrain? Trends Neurosci [Internet]. 1996;19(9):387–93. Available from: http://dx.doi.org/10.1016/S0166-2236(96)10035-7
19. Levison SW, Goldman JE. Both oligodendrocytes and astrocytes develop from progenitors in the subventricular zone of postnatal rat forebrain. Neuron. 1993;10(2):201–12.
20. Palmer TD, Willhoite AR, Gage FH. Vascular niche for adult hippocampal neurogenesis. J Comp Neurol. 2000;425(4):479–94.
21. Mohammad K, Dakik P, Medkour Y, Mitrofanova D, Titorenko VI. Quiescence entry, maintenance, and exit in adult stem cells. Int J Mol Sci. 2019;20(9):1–43.
22. Ehm O, Göritz C, Covic M, Schäffner I, Schwarz TJ, Karaca E, et al. RBPJκ-dependent signaling is essential for long-term maintenance of neural stem cells in the adult hippocampus. J Neurosci. 2010;30(41):13794–807.
23. Than-Trong E, Ortica-Gatti S, Mella S, Nepal C, Alunni A, Bally-Cuif L. Neural stem cell quiescence and stemness are molecularly distinct outputs of the notch3 signalling cascade in the vertebrate adult brain. Dev.

2018;145(10).

24. Kempermann G, Gage FH, Aigner L, Song H, Curtis MA, Thuret S, et al. Human Adult Neurogenesis: Evidence and Remaining Questions. Cell Stem Cell. 2018;23(1):25–30.
25. Boldrini M, Fulmore CA, Tartt AN, Simeon LR, Pavlova I, Poposka V, et al. Human Hippocampal Neurogenesis Persists throughout Aging. Cell Stem Cell. 2018;22(4):589-599.e5.
26. Sorrells SF, Paredes MF, Cebrian-Silla A, Sandoval K, Qi D, Kelley KW, et al. Human hippocampal neurogenesis drops sharply in children to undetectable levels in adults. Nature [Internet]. 2018;555(7696):377–81. Available from: http://dx.doi.org/10.1038/nature25975
27. Casarosa S, Zasso J, Conti L. Systems for ex-vivo Isolation and Culturing of Neural Stem Cells. Neural Stem Cells - New Perspect. 2013;3–28.
28. Mihaylova MM, Sabatini DM, Yilmaz ÖH. Dietary and metabolic control of stem cell function in physiology and cancer. Cell Stem Cell. 2014;14(3):292–305.
29. Pillai SM, Sereda NH, Hoffman ML, Valley E V., Crenshaw TD, Park YK, et al. Effects of poor maternal nutrition during gestation on bone development and mesenchymal stem cell activity in offspring. PLoS One. 2016;11(12):1–16.
30. Palacios C. The role of nutrients in bone health, from A to Z. Crit Rev Food Sci Nutr. 2006;46(8):621–8.
31. Bruder SP, Fink DJ, Caplan AI. Mesenchymal stem cells in bone

development, bone repair, and skeletal regenaration therapy. J Cell Biochem. 1994;56(3):283–94.

32. Wu CL, Diekman BO, Jain D, Guilak F. Diet-induced obesity alters the differentiation potential of stem cells isolated from bone marrow, adipose tissue and infrapatellar fat pad: The effects of free fatty acids. Int J Obes. 2013;37(8):1079–87.

33. Cerletti M, Jang YC, Finley LWS, Haigis MC, Wagers AJ. Short-term calorie restriction enhances skeletal muscle stem cell function. Cell Stem Cell [Internet]. 2012;10(5):515–9. Available from: http://dx.doi.org/10.1016/j.stem.2012.04.002

34. Richmond CA, Shah MS, Carlone DL, Breault DT. Factors regulating quiescent stem cells: insights from the intestine and other self-renewing tissues. J Physiol. 2016;594(17):4805–13.

35. Richmond CA, Shah MS, Deary LT, Trotier DC, Thomas H, Ambruzs DM, et al. Dormant Intestinal Stem Cells Are Regulated by PTEN and Nutritional Status. Cell Rep [Internet]. 2015;13(11):2403–11. Available from: http://dx.doi.org/10.1016/j.celrep.2015.11.035

36. McLeod CJ, Wang L, Wong C, Jones DL. Stem cell dynamics in response to nutrient availability. Curr Biol [Internet]. 2010;20(23):2100–5. Available from: http://dx.doi.org/10.1016/j.cub.2010.10.038

37. Richmond CA, Shah MS, Carlone DL, Breault DT. An enduring role for quiescent stem cells. Dev Dyn. 2016;245(7):718–26.

38. Yilmaz ÖH, Katajisto P, Lamming DW, Gültekin Y, Bauer-Rowe KE,

Sengupta S, et al. MTORC1 in the Paneth cell niche couples intestinal stem-cell function to calorie intake. Nature. 2012;486(7404):490–5.

39. Efeyan A, Comb WC, Sabatini DM. Nutrient-sensing mechanisms and pathways. Nature. 2015;517(7534):302–10.
40. Grönke S, Clarke DF, Broughton S, Andrews TD, Partridge L. Molecular evolution and functional characterization of Drosophila insulin-like peptides. PLoS Genet. 2010 Feb;6(2).
41. Grönke S, Clarke D-F, Broughton S, Andrews TD, Partridge L. Molecular Evolution and Functional Characterization of Drosophila Insulin-Like Peptides. PLoS Genet [Internet]. 2010;6(2):e1000857. Available from: http://dx.plos.org/10.1371/journal.pgen.1000857
42. Grö Nke S, Clarke D-F, Broughton S, Andrews TD, Partridge L. Molecular Evolution and Functional Characterization of Drosophila Insulin-Like Peptides. PLoS Genet [Internet]. 2010 [cited 2017 Apr 14];6(2). Available from: http://www.mpg.de/english/portal/index.html.
43. Gontijo AM, Garelli A. The biology and evolution of the Dilp8-Lgr3 pathway: A relaxin-like pathway coupling tissue growth and developmental timing control. Mech Dev [Internet]. 2018;154(April):44–50. Available from: https://doi.org/10.1016/j.mod.2018.04.005
44. Garelli A, Heredia F, Casimiro AP, Macedo A, Nunes C, Garcez M, et al. Dilp8 requires the neuronal relaxin receptor Lgr3 to couple growth to developmental timing. Nat Commun [Internet]. 2015;6:1–14. Available from: http://dx.doi.org/10.1038/ncomms9732

45. Britton JS, Edgar B a. Environmental control of the cell cycle in Drosophila: nutrition activates mitotic and endoreplicative cells by distinct mechanisms. Development [Internet]. 1998;125(11):2149–58. Available from: http://dev.biologists.org/content/develop/125/11/2149.full.pdf

46. Sipe CW, Siegrist SE. Eyeless uncouples mushroom body neuroblast proliferation from dietary amino acids in drosophila. Elife. 2017;6:1–11.

47. Chell JM, Brand AH. Nutrition-responsive glia control exit of neural stem cells from quiescence. Cell [Internet]. 2010;143(7):1161–73. Available from: http://dx.doi.org/10.1016/j.cell.2010.12.007

48. Sousa-Nunes R, Yee LL, Gould AP. Fat cells reactivate quiescent neuroblasts via TOR and glial insulin relays in Drosophila. Nature. 2011 Mar 24;471(7339):508–13.

49. Homem CCF, Repic M, Knoblich JA. Proliferation control in neural stem and progenitor cells. Nat Rev Neurosci. 2015;16(11):647–59.

50. Homem CCF, Knoblich JA. Drosophila neuroblasts: A model for stem cell biology. Dev. 2012;139(23):4297–310.

51. Tsuji T, Hasegawa E, Isshiki T. Neuroblast entry into quiescence is regulated intrinsically by the combined action of spatial Hox proteins and temporal identity factors. Development. 2008;135(23):3859–69.

52. Ding R, Weynans K, Bossing T, Barros CS, Berger C. The Hippo signalling pathway maintains quiescence in Drosophila neural stem cells. Nat Commun. 2016 Jan 29;7.

53. Voigt A, Pflanz R, Schäfer U, Jäckle H. Perlecan participates in

proliferation activation of quiescent Drosophila neuroblasts. Dev Dyn. 2002;224(4):403–12.

54. Ebens AJ, Garren H, Cheyette BNR, Zipursky SL. The Drosophila anachronism locus: A glycoprotein secreted by glia inhibits neuroblast proliferation. Cell. 1993;74(1):15–27.

55. Chell JM, Brand AH. Nutrition-responsive glia control exit of neural stem cells from quiescence. Cell. 2010 Dec 23;143(7):1161–73.

56. Brand AH, Spe´der P. Gap Junction Proteins in the Blood-Brain Barrier Control Nutrient-Dependent Reactivation of Drosophila Neural Stem Cells. 2014;309–21.

57. Spéder P, Brand AH. Systemic and local cues drive neural stem cell niche remodelling during neurogenesis in drosophila. Elife. 2018;7:1–16.

58. Gil-Ranedo J, Gonzaga E, Jaworek KJ, Berger C, Bossing T, Barros CS. STRIPAK Members Orchestrate Hippo and Insulin Receptor Signaling to Promote Neural Stem Cell Reactivation. Cell Rep [Internet]. 2019;27(10):2921-2933.e5. Available from: https://linkinghub.elsevier.com/retrieve/pii/S2211124719306345

59. Otsuki L, Brand AH. The vasculature as a neural stem cell niche. Neurobiol Dis [Internet]. 2017;107:4–14. Available from: http://dx.doi.org/10.1016/j.nbd.2017.01.010

60. Scadden DT. Nice neighborhood: Emerging concepts of the stem cell niche. Vol. 157, Cell. Cell Press; 2014. p. 41–50.

61. Yabut OR, Pleasure SJ. The Crossroads of Neural Stem Cell Development

and Tumorigenesis. Opera medica Physiol [Internet]. 2016;2(3–4):181–7. Available from: http://www.ncbi.nlm.nih.gov/pubmed/28795171%0Ahttp://www.pubmedcentral.nih.gov/articlerender.fcgi?artid=PMC5546789

62. Song H, Stevens CF, Gage FH. Astroglia induce neurogenesis from adult neural stem cells. Nature. 2002;417(6884):39–44.

63. Lim DA, Tramontin AD, Trevejo JM, Herrera DG, García-Verdugo JM, Alvarez-Buylla A. Noggin antagonizes BMP signaling to create a niche for adult neurogenesis. Neuron. 2000;28(3):713–26.

64. Mirzadeh Z, Merkle FT, Soriano-Navarro M, Garcia-Verdugo JM, Alvarez-Buylla A. Neural Stem Cells Confer Unique Pinwheel Architecture to the Ventricular Surface in Neurogenic Regions of the Adult Brain. Cell Stem Cell. 2008 Sep 11;3(3):265–78.

65. Kaneko N, Sawamoto K. Go with the Flow: Cerebrospinal Fluid Flow Regulates Neural Stem Cell Proliferation. Cell Stem Cell [Internet]. 2018;22(6):783–4. Available from: https://doi.org/10.1016/j.stem.2018.05.015

66. Ottone C, Krusche B, Whitby A, Clements M, Quadrato G, Pitulescu ME, et al. Direct cell-cell contact with the vascular niche maintains quiescent neural stem cells. Nat Cell Biol [Internet]. 2014;16(11):1045–56. Available from: http://www.pubmedcentral.nih.gov/articlerender.fcgi?artid=4298702&tool=pmcentrez&rendertype=abstract

67. Bjornsson CS, Apostolopoulou M, Tian Y, Temple S. It takes a village: Constructing the neurogenic niche. Dev Cell [Internet]. 2015;32(4):435–46. Available from: http://dx.doi.org/10.1016/j.devcel.2015.01.010

68. Song H, Berg DA, Bond AM, Ming G li. Radial glial cells in the adult dentate gyrus: What are they and where do they come from? F1000Research. 2018;7(0).

69. Fuentealba LC, Obernier K, Alvarez-Buylla A. Adult neural stem cells bridge their niche. Cell Stem Cell [Internet]. 2012;10(6):698–708. Available from: http://dx.doi.org/10.1016/j.stem.2012.05.012

70. Fournier NM, Duman RS. Role of vascular endothelial growth factor in adult hippocampal neurogenesis: Implications for the pathophysiology and treatment of depression. Behav Brain Res [Internet]. 2012;227(2):440–9. Available from: http://dx.doi.org/10.1016/j.bbr.2011.04.022

71. Bonaguidi MA, Peng CY, McGuire T, Falciglia G, Gobeske KT, Czeisler C, et al. Noggin expands neural stem cells in the adult hippocampus. J Neurosci. 2008;28(37):9194–204.

72. Doyle SE, Pahl MC, Siller KH, Ardiff L, Siegrist SE. Neuroblast niche position is controlled by phosphoinositide 3-kinase-dependent DE-cadherin adhesion. Dev. 2017 Mar 1;144(5):820–9.

73. Doe CQ. Neural stem cells: Balancing self-renewal with differentiation. Development. 2008;135(9):1575–87.

74. Loyer N, Januschke J. The last-born daughter cell contributes to division orientation of Drosophila larval neuroblasts. Nat Commun [Internet].

2018;9(1):1–12. Available from: http://dx.doi.org/10.1038/s41467-018-06276-0

75. Freeman MR. Drosophila central nervous system glia. Cold Spring Harb Perspect Biol. 2015;7(11).

76. Unhavaithaya Y, Orr-Weaver TL. Polyploidization of glia in neural development links tissue growth to blood-brain barrier integrity. Genes Dev. 2012 Jan 1;26(1):31–6.

77. Limmer S, Weiler A, Volkenhoff A, Babatz F, Klämbt C. The drosophila blood-brain barrier: Development and function of a glial endothelium. Front Neurosci. 2014;8(OCT):1–19.

78. Kanai MI, Kim MJ, Akiyama T, Takemura M, Wharton K, O'Connor MB, et al. Regulation of neuroblast proliferation by surface glia in the Drosophila larval brain. Sci Rep. 2018;8(1):1–15.

79. Mas-Bargues C, Sanz-Ros J, Román-Domínguez A, Inglés M, Gimeno-Mallench L, El Alami M, et al. Relevance of oxygen concentration in stem cell culture for regenerative medicine. Int J Mol Sci. 2019;20(5).

80. Ezashi T, Das P, Roberts RM. Low O2 tensions and the prevention of differentiation of hES cells. Proc Natl Acad Sci U S A. 2005;102(13):4783–8.

81. Mohyeldin A, Garzón-Muvdi T, Quiñones-Hinojosa A. Oxygen in stem cell biology: A critical component of the stem cell niche. Cell Stem Cell. 2010;7(2):150–61.

82. Li L, Candelario KM, Thomas K, Wang R, Wright K, Messier A, et al.

Hypoxia inducible factor-1α (HIF-1α) is required for neural stem cell maintenance and vascular stability in the adult mouse SVZ. J Neurosci. 2014;34(50):16713–9.

83. Harms KM, Li L, Cunningham LA. Murine Neural Stem/Progenitor Cells Protect Neurons against Ischemia by HIF-1α-Regulated VEGF Signaling. PLoS One. 2010;5(3).
84. Javaherian A, Kriegstein A. A stem cell niche for intermediate progenitor cells of the embryonic cortex. Cereb Cortex. 2009;19(SUPPL. 1).
85. Westneat MW, Betz O, Blob RW, Fezzaa K, Cooper WJ, Lee WK. Tracheal respiration in insects visualized with synchrotron x-ray imaging. Science (80-). 2003;299(5606):558–60.
86. Pereanu W, Spindler S, Cruz L, Hartenstein V. Tracheal development in the Drosophila brain is constrained by glial cells. Dev Biol. 2007 Feb 1;302(1):169–80.
87. Magistretti PJ, Allaman I. A Cellular Perspective on Brain Energy Metabolism and Functional Imaging. Neuron [Internet]. 2015;86(4):883–901. Available from: http://dx.doi.org/10.1016/j.neuron.2015.03.035
88. Folli F, Bonfanti L, Renard E, Kahn CR, Merighi A. Insulin receptor substrate-1 (IRS-1) distribution in the rat central nervous system. J Neurosci. 1994;14(11 I):6412–22.
89. Blázquez E, Velázquez E, Hurtado-Carneiro V, Ruiz-Albusac JM. Insulin in the brain: Its pathophysiological implications for states related with central insulin resistance, type 2 diabetes and alzheimer’s disease. Front

Endocrinol (Lausanne). 2014;5(OCT):1–21.

90. Banks WA, Owen JB, Erickson MA. Insulin in the brain: There and back again. Pharmacol Ther. 2012;136(1):82–93.

91. Lee SH, Zabolotny JM, Huang H, Lee H, Kim YB. Insulin in the nervous system and the mind: Functions in metabolism, memory, and mood. Mol Metab [Internet]. 2016;5(8):589–601. Available from: http://dx.doi.org/10.1016/j.molmet.2016.06.011

92. Unger JW, Livingston JN, Moss AM. Insulin receptors in the central nervous system: Localization, signalling mechanisms and functional aspects. Prog Neurobiol. 1991;36(5):343–62.

93. Banks WA, Kastin AJ. Differential permeability of the blood-brain barrier to two pancreatic peptides: Insulin and amylin. Peptides. 1998;19(5):883–9.

94. Banks WA, Jaspan JB, Kastin AJ. Selective, physiological transport of insulin across the blood-brain barrier. Novel demonstration by species-specific radioimmunoassays. Peptides. 1997;18(8):1257–62.

95. Devaskar SU, Giddings SJ, Rajakumar PA, Carnaghi LR, Menon RK, Zahm DS. Insulin gene expression and insulin synthesis in mammalian neuronal cells. J Biol Chem. 1994;269(11):8445–54.

96. Gray SM, Meijer RI, Barrett EJ. Insulin regulates brain function, but how does it get there? Diabetes. 2014;63(12):3992–7.

97. Molnár G, Faragó N, Kocsis ÁK, Rózsa M, Lovas S, Boldog E, et al. GABAergic neurogliaform cells represent local sources of insulin in the cerebral cortex. J Neurosci. 2014;34(4):1133–7.

98. Arsenijevic Y, Weiss S, Schneider B, Aebischer P. Insulin-like growth factor-1 is necessary for neural stem cell proliferation and demonstrates distinct actions of epidermal growth factor and fibroblast growth factor-2. J Neurosci. 2001;21(18):7194–202.

99. Ziegler AN, Schneider JS, Qin M, Tyler WA, Pintar JE, Fraidenraich D, et al. IGF-II promotes stemness of neural restricted precursors. Stem Cells. 2012;30(6):1265–76.

100. Ziegler AN, Feng Q, Chidambaram S, Testai JM, Kumari E, Rothbard DE, et al. Insulin-like Growth Factor II: An Essential Adult Stem Cell Niche Constituent in Brain and Intestine. Stem Cell Reports [Internet]. 2019;12(4):816–30. Available from: https://doi.org/10.1016/j.stemcr.2019.02.011

101. Ziegler AN, Levison SW, Wood TL. Insulin and IGF receptor signalling in neural-stem-cell homeostasis. Vol. 11, Nature Reviews Endocrinology. Nature Publishing Group; 2015. p. 161–70.

102. Åberg MAI, Åberg ND, Hedbäcker H, Oscarsson J, Eriksson PS. Peripheral infusion of IGF-I selectively induces neurogenesis in the adult rat hippocampus. J Neurosci. 2000;20(8):2896–903.

103. Wands JR. Alzheimer ' s Disease Is Type 3 Diabetes — Evidence Reviewed. 2015;2(6):1101–13.

104. Arnold SE, Arvanitakis Z, Macauley-Rambach SL, Koenig AM, Wang HY, Ahima RS, et al. Brain insulin resistance in type 2 diabetes and Alzheimer disease: Concepts and conundrums. Nat Rev Neurol [Internet].

2018;14(3):168–81. Available from: http://dx.doi.org/10.1038/nrneurol.2017.185

105. Morris JK, Burns JM. Insulin: An emerging treatment for alzheimer's disease dementia? Curr Neurol Neurosci Rep. 2012;12(5):520–7.
106. Boulan L, Milán M, Léopold P. The systemic control of growth. Cold Spring Harb Perspect Biol. 2015 Dec 1;7(12).
107. Yamanaka N, Rewitz KF, O'Connor MB. Ecdysone Control of Developmental Transitions: Lessons from Drosophila Research . Annu Rev Entomol. 2013 Jan 7;58(1):497–516.
108. Hariharan IK. Organ Size Control: Lessons from Drosophila. Vol. 34, Developmental Cell. Cell Press; 2015. p. 255–65.
109. Koyama T, Mirth CK. Unravelling the diversity of mechanisms through which nutrition regulates body size in insects. Curr Opin Insect Sci [Internet]. 2018;25:1–8. Available from: http://dx.doi.org/10.1016/j.cois.2017.11.002
110. Thomas Danielsen E, Moeller ME, Rewitz KF. Nutrient signaling and developmental timing of maturation [Internet]. 1st ed. Vol. 105, Current Topics in Developmental Biology. Elsevier Inc.; 2013. 37–67 p. Available from: http://dx.doi.org/10.1016/B978-0-12-396968-2.00002-6
111. Nijhout HF, Riddiford LM, Shingleton AW, Suzuki Y, Callier V, Frederik H. The Developmental Control of Size in Insects.
112. Chantranupong L, Wolfson RL, Sabatini DM. Nutrient-sensing mechanisms across evolution. Vol. 161, Cell. Cell Press; 2015. p. 67–83.

113. Del Valle Rodríguez A, Didiano D, Desplan C. Power tools for gene expression and clonal analysis in Drosophila. Nat Methods. 2012;9(1):47–55.

114. Engelman JA, Luo J, Cantley LC. The evolution of phosphatidylinositol 3-kinases as regulators of growth and metabolism. Nat Rev Genet. 2006;7(8):606–19.

115. Alamy M, Bengelloun WA. Malnutrition and brain development: An analysis of the effects of inadequate diet during different stages of life in rat. Neurosci Biobehav Rev [Internet]. 2012;36(6):1463–80. Available from: http://dx.doi.org/10.1016/j.neubiorev.2012.03.009

116. Semba RD, Shardell M, Sakr Ashour FA, Moaddel R, Trehan I, Maleta KM, et al. Child Stunting is Associated with Low Circulating Essential Amino Acids. EBioMedicine. 2016 Apr 1;6:246–52.

117. Semba RD, Zhang P, Gonzalez-Freire M, Moaddel R, Trehan I, Maleta KM, et al. The association of serum choline with linear growth failure in young children from rural Malawi. Am J Clin Nutr. 2016 Jul 1;104(1):191–7.

118. Rafalski VA, Brunet A. Energy metabolism in adult neural stem cell fate. Prog Neurobiol [Internet]. 2011;93(2):182–203. Available from: http://dx.doi.org/10.1016/j.pneurobio.2010.10.007

119. Colombani J, Raisin S, Pantalacci S, Radimerski T, Montagne J, Lé Opold P. A Nutrient Sensor Mechanism Controls Drosophila Growth mycin; for review, Gingras et al., 2001; Schmelzle and Hall, 2000), a conserved kinase recently shown to partic-ipate in a nutrient-sensitive complex both in

mammalian [Internet]. Vol. 114, Cell. 2003. Available from: http://www.cell.com/cgi/content/

120. Géminard C, Rulifson EJ, Léopold P. Remote Control of Insulin Secretion by Fat Cells in Drosophila. Cell Metab. 2009 Sep 2;10(3):199–207.
121. Rajan A, Perrimon N. Drosophila cytokine unpaired 2 regulates physiological homeostasis by remotely controlling insulin secretion. Cell. 2012 Sep 28;151(1):123–37.
122. Koyama T, Mirth CK. Growth-Blocking Peptides As Nutrition-Sensitive Signals for Insulin Secretion and Body Size Regulation. PLoS Biol. 2016 Feb 29;14(2).
123. Delanoue R, Meschi E, Agrawal N, Mauri A, Tsatskis Y, Mcneill H, et al. Drosophila insulin release is triggered by adipose Stunted ligand to brain Methuselah receptor [Internet]. Available from: http://science.sciencemag.org/
124. Spé Der P, Brand AH. Systemic and local cues drive neural stem cell niche remodelling during neurogenesis in Drosophila. Available from: https://doi.org/10.7554/eLife.30413.001
125. Lin S, Marin EC, Yang CP, Kao CF, Apenteng BA, Huang Y, et al. Extremes of lineage plasticity in the drosophila brain. Curr Biol. 2013 Oct 7;23(19):1908–13.
126. Javaherian A, Kriegstein A. A stem cell niche for intermediate progenitor cells of the embryonic cortex. Cereb Cortex. 2009 Jul;19(SUPPL. 1).
127. Weinkove D, Neufeld TP, Twardzik T, Waterfield MD, Leevers SJ.

Regulation of imaginal disc cell size, cell number and organ size by Drosophila class I A phosphoinositide 3-kinase and its adaptor [Internet]. 1999. Available from: http://biomednet.com/elecref/0960982200901019

128. Puig O, Marr MT, Ruhf ML, Tjian R. Control of cell number by Drosophila FOXO: Downstream and feedback regulation of the insulin receptor pathway. Genes Dev. 2003 Aug 15;17(16):2006–20.
129. Siegrist SE, Haque NS, Chen CH, Hay BA, Hariharan IK. Inactivation of Both foxo and reaper Promotes Long-Term Adult Neurogenesis in Drosophila. Curr Biol [Internet]. 2010;20(7):643–8. Available from: http://dx.doi.org/10.1016/j.cub.2010.01.060
130. Puig O, Tjian R. Transcriptional feedback control of insulin receptor by dFOXO/FOXO1. Genes Dev. 2005;19(20):2435–46.
131. Britton JS, Lockwood WK, Li L, Cohen SM, Edgar BA. Drosophila's Insulin/PI3-Kinase Pathway Coordinates Cellular Metabolism with Nutritional Conditions generating a variety of second messengers. The critical second messenger produced by the class I A PI3-kinases is generated when phosphatidylinositol-4,5-P 2 (PIP 2 ; mostly found in lipid membranes) is phosphorylated in 1 Molecular and Cellular Biology Program and the third position, producing phosphatidylinositol-3,4,5-2 Division of Basic Sciences P 3 (PIP 3 ; Rameh and Cantley. Vol. 2, Developmental Cell. 2002.
132. Engler A, Rolando C, Giachino C, Saotome I, Erni A, Brien C, et al. Notch2 Signaling Maintains NSC Quiescence in the Murine Ventricular-

Subventricular Zone. Cell Rep. 2018 Jan 23;22(4):992–1002.

133. Read RD. Pvr receptor tyrosine kinase signaling promotes post-embryonic morphogenesis, and survival of glia and neural progenitor cells in drosophila. Dev. 2018 Dec 1;145(23).
134. Inaba M, Buszczak M, Yamashita YM. Nanotubes mediate niche-stem-cell signalling in the Drosophila testis. Nature. 2015;523(7560):329–32.
135. Sato M, Kornberg TB. Wilk et al., 1996) and Tango (Ohshiro and Saigo. Vol. 3, Developmental Cell. 2002.
136. Shen Q, Wang Y, Kokovay E, Lin G, Chuang SM, Goderie SK, et al. Adult SVZ Stem Cells Lie in a Vascular Niche: A Quantitative Analysis of Niche Cell-Cell Interactions. Cell Stem Cell. 2008 Sep 11;3(3):289–300.
137. Tata M, Wall I, Joyce A, Vieira JM, Kessaris N, Ruhrberg C. Regulation of embryonic neurogenesis by germinal zone vasculature. Proc Natl Acad Sci U S A. 2016 Nov 22;113(47):13414–9.
138. Brogiolo W, Stocker H, Ikeya T, Rintelen F, Fernandez R, Hafen E. An evolutionarily conserved function of the drosophila insulin receptor and insulin-like peptides in growth control. Curr Biol. 2001;11(4):213–21.
139. Ikeya T, Galic M, Belawat P, Nairz K, Hafen E. Nutrient-dependent expression of insulin-like peptides from neuroendocrine cells in the CNS contributes to growth regulation in Drosophila. Curr Biol. 2002;12(15):1293–300.
140. Bader R, Sarraf-Zadeh L, Peters M, Moderau N, Stocker H, Kö hler K, et al. The IGFBP7 homolog Imp-L2 promotes insulin signaling in distinct

neurons of the Drosophila brain. J Cell Sci. 2013 Jun;126(12):2571–6.

141. Colombani J, Andersen DS, Léopol P. Secreted peptide dilp8 coordinates Drosophila tissue growth with developmental timing. Science (80-). 2012;336(6081):582–5.

142. Garelli A, Gontijo AM, Miguela V, Caparros E, Dominguez M. Imaginal discs secrete insulin-like peptide 8 to mediate plasticity of growth and maturation. Science (80-). 2012;336(6081):579–82.

143. Jaszczak JS, Wolpe JB, Bhandari R, Jaszczak RG, Halme A. Growth coordination during Drosophila melanogaster imaginal disc regeneration is mediated by signaling through the relaxin receptor Lgr3 in the prothoracic gland. Genetics. 2016 Oct 1;204(2):703–9.

144. Colombani J, Andersen DS, Boulan L, Boone E, Romero N, Virolle V, et al. Drosophila Lgr3 Couples Organ Growth with Maturation and Ensures Developmental Stability. Curr Biol. 2015 Oct 19;25(20):2723–9.

145. Garelli A, Heredia F, Casimiro AP, Macedo A, Nunes C, Garcez M, et al. Dilp8 requires the neuronal relaxin receptor Lgr3 to couple growth to developmental timing. Nat Commun. 2015 Oct 29;6.

146. Lim DA, Alvarez-Buylla A. The adult ventricular–subventricular zone (V-SVZ) and olfactory bulb (OB) neurogenesis. Cold Spring Harb Perspect Biol. 2016 May 1;8(5).

147. Rushing G V., Bollig MK, Ihrie RA. Heterogeneity of Neural Stem Cells in the Ventricular–Subventricular Zone. 2019;1–30.

148. Silva-Vargas V, Maldonado-Soto AR, Mizrak D, Codega P, Doetsch F.

Age-Dependent Niche Signals from the Choroid Plexus Regulate Adult Neural Stem Cells. Cell Stem Cell. 2016 Nov 3;19(5):643–52.

149. Suzawa M, Muhammad NM, Joseph BS, Bland ML. The Toll Signaling Pathway Targets the Insulin-like Peptide Dilp6 to Inhibit Growth in Drosophila. Cell Rep. 2019 Aug;28(6):1439-1446.e5.
150. Albertson R, Doe CQ. Dlg, Scrib and Lgl regulate neuroblast cell size and mitotic spindle asymmetry. Nat Cell Biol. 2003;5(2):166–70.
151. Langevin J, Le Borgne R, Rosenfeld F, Gho M, Schweisguth F, Bellaïche Y. Lethal giant larvae controls the localization of Notch-signaling regulators Numb, neuralized, and Sanpodo in Drosophila sensory-organ precursor cells. Curr Biol. 2005 May 24;15(10):955–62.
152. Thacker SA, Bonnette PC, Duronio RJ. The Contribution of E2F-Regulated Transcription to Drosophila PCNA Gene Function constructs (Figure 1B) and performed in situ hybridiza-tion of embryos carrying these transgenes with a GFP probe. The results indicate that a 100-bp sequence con-taining the two E2F binding sites reproduces the entire complex embryonic profile of cell cycle-correlated. Vol. 13, Current Biology. 2003.
153. Schwabe T, Bainton RJ, Fetter RD, Heberlein U, Gaul U. GPCR signaling is required for blood-brain barrier formation in Drosophila. Cell. 2005 Oct 7;123(1):133–44.
154. Park S, Alfa RW, Topper SM, Kim GES, Kockel L, Kim SK. A Genetic Strategy to Measure Circulating Drosophila Insulin Reveals Genes Regulating Insulin Production and Secretion. PLoS Genet. 2014 Aug

7;10(8).

155. Hawkes CP, Grimberg A. Insulin-like growth factor-I is a marker for the nutritional state. Pediatr Endocrinol Rev. 2015;13(2):499–511.

156. Hsu D, Olefsky JM. Characterization of insulin-like growth factor (IGF) binding proteins and their role in modulating IGF-I action in BHK cells. J Biol Chem. 1992;267(35):25576–82.

157. Yamanaka Y, Wilson EM, Rosenfeld RG, Oh Y. Inhibition of insulin receptor activation by insulin-like growth factor binding proteins. J Biol Chem. 1997;272(49):30729–34.

158. Rulifson EJ, Kim SK, Nusse R. Ablation of insulin-producing neurons in files: Growth and diabetic phenotypes. Science (80-). 2002;296(5570):1118–20.

159. Delanoue R, Meschi E, Agrawal N, Mauri A, Tsatskis Y, McNeill H, et al. Drosophila insulin release is triggered by adipose Stunted ligand to brain Methuselah receptor. Science (80-). 2016;353(6307).

160. Meschi E, Léopold P, Delanoue R. An EGF-Responsive Neural Circuit Couples Insulin Secretion with Nutrition in Drosophila. Dev Cell. 2019;48(1):76-86.e5.

161. Liu Y, Liao S, Veenstra JA, Nässel DR. Drosophila insulin-like peptide 1 (DILP1) is transiently expressed during non-feeding stages and reproductive dormancy. Sci Rep [Internet]. 2016;6(May). Available from: http://dx.doi.org/10.1038/srep26620

162. Nässel DR, Kubrak OI, Liu Y, Luo J, Lushchak O V. Factors that regulate

insulin producing cells and their output in drosophila. Front Physiol. 2013;4 SEP(September):1–12.

163. Géminard C, Rulifson EJ, Léopold P. Remote Control of Insulin Secretion by Fat Cells in Drosophila. Cell Metab [Internet]. 2009;10(3):199–207. Available from: http://dx.doi.org/10.1016/j.cmet.2009.08.002
164. Brankatschk M, Dunst S, Nemetschke L, Eaton S. Delivery of circulating lipoproteins to specific neurons in the Drosophila brain regulates systemic insulin signaling. Elife. 2014;3(October2014):1–19.
165. Honegger B, Galic M, Köhler K, Wittwer F, Brogiolo W, Hafen E, et al. Imp-L2, a putative homolog of vertebrate IGF-binding protein 7, counteracts insulin signaling in Drosophila and is essential for starvation resistance. J Biol. 2008;7(3).
166. Delanoue R, Meschi E, Agrawal N, Mauri A, Tsatskis Y, McNeill H, et al. Drosophila insulin release is triggered by adipose Stunted ligand to brain Methuselah receptor. Science (80-). 2016;353(6307):1553–6.
167. Wu Q, Zhang Y, Xu J, Shen P. Regulation of hunger-driven behaviors by neural ribosomal S6 kinase in Drosophila. Proc Natl Acad Sci U S A. 2005;102(37):13289–94.
168. Rulifson EJ, Kim SK, Nusse R. Ablation of Insulin-Producing Neurons in Flies_ Growth and Diabetic Phenotypes — Supplemental Data.pdf. Science (80-). 2002;296(May):1118–21.
169. Broughton S, Alic N, Slack C, Bass T, Ikeya T, Vinti G, et al. Reduction of DILP2 in Drosophila Triages a Metabolic Phenotype from Lifespan

Revealing Redundancy and Compensation among DILPs. 2008 [cited 2017 Jul 1]; Available from: http://journals.plos.org/plosone/article/file?id=10.1371/journal.pone.0003721&type=printable

170. Alfa RW, Kim SK, Topper SM, Kockel L, Kim GES, Park S. A Genetic Strategy to Measure Circulating Drosophila Insulin Reveals Genes Regulating Insulin Production and Secretion. PLoS Genet. 2014;10(8):e1004555.
171. Sarraf-Zadeh L, Christen S, Sauer U, Cognigni P, Miguel-Aliaga I, Stocker H, et al. Local requirement of the Drosophila insulin binding protein imp-L2 in coordinating developmental progression with nutritional conditions. Dev Biol [Internet]. 2013;381(1):97–106. Available from: http://dx.doi.org/10.1016/j.ydbio.2013.06.008
172. Garbe JC, Yang E, Fristrom JW. IMP-L2: An essential secreted immunoglobulin family member implicated in neural and ectodermal development in Drosophila. Development. 1993;119(4):1237–50.
173. Post S, Karashchuk G, Wade JD, Sajid W, De Meyts P, Tatar M. Drosophila insulin-like peptides DILP2 and DILP5 differentially stimulate cell signaling and glycogen phosphorylase to regulate longevity. Front Endocrinol (Lausanne). 2018;9(MAY):1–16.
174. Plum L, Schubert M, Brüning JC. The role of insulin receptor signaling in the brain. Trends Endocrinol Metab. 2005;16(2):59–65.
175. Zhao S, Zhu Y, Schultz RD, Li N, He Z, Zhang Z, et al. Partial Leptin

Reduction as an Insulin Sensitization and Weight Loss Strategy. Cell Metab. 2019;30(4):706-719.e6.

176. Siegrist SE, Haque NS, Chen CH, Hay BA, Hariharan IK. Inactivation of Both foxo and reaper Promotes Long-Term Adult Neurogenesis in Drosophila. Curr Biol. 2010 Apr 13;20(7):643–8.
177. Doyle SE, Pahl MC, Siller KH, Ardiff L, Siegrist SE. Neuroblast niche position is controlled by Phosphoinositide 3-kinase-dependent DE-Cadherin adhesion. Development [Internet]. 2017;144(5):820–9. Available from: http://dev.biologists.org/lookup/doi/10.1242/dev.136713
178. Schindelin J, Arganda-Carreras I, Frise E, Kaynig V, Longair M, Pietzsch T, et al. Fiji: An open-source platform for biological-image analysis. Nat Methods. 2012;9(7):676–82.
179. Liu Y, Liao S, Veenstra JA, Nässel DR. Drosophila insulin-like peptide 1 (DILP1) is transiently expressed during non-feeding stages and reproductive dormancy. Nat Publ Gr [Internet]. 2016;1–15. Available from: http://dx.doi.org/10.1038/srep26620
180. Miguel-Aliaga I, Thor S, Gould AP. Postmitotic specification of Drosophila insulinergic neurons from pioneer neurons. PLoS Biol. 2008;6(3):0538–51.
181. Nässel DR, Enell LE, Santos JG, Wegener C, Johard HAD. A large population of diverse neurons in the Drosophila central nervous system expresses short neuropeptide F, suggesting multiple distributed peptide functions. BMC Neurosci. 2008;9:1–35.
182. Sano H, Nakamura A, Texada MJ, Truman JW, Ishimoto H, Kamikouchi A,

et al. The Nutrient-Responsive Hormone CCHamide-2 Controls Growth by Regulating Insulin-like Peptides in the Brain of Drosophila melanogaster. PLoS Genet. 2015;11(5):1–26.

183. Manière G, Ziegler AB, Geillon F, Featherstone DE, Grosjean Y. Direct Sensing of Nutrients via a LAT1-like Transporter in Drosophila Insulin-Producing Cells. Cell Rep. 2016;17(1):137–48.
184. Shim J, Gururaja-Rao S, Banerjee U. Nutritional regulation of stem and progenitor cells in Drosophila. Dev. 2013;140(23):4647–56.
185. Mishra B, Ghannad-Rezaie M, Li J, Wang X, Hao Y, Ye B, et al. Using microfluidics chips for live imaging and study of injury responses in Drosophila larvae. J Vis Exp. 2014;(84):1–15.
186. Farca-Luna A, Sprecher SG. Plasticity in the Drosophila larval visual system. Front Cell Neurosci. 2013;(JUNE).
187. Bhatt PK, Neckameyer WS. Functional analysis of the larval feeding circuit in Drosophila. J Vis Exp. 2013;(81):1–7.
188. Jeibmann A, Paulus W. Drosophila melanogaster as a model organism of brain diseases. Int J Mol Sci. 2009;10(2):407–40.
189. Echalier G, Ohanessian A. In vitro Culture of Drosophila melanogaster Embryonic Cells Author (s): G . Echalier and A . Ohanessian IN VITRO CULTURE OF DROSOPHILA MELANOGASTER EMBRYONIC CELLS. In Vitro. 1970;6(3):162–72.
190. Pahl MC, Doyle SE, Siegrist SE. E93 Integrates Neuroblast Intrinsic State with Developmental Time to Terminate MB Neurogenesis via Autophagy.

Curr Biol [Internet]. 2019;29(5):750-762.e3. Available from: https://doi.org/10.1016/j.cub.2019.01.039

191. Lewis GM, Kucenas S. Motor nerve transection and time-lapse imaging of glial cell behaviors in live zebrafish. J Vis Exp. 2013;(76):1–6.
192. Rawlings JS, Rosler KM, Harrison DA. The JAK/STAT signaling pathway. J Cell Sci. 2004;117(8):1281–3.
193. Zeidler MP, Bach EA, Perrimon N. The roles of the Drosophila JAK/STAT pathway. Oncogene. 2000;19(21):2598–606.
194. Zoranovic T, Grmai L, Bach EA. Regulation of proliferation, cell competition, and cellular growth by the Drosophila JAK-STAT pathway . Jak-Stat. 2013;2(3):e25408.
195. Bausek N. JAK-STAT signaling in stem cells and their niches in Drosophila . Jak-Stat. 2013;2(3):e25686.
196. Bach EA, Ekas LA, Ayala-Camargo A, Flaherty MS, Lee H, Perrimon N, et al. GFP reporters detect the activation of the Drosophila JAK/STAT pathway in vivo. Vol. 7, Gene Expression Patterns. 2007. p. 323–31.
197. Evans CJ, Olson JM, Ngo KT, Kim E, Lee NE, Kuoy E, et al. G-TRACE: Rapid Gal4-based cell lineage analysis in Drosophila. Nat Methods. 2009;6(8):603–5.
198. Awasaki T, Lai S-L, Ito K, Lee T. Organization and postembryonic development of glial cells in the adult central brain of Drosophila. J Neurosci. 2008;28(51):13742–53.
199. Bai J, Montell D. Eyes absent, a key repressor of polar cell fate during

Drosophila oogenesis. Development. 2002;129(23):5377–88.